수의학박사학위논문

마우스 위암과 간암 모델에서 Osteopontin의 역할

The roles of osteopontin on gastric and hepatic carcinogenesis in mouse model

2017년 2월

서울대학교 대학원

수의학과 수의병리학 전공

이 수 형

ABSTRACT

The roles of osteopontin on gastric and hepatic carcinogenesis in mouse model

(Supervisor: Dae-Yong Kim, D.V.M., Ph.D.)

Su-Hyung Lee

Department of Veterinary Pathology, College of Veterinary Medicine,
Graduate School, Seoul National University

Osteopontin (OPN), coded by secreted phosphoprotein 1 (*Spp1*) gene, plays a variety of roles in pathophysiological processes, including inflammation and carcinogenesis. Clinically, the elevated OPN levels in plasma or tissue from patients were identified in inflammatory diseases such as Crohn's disease and rheumatoid arthritis, and in various cancers. In this study, we demonstrated the role of OPN in *Helicobacter pylori (H. pylori)*-induced gastritis, gastric cancer and chemically induced hepatocellular carcinoma using C57BL/6-Spp1$^{tm1Blh(-/-)}$ (OPN KO) mice and OPN knockdown human cancer cell lines. In *H. pylori*-

induced gastritis model, the degree of inflammation of OPN KO mice was lower compared to that of WT mice, with a significant reduction in infiltratied macrophages and the expression of IL-1β, TNF-α, and IFN-γ. Similar to these results, mRNA expression of the pro-inflammatory cytokines was reduced in OPN KD gastric cancer cell lines exposed to *H. pylori*, and the conditioned media (CM) from these cells decreased the migration of monocytic and macrophage-like cell lines. Furthermore, *H. pylori*-infected OPN KO mice had a lower number of proliferative gastric epithelial cells than WT mice, in association with a reduction in mitogen-activated protein kinase (MAPK) pathway activation. OPN KD gastric cancer cell lines also showed the suppression of the G1/S cell-cycle after *H. pylori* co-culture and reduced MAPK activation after IL-1β and TNF-α treatment. In *H. pylori* and chemical-induced gastric cancer model, the overall incidence of gastric tumors was significantly decreased in OPN KO mice compared to WT mice. Apoptotic cell death was significantly enhanced in OPN KO mice, and was accompanied by upregulation of signal transducer and activator of transcription 1 (STAT1) and inducible nitric oxide synthase (iNOS). In AGS and THP-1 cells, OPN suppression also caused STAT1 upregulation and iNOS overexpression, which resulted in apoptosis of AGS cells. In addition, a negative correlation was clearly identified between expression of OPN and iNOS in human gastric cancer tissues. Our data demonstrate that loss of OPN decreases *H. pylori*-induced

gastric carcinogenesis by suppressing pro-inflammatory immune response and augmenting STAT1 and iNOS-mediated apoptosis of gastric epithelial cells. Furthermore, the overall incidence of chemically induced hepatic tumors at 36 weeks was significantly decreased in OPN KO mice compared to WT mice. Consistent with the result of gastric cancer model, apoptosis was significantly enhanced in OPN KO mice and was accompanied by downregulation of epidermal growth factor receptor (EGFR). In Hep3B and Huh7, OPN suppression also caused the decreased mRNA and protein levels of EGFR with the downregulation of c-Jun, which resulted in the increased apoptotic cell death of both cell lines. In addition, a positive correlation was clearly identified between expression of OPN and EGFR in human HCC tissues. Taken together, these data demonstrate that the loss of OPN decreases the degree of *H. pylori*-associated gastritis, which resulting in the suppression of gastric cancer development. In addition, it can be concluded that loss of OPN inhibits gastric and hepatic carcinogenesis through promotion of apoptotic cell death in cancer cells.

Keywords: Osteopontin, *H. pylori*, macrophage, iNOS, EGFR, gastric cancer, hepatocellular carcinoma

Student Number: 2011-21693

CONTENTS

ABBREVIATIONS

OPN: osteopontin

Bcl-2: B-cell lymphoma 2

Bcl-xL: B-cell lymphoma-extra large

CM: conditioned media

CFU: colony-forming unit

DEN: diethylnitrosamine

EGFR: epidermal growth factor receptor

FACS: flow cytometry

GAPDH: glyceraldehydes 3-phosphate dehydrogenase

GM-CSF: granulocyte-macrophage colony-stimulating factor

HCC: hepatocellular carcinoma

H. pylori: Helicobacter pylori

IFN-γ : interferon gamma

IL-1β : interleukin 1 beta

iNOS: inducible nitric oxide synthase

KD: knockdown

KO: knockout

LPS: lipopolysaccharide

MAPK: mitogen-activated protein kinase

MCP-1: monocyte chemoattractant protein-1

MMP: matrix metalloproteinase

MNU: *N*-methyl-*N*-nitrosourea

MOI: multiplicity of infection

NO: nitric oxide

PCNA: proliferating cell nuclear antigen

PI3K: phosphoinositide 3-kinase

PMA: phorbol 12-myristate 13-acetate

QRT-PCR: quantitative real-time reverse-transcription polymerase chain reaction

rhOPN: recombinant human osteopontin

shRNA: short hairpin ribonucleic acid

SPP1: secreted phosphoprotein 1

SS1: Sydney strain 1

STAT1: signal transducer and activator of transcription 1

TFF2: trefoil factor 2

TMA: tissue-microarray

TNF-α: Tumor necrosis factor alpha

TUNEL: terminal deoxynucleotidyl transferase dUTP nick end labeling

WT: wild type

LITERATURE REVIEW

Introduction

Since osteopontin (OPN), encoded by the human *SPP1* or mouse *Spp1* (secreted phosphoprotein 1) gene, was originally discovered as a bone-specific sialoprotein in a rat osteosarcoma (Oldberg, Franzen et al. 1986), a variety of studies for the function and structure of OPN has been carried out. It was initially identified that OPN had a specific structure containing abundant negatively charged amino acids which could make OPN acting as a mineralization inhibitor (Sodek, Ganss et al. 2000). OPN is also able to anchor osteoclast to the mineral matrix of bone, resulting in promotion of bone remodeling. Apart from these mineralization-associated role, OPN has known to be concerned in many pathophysiological events including wound healing, (Liaw, Birk et al. 1998) immune response (Cho and Kim 2009) and carcinogenesis (Singhal, Bautista et al. 1997, Cook, Chambers et al. 2006).

A wide range of the roles of OPN is accomplished by various isoform that formed by alternative translation or post-translational modification (Laffon, Garcia-Vicuna et al. 1991, Shinohara, Kim et al. 2008). *SPP1*, OPN coding gene, has seven exons, and six of seven exons contain coding sequence (Kiefer, Bauer et al. 1989). Full length OPN has several cleavage sites recognized by matrix metalloproteinases (MMPs) 3, 7 or

thrombin, and cleaved variants of OPN are called OPN-b and OPN-c that each variant lacks exon 5 or exon 4, respectively (Fig. 1) (Ahmed, Behera et al. 2011). Moreover, Shinohara *et al.* identified that alternative translation could generate secreted and intracellular forms of OPN (sOPN and iOPN) that had different roles in dendritic cells (Shinohara, Kim et al. 2008).

The pathophysiological effect of sOPN is mediated by binding to cell surface receptors, such as various integrins, CD44 variants and epidermal growth factor receptor (Fig. 2) (Lin, Huang et al. 2000, Lin and Yang-Yen 2001). OPN binding to these receptors allows activation of a variety of signaling pathways, which lead to pro-inflammatory response, neovascularization, cell survival and proliferation (Ahmed, Behera et al. 2011). iOPN also regulates cell migration, fusion, and immune cell function (Shinohara, Kim et al. 2008, Shinohara, Kim et al. 2008).

OPN knockout (KO) mice showed no difference in embryogenesis and reproductive phenotype compared to wild-type (WT) mice on the initial study for the mice phenotype (Liaw, Birk et al. 1998). It was also known that OPN KO mice did not represent any gross physical or behavioral abnormalities in normal condition according to the strain description of vendor (https://www.jax.org/strain/004936). For this reason, OPN KO mice has been employed by many researchers to identify the more detailed functions of OPN *in vivo*, and several studies presented the

difference between OPN KO mice and WT mice in diverse pathophysiological conditions (Kiefer, Neschen et al. 2011, Uaesoontrachoon, Wasgewatte Wijesinghe et al. 2013).

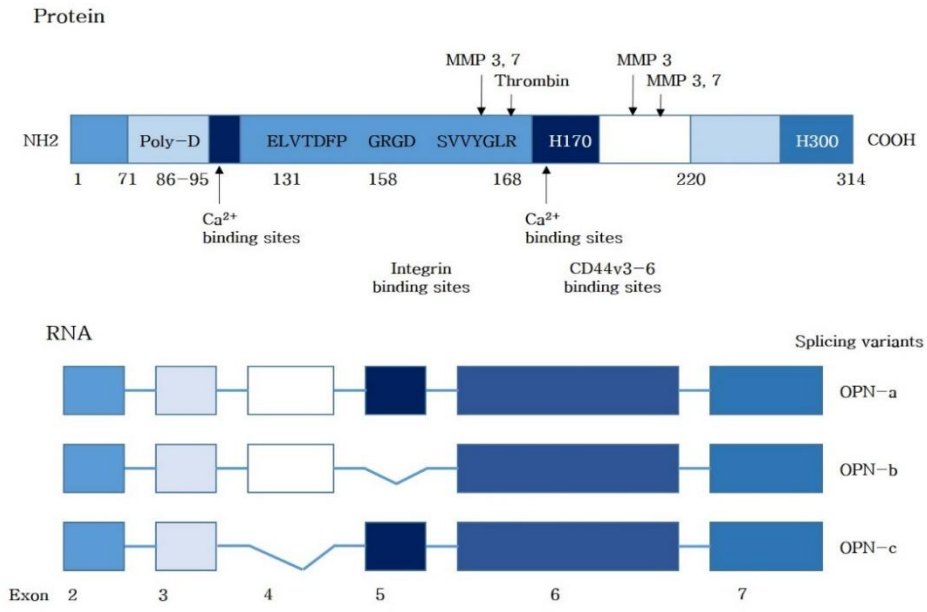

Fig 1. Schematic illustration of post−translational or alternative splicing variants of OPN (Ahmed, Behera et al. 2011).

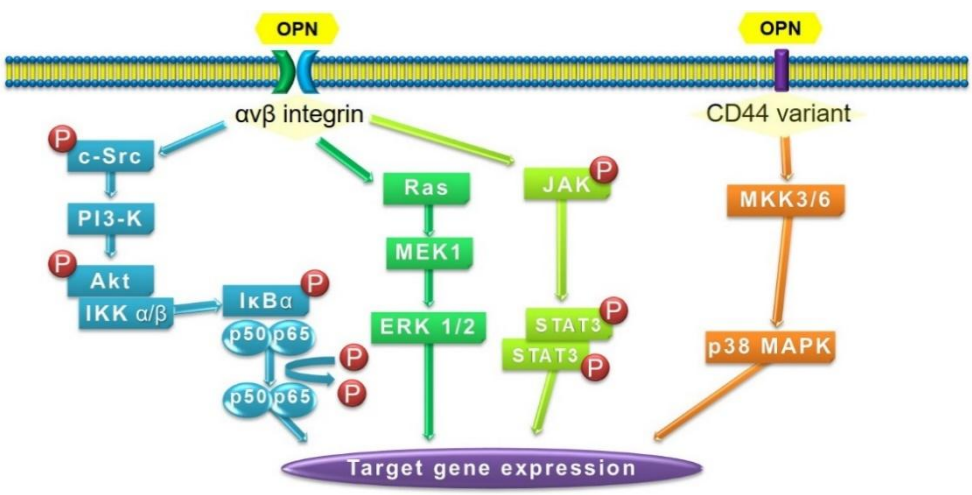

Fig 2. Schematic illustration of OPN, its receptor and related signaling pathway (Ahmed, Behera et al. 2011).

OPN in inflammatory response

It has been shown that OPN is expressed in a wide range of immune cells, regulating immune cell function and differentiation. One of the typical roles of OPN is chemotaxis of inflammatory cell, especially macrophage, through the coordination with CD44 variants and integrins (Giachelli, Lombardi et al. 1998, Zhu, Suzuki et al. 2004). Monocyte, precursor cell of macrophage, show low expression level of OPN while phorbol 12-myristate 13-acetate-induced macrophage show significantly higher expression level of OPN (Atkins, Berry et al. 1998). In addition, cytokines, such as tumor necrosis factor-alpha (TNF-α), interferon-gamma (IFN-γ) and interleukin-6 (IL-6), also induce OPN expression in monocyte and macrophage, and vice versa (Miyazaki, Tashiro et al. 1995, Li, O'Regan et al. 2003). The highly expressed OPN in macrophage plays important roles in induction of cytokine expression, phagocytosis, antigen presentation and recruitment of more inflammatory cells (Rittling 2011). OPN, known as early T lymphocyte activation gene 1, is also highly expressed in activated T cell following T cell receptor ligation, and important for prevention from apoptosis and induction of cell-mediated immune response (Shinohara, Jansson et al. 2005, Lund, Giachelli et al. 2009). The interaction between iOPN and Myeloid differentiation primary response gene 88 (MyD88) in plasmacytoid dendritic cell (DC) induces expression of IFN-α which can activate T helper 1 (Th1) cell-mediated immunity (Shinohara, Lu et

al. 2006). Furthermore, it was found that Th17 cell activation was mainly regulated by OPN. Classical DC-derived iOPN prevent IL-27 production that lead to Th17 activation (Shinohara, Kim et al. 2008, Cantor and Shinohara 2009).

Based on above findings, it is reasonable that host responses to a variety of pathologic stimuli, including infection, wound, autoimmune response, in mice lacking OPN is clearly different from those in WT mice (Lund, Giachelli et al. 2009), and OPN overexpression in plasma or tissue is observed in inflammatory disease. Infected with intracellular bacterium or viral pathogens, OPN deficient T cell show decreased expression levels of IL-12 and IFN-γ while increased IL-10 expression, thereby impairment of Th1 immune response to pathogen (Ashka, Weber et al. 2000). Furthermore, lack of OPN caused attenuation of neurological deficit and paralysis by promoting apoptotic cell death of activated T cell in experimental autoimmune encephalomyelitis and multiple sclerosis models (Hur, Youssef et al. 2007). On the other hand, OPN-transgenic (Tg) mice showed more severe inflammatory response accompanied by enhancement of Th1 cytokine expression and T cell proliferation in autoimmune disease and atherosclerosis models (Isoda 2003, Higuchi, Tamura et al. 2004, Husain-Krautter, Kramer et al. 2015).

OPN in cancer

Past decades, several clinical studies have been shown that OPN is overexpressed in cancer tissues and plasmas from patients, and the elevated OPN levels implicated progression and poor prognosis (Brown, Papadopoulos-Sergiou et al. 1994, Higashiyama, Ito et al. 2007, Lin, Li et al. 2011). Additionally, mutation as well as amplification of OPN is also observed in various epithelial cancers (Table 1 and 2) (Weber, Lett et al. 2011).

OPN is widely involved in carcinogenesis, such as cell proliferation, evading cell death, angiogenesis, invasion and metastasis by the activation of target molecules (Fig. 3). Generally, imbalance between proliferation and apoptosis is important process in cancer development (Murakami, Fujioka et al. 1997, Osman, Bloom et al. 2013). Luo *et al.* identified that OPN stimulated the growth of pre-neoplastic cell via mitogen-activated protein kinase (MAPK) activation (Luo, Ruhland et al. 2011). The suppressive effect of OPN on apoptosis was demonstrated by small interfering RNA-mediated OPN silencing (Zhang, Liu et al. 2010). These proliferating activity and anti-apoptotic effect is associated with cell cycle regulation. Xu *et al.* showed OPN downregulation resulted in G1/S arrest and increased apoptosis (Xu, Guo et al. 2015). Moreover, OPN is also closely related with cancer cell invasion and metastasis (Wu, Wu et al. 2007, Zhao, Dong et al. 2008). Increased expression of MMP, one of the key molecule in invasion and metastasis, through nuclear

translocation of β−catenin by OPN promoted cell survival and metastatic potential (Zhao, Dong et al. 2008, Robertson and Chellaiah 2010). These effect is mainly mediated by binding of sOPN to its receptors. Through binding to CD44 variants, OPN causes to p38 phosphorylation and phosphoinositide 3−kinase (PI3K)/Akt signaling activation, resulting in cancer cell survival and increase of motility (Kumar, Behera et al. 2010). Tumor cell growth, angiogenesis and metastasis is accelerated by PI3K/Akt, ERK and signal transducer and activator of transcription 3 (STAT3) activation through binding to integrins (Fig. 2) (Tang, Wang et al. 2007, Behera, Kumar et al. 2010). Meanwhile, these proliferating activity of OPN was also identified in OPN−Tg mice model (Hubbard, Chen et al. 2013). In this study, more numerous ducts, increased lobulogenesis and lactational change in mammary glands were prominently observed in OPN−Tg mice compared to WT littermate controls. This study also provided an implication of the role of OPN in carcinogenesis.

Importance of microenvironment in carcinogenesis has attracted scientist's attention for several decades. Being one of the most important regulator for macrophage functions, OPN is able to affect tumor development and progression through the establishment of tumor−favorable microenvironment (Rittling 2011, Shevde and Samant 2014). Tumor cells secrete a variety of cytokines and chemokines, resulting in inflammatory cell recruitment in tumor tissue (Coussens and Werb 2002).

In particular, macrophages infiltrated in tumor tissue are called tumor-associated macrophages (TAMs) which are mainly attracted by monocyte chemoattractant protein (Coussens and Werb 2002). TAMs play a contrasting role in carcinogenesis; TAMs may kill tumor cells, whereas angiogenesis, tumor cell invasion and metastasis are promoted by infiltrated TAMs (Brigati, Noonan et al. 2002, Tsung, Dolan et al. 2002). According to previous studies, these tumor-promoting TAMs highly expressed OPN, implying that OPN may accelerate tumor progression via TAM regulation (Kumar, Behera et al. 2010, Kale, Raja et al. 2014).

In gastric and hepatic cancers, *in vitro* mechanistic and clinical studies for the role of OPN have been extensively performed. Clinically, it was clearly proved OPN expression was upregulated in tumor tissues of gastric cancer and hepatocellular carcinoma (HCC) compared to the adjacent normal tissues, and OPN expression level was positively correlated with pathological grade, including invasiveness and lymph node metastasis (Pan, Ou et al. 2003, Dai, Bao et al. 2007, Imano, Satou et al. 2009, Tsai, Tsai et al. 2012). In addition, OPN downregulation in gastric or hepatic cancer cell lines also led to the suppression of cell proliferation and metastatic potential *in vitro* and xenograft studies (Gong, Lu et al. 2008, Zhao, Dong et al. 2008, Yoo, Gredler et al. 2011). Gong *et al.* showed that small interfering RNA (siRNA)-induced OPN suppression in human gastric cancer cell line inhibited ERK activation and

DNA binding activity of nuclear factor-kappa B (NF-κB), thereby reducing cell growth, migration and invasion (Gong, Lu et al. 2008). OPN also promoted lung metastasis and chemoresistance of human HCC cell line through NF-κB activation (Zhao, Dong et al. 2008). Taken together, OPN may be positively related to tumorigenesis of gastric cancer and HCC *in vivo*.

Table 1. *SPP1* gene overexpression in various types of cancers and correlation of expression level of SPP1 gene between cancerous and non-cancerous tissues (Weber, Lett et al. 2011).

Cancer type	Studies	Patients	Pearson p-value	Correlation coefficiency
All	153	13526	<0.001	0.84
Ampullary	3	140	<0.001	0.86
Bladder	1	78	<0.001	1
Bone	2	85	<0.001	1
Breast	13	743	<0.001	0.87
Cervical	4	654	<0.001	1
Colorectal	10	675	<0.001	0.95
Endometrial	4	214	<0.001	0.74
Esophageal	5	215	<0.001	0.94
Gastric	11	740	<0.001	1
Glioma	1	33	<0.001	1
Head and neck	5	374	<0.001	0.67
Leuk/lymph	2	190	<0.001	0.65
Liver	10	1424	<0.001	0.95
Lung	11	1769	<0.001	1
Medulloblastoma	2	45	<0.001	1

Melanoma	8	419	<0.001	0.95
Mesothelioma	6	663	<0.001	0.96
Myeloma	6	431	<0.001	1
Oral	4	312	<0.001	0.8
Ovarian	19	2410	<0.001	0.7
Pancreatic	3	259	<0.001	1
Pilomatricoma	1	7	0.008	1
Prostate	11	909	<0.001	0.71
Renal	3	231	0.044	0.13
Soft tissue sarcoma	1	30	<0.001	1
Thyroid	7	182	<0.001	1

Table 2. Frequency of *SPP1* gene mutation in various types of cancers (http://cancer.sanger.ac.uk/cosmic/gene/analysis?ln=SPP1).

Tissue	Point mutation	
	Frequency (%)	Samples (n)
Pituitary	6.67	15
NS	1.85	54
Large intestine	1.42	1552
Skin	1.19	1094
Stomach	1.18	592
Cervix	0.93	322
Lung	0.64	1868
Endometrium	0.62	640
Biliary tract	0.61	329
Oesophagus	0.37	1073
Soft tissue	0.35	567
Kidney	0.34	1479
Prostate	0.15	1295
Urinary tract	0.15	667
Breast	0.14	1397

Pancreas	0.13	1539
Ovary	0.12	831
Haematopoietic and lymphoid	0.1	2925
Upper aerodigestive tract	0.1	998
Central nervous system	0.05	2163

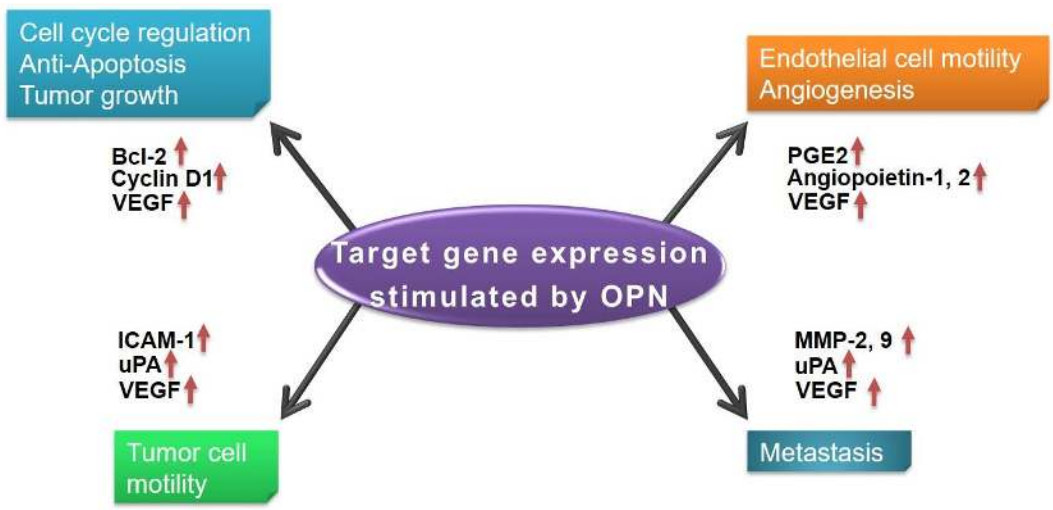

Fig 3. A wide range of effect of OPN on carcinogenesis and associated target molecules.

Summary

OPN is closely related to a wide range of pathophysiological conditions especially inflammation and cancer, and OPN upregulation in tissue and plasma from patients is commonly observed. Although mechanistic studies *in vitro* have been also carried out for several years, few studies have shown how OPN affects the development and progression of disease *in vivo*.

In the present study, we showed the effect and underlying mechanisms of OPN-associated development and progression of inflammation and cancer using specific disease model combined with genetically engineered mouse. Specifically, the role of OPN in *Helicobacter pylori*-induced multistep carcinogenesis was studied (Fig. 4).

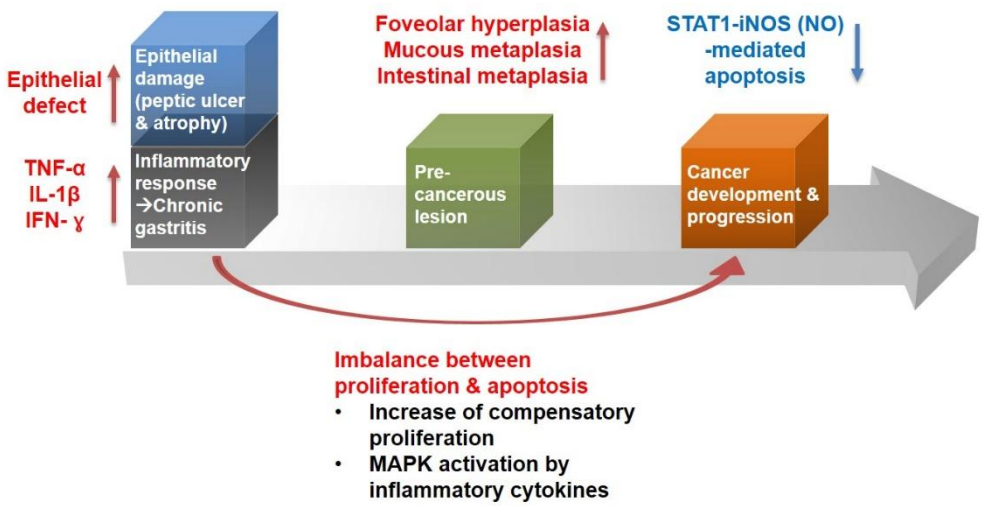

Fig 4. The effect of OPN on *Helicobacter pylori*-induced multistep gastric carcinogenesis.

CHAPTER I.

OSTEOPONTIN DEPLETION DECREASES INFLAMMATION AND GASTRIC EPITHELIAL PROLIFERATION DURING HELICOBACTER pylori INFECTION IN MICE

Abstract

Osteopontin (OPN) is a multi-functional protein that plays a role in many physiological and pathological processes, including inflammation and tumorigenesis. Here, we investigated the involvement of OPN in *Helicobacter pylori* (*H. pylori*)-induced gastritis using OPN knockout (KO) mice and OPN knockdown (KD) cell lines. *H. pylori*-infected OPN KO mice showed significantly reduced gastritis compared with wild type (WT) mice with decreased infiltration of macrophages and a reduction in *H. pylori*-induced up-regulation of IL-1β, TNF-α, and IFN-γ. *H. pylori*-exposed OPN KD gastric cancer cells and macrophage-like cells showed an attenuated induction of these cytokines. We also demonstrated a reduction in the migration of monocytic and macrophage-like cells toward conditioned media harvested from *H. pylori*-exposed OPN KD gastric cancer cells as well as reduced migration ability of OPN KD cells itself. In addition, *H. pylori*-infected OPN KO mice showed decreased epithelial cell proliferation compared with *H. pylori*-infected WT mice, in association with a reduction in MAPK pathway activation. OPN KD gastric cancer cell lines also showed lower proliferative activity and reduced MAPK activation than shRNA-control cells after *H. pylori* co-culture or after IL-1β and TNF-α treatment. Taken together, these results indicate that OPN exerts a considerable influence on *H. pylori*-induced gastritis by modulating the production of cytokines and contributing to macrophage infiltration.

Moreover, OPN-mediated activation of the MAPK pathway in gastric epithelial cells might contribute to epithelial changes following *H. pylori* infection.

Introduction

Helicobacter pylori (*H. pylori*) is a gram-negative bacterial pathogen that selectively colonizes the human stomach (Konturek, Bielanski et al. 1999, Peek, Fiske et al. 2010). Approximately half of the world's population is infected with *H. pylori*, and its infection is strongly associated with chronic gastritis, peptic ulcers, and gastric cancer(Konturek, Bielanski et al. 1999, Peek, Fiske et al. 2010). *H. pylori*-infected gastric mucosa progresses through stages of chronic gastritis, glandular atrophy, intestinal metaplasia, dysplasia, and gastric cancer (Fox and Wang 2007). *H. pylori* produce a variety of virulence factors, such as CagA and VacA that can affect host intracellular signaling pathways and play an important role in determining the outcome of *H. pylori* infection (Fox and Wang 2007). However, they are not absolute determinants of clinical outcomes because most individuals remain asymptomatic after *H. pylori* infection (Wroblewski, Peek et al. 2010). The variable outcomes of *H. pylori* infection can be attributed to inflammatory responses governed by host factors as well as *H. pylori* virulence factors (Blaser and Berg 2001). Indeed, polymorphisms of host interleukin (IL)-1β and tumor necrosis factor (TNF)-α are reported to be associated with the risk of *H. pylori*-associated gastric cancer development (Wroblewski, Peek et al. 2010).

H. pylori-induced chronic inflammation induces DNA alterations and imbalanced epithelial cell turnover, providing opportunities for mitotic

error that could ultimately contribute to the development of gastric cancer (Correa 1992, Chan, Chu et al. 2007, Fox and Wang 2007, Milne, Carneiro et al. 2009). Infiltrating macrophages, in particular, produce various cytokines and growth factors such as IL-1β that could attract more inflammatory cells and induces the proliferation of gastric epithelial cells (Peek, Moss et al. 1997, Xia, Lam et al. 2005). A recent study demonstrated that IL-1β physiologically induced by *H. pylori* infection enhanced gastric inflammation and the number of gastric tumors using *Il1b*-mull mice (Shigematsu, Niwa et al. 2013). Moreover, host factors secreted from gastric epithelial cells, such as Sonic Hedgehog (Shh), could also be involved in the initiation of gastritis, acting as a macrophage chemoattractant during *H. pylori* infection(Schumacher, Donnelly et al. 2012). The interaction between gastric epithelial cells and infiltrating macrophages during *H. pylori* infection might play an important role in the development of gastritis and *H. pylori*-related pathogenic changes in gastric epithelial cells. Therefore, host factors involved in such interactions during *H. pylori* infection need to be further investigated.

Osteopontin (OPN), encoded by a secreted phosphoprotein 1 (*SPP1*) gene, is a multifunctional glycol-phosphoprotein that play important roles in a wide range of pathophysiological processes, such as inflammation, angiogenesis, bone remodeling, and cell migration (Chan, Chu et al. 2007, Milne, Carneiro et al. 2009). OPN, functioning as chemoattractive Th1 cytokine, promotes the migration of inflammatory

cells (Shinohara, Lu et al. 2006, Chan, Chu et al. 2007). Clinically, increased plasma OPN levels were proven in many chronic inflammatory diseases such as Crohn's disease and rheumatoid arthritis and various cancers including gastric cancer (Chan, Chu et al. 2007). A recent study showed that increased gastric OPN expression in response to *H. pylori* infection correlates well with the degree of gastric inflammation and intestinal metaplasia in human (Chang, Yang et al. 2011). However, the exact functional roles of OPN in *H. pylori*–induced gastritis have not yet been fully investigated. Previous reports have focused on the role of OPN in macrophage functions in various immunological disorders (Chan, Chu et al. 2007), while the role of OPN in epithelial cells in response to infectious pathogens, such as *H. pylori*, has been not studied.

In this study, we investigated the possible roles of OPN during *H. pylori*–induced gastritis using OPN knockout (KO) mice and stable OPN knockdown (KD) cell lines. The results showed that OPN is an important mediator of *H. pylori*–induced gastritis and regulates cytokine production, macrophage migration, and proliferation of gastric epithelial cells in response to *H. pylori* infection. Our results provide important insights into the role of OPN in inflammatory processes and gastric epithelial changes that occur in response to *H. pylori* infection.

Materials and Methods

Mice

Female C57BL/6-Spp1$^{tm1Blh(-/-)}$ (OPN KO) mice were purchased from Jackson Laboratory (Bar Harbor, ME, USA) and wild type (WT) littermates were purchased from Orientbio (Seongnam, Korea) at 5 weeks old. Mouse studies were conducted with the approval of the Animal Care and Use Committees of Seoul National University (certification number: SNU-100729-1). The mice were used in the study after one week adjustment to the facility

Cell cuture and isolation of peritoneal macrophages

Human gastric cancer cell line AGS, human monocytic cell line THP-1, and mouse macrophage-like cell line RAW267.4 were purchased from American Type Culture Collection (Manassas, VA, USA). NCC-S1M, mouse gastric cancer cell line, was primarily cultured from a spontaneous gastric carcinoma arising in a *Villin-cre;Trp53*$^{F/F}$*;Smad4*$^{F/F}$*;Cdh1*$^{F/wt}$ mouse (Park, Park et al. 2014). All the cell lines were cultured at 37 ℃ in a 5% CO_2 humidified incubator in RPMI-1640 medium (Gibco, Grand Island, NY, USA) containing 10 % fetal bovine serum (Gibco), 1% penicillin and streptomycin (Invitrogen Biotechnology, Grand Island, NY, USA), and 0.05 mM mercaptoethanol was additionally supplemented to culture THP-1 cell line. To produce differentiated macrophage-like

cells (Di-THP-1), THP-1 cells were seeded on the 6-well plates at 1 x 10^6 cells with 200nM of phorbol 12-myristate 13-acetate (PMA; Sigma-Aldrich, St. Louis, MO, USA) and incubated for 24 hours.

To isolate peritoneal macrophages from mice, we used previously described method (Coligan). Briefly, female 5 week-old WT and OPN KO mice were injected intra-peritoneally with 10 ml cold PBS after CO_2 euthanasia and the peritoneal fluid was withdrawn by syringe suction. Peritoneal cells in the fluid were allowed to adhere in tissue culture plates in cell culture media for 1 hour. Non-adherent cells were removed by washing with warm PBS. We verified greater than 85% macrophages in the preparation by flow cytometry using anti-mouse F4/80 antigen PE (1:500; 12-4801-80, eBioscience, San Diego, CA, USA).

Helicobacter pylori infection and in vitro co-culture

Mouse adapted *H. pylori* Sydney strain 1 (SS1) was grown on brain heart infusion agar plates (Difco, Detroit, MI, USA) containing 10% sheep blood under microaerobic conditions produced by GasPak jars (Difco) and Campy-Paks (Becton Dickinson, Cockeysville, MD, USA) at 37 ℃. After 24 hours of fasting, 6 week-old OPN KO and WT mice (n=20 and 20, respectively) were orally administered with a 0.1-mL suspension of *H. pylori* containing 1X10^9 colony-forming units (CFU)/mL for three times every other day in 1 week. . Twenty additional mice in each group were used as sham-infected controls. Ten mice in

each group were sacrificed at 8 and 16 weeks after H. pylori infection, respectively. To quantify *H. pylori* in mouse stomach, total DNA was extracted from mouse stomachs using QIAamp DNA mini kit (Qiagen, Hilden, Germany) according to the manufacturer's instruction and was amplified using specific primers for the 16S rDNA gene of *H. pylori* SS1 with TaqMan probe (Roussel, Harris et al. 2007). The quantity of *H. pylori* 16S gene was normalized to that of mouse GAPDH gene.

For the *in-vitro* co-culture experiment, *H. pylori* strain 60190 was used because of the low viability of *H. pylori* SS1 in RPMI 1640 media and the similar pathogenicity with *H. pylori* SS1 (CagA (+), VacA (+)). H. pylori strain 60190 was kindly provided by Dr. Yong Chan Lee (Department of Internal Medicine, Yonsei University, Korea). *H. pylori* 60190 was grown according to the same method used for the cultivation of *H. pylori* SS1. The conditions for *H. pylori* co-culture were described previously (Lee, Kim et al. 2010, Chang, Yang et al. 2011). Briefly, AGS, NCC-S1M, Di-THP-1, RAW264.7 cells, and peritoneal macrophages were seeded on 6-well plates at a density of 1.5 x 10^5 cells per well in RPMI-1640 medium with 10% fetal bovine serum (FBS). Then, 12 hours after seeding, the culture medium was replaced with RPMI-1640 containing 1% FBS and no antibiotics. After 12 hours, *H. pylori* was suspended in the RPMI-1640 medium and added to the cells at a concentration of 10 multiplicity of infection (MOI). To verify the *H. pylori* viability in the co-culture condition, supernatants and scrapped

gastric cancer cells after co-culture for 24 hours were collected and grown on brain heart infusion agar plates containing 10% sheep blood under microaerobic conditions. After 3 days of incubation, *H. pylori* colonies were identified by colony morphology, urease activity, and PCR (data not shown). To prepare the conditioned media (CM), the culture media were harvested at 24 hours after *H. pylori* co-culture and filtered using a 0.45 micron filter.

The cell proliferation was determined using the MTT assay. 24 hours after *H. pylori* co-culture, 200 ㎕ of MTT solution (5mg/ml in PBS) was added to each well in 1 ml of media. Formazane formation was terminated after 2 hours by removing the MTT solution. 500 ㎕ DMSO was added into each well to dissolve the precipitation. The absorbance was detected at 570 nm with a Microplate Reader.

Flow cytometry for cell cycle analysis was performed by using the co-cultured cells with *H. pylori* for 24 hours. Cells were harvested, washed with PBS, fixed in 70% ethanol at 4℃ overnight, washed with cold PBS, and stained with propidium iodide (PI) staining solution (50 ㎍/mL PI and 0.1 mg/mL RNase A in PBS) at RT for 30 minutes. Cell cycles were then analyzed using FACSCalibur (BD Biosciences, San Jose, CA).

Necropsy and histopathological examination

Mice were sacrificed 24 hours after fasting and stomachs were incised along the greater curvature. The stomach was spread onto a filter paper

and cut in half along the lesser curvature. One part was stored in a −70° C deep freezer for subsequent analysis. The other part was fixed in neutral buffered 10% formalin for 1 day. Then the formalin-fixed stomachs were cut into three strips and processed by standard method. 5 μm paraffin-embedded sections were stained with hematoxylin and eosin (H&E). The degrees of mucosal inflammation after *H. pylori* infection were graded on the basis of previously delineated criteria (Rogers, Taylor et al. 2005).

Immunohistochemistry (IHC) and double immunofluorescence

The replicate paraffin sections were dewaxed, rehydrated and subjected to antigen retrieval by heating at 100 ° C for 20 minutes in 0.01 M citrate buffer (pH 6.0). The ImmPRESS Peroxidase Polymer kit (Vector Laboratories, Burlingame, CA) was used for immunostaining according to the manufacturer' s protocol. Briefly, the slides were incubated with the 2.5% horse serum for blocking and then incubated for 30 minutes at room temperature with the primary antibodies. Rabbit polyclonal anti-Ki-67 (1:200; ab15580, Abcam, Cambridge, MA, USA), rabbit monoclonal anti-CD3 (1:100; ab16669, Abcam), rat monoclonal anti-F4/80 (1:200; ab6640, Abcam), mouse monoclonal anti spasmolytic polypeptide antibody (TFF2) (1:50; ab49536, Abcam), and goat polyclonal anti-OPN (1:100; AF808, R&D systems, Minneapolis, MN, USA) were used as primary antibodies. After washing, the slides were

then incubated for 30 minutes with peroxidase polymer-linked appropriate secondary antibodies. The slides were subjected to colorimetric detection with ImmPact DAB substrate (SK-4105, Vector Laboratories). The slides were counterstained with Meyer's hematoxylin for 10 seconds. Negative controls were performed by omitting the primary antibody and substitution with diluent.

For double immunofluorescence analysis, the slides were incubated with 5% goat serum for first blocking. The first primary antibody against F4/80 (1:100; ab6640, Abcam) was incubated overnight at 4℃. After washing, the Texas red goat anti-rat secondary antibody (1:250; TI-9400, Vector Laboratories) was incubated for 1 hour at room temperature. Then, the slides were incubated with 5% rabbit serum for second blocking. After blocking, second primary antibody against OPN (1:50; AF808, R&D systems) was incubated overnight for 1 hour and the FITC rabbit anti-goat secondary antibody (1:250; FI-5000, Vector Laboratories) was incubated for 1 hour at room temperature. Slides were mounted with Vectashield mounting media (H-1200, Vector Laboratories). Stained slides were evaluated using Zeiss Axio Imager HBO 100 (Carl Zeiss, Oberkochen, Germany).

Lentiviral shRNA for stable OPN knockdown

The lentiviral human SPP1 and mouse Spp1 shRNA constructs were purchased from Sigma-Aldrich with pLKO.1-puro eGFP control vector

(SHC005, Sigma). The target constructs were generated from accession number NM_000582 (CCGGCCGAGGTGATAGTGTGGTTTACTCGAGTAAACCACACTATCACCTCGGTTTTT) and NM_009263 (CCGGAGGATGACTTTAAGCAAGAAACTCGAGTTTCTTGCTTAAAGTCATCCTTTTTTG). Lentiviruses were produced by cotransfecting shRNA-expressing vector and pMD2.G and psPAX2 constructs (Addgene, Cambridge, MA, USA) into 293T cells by using lipofectamine 2000 (Invitrogen). Viral supernatants were harvested 48 hours after transfection, filtered through a 0.45 μm filter, titered and used for viral transduction with 10 μg/mL polybrene. AGS and NCC-S1M cell lines were selected for OPN knockdown because AGS cell line was one of the gastric cancer cell lines showing relatively high expression of OPN based on Quantitative real-time RT-PCR and western blot analysis (data not shown) and NCC-S1M showed a considerably increased OPN expression compared with mouse normal gastric epithelium (Fig. 5B). Cells were treated by 2 μg/ml puromycin at 48 hours after viral transduction and were selected for 3 days. The knockdown efficiency was determined by quantitative real-time RT-PCR and western blotting (Fig. 5A and B).

In vitro migration assay

We performed a modified Boyden chamber migration assay to measure migration of mouse peritoneal macrophages, THP-1 cells, and

RAW267.4 cells using transwell-24 well inserts with an 8 μm porous membrane (353097, BD Biosciences). Either medium containing *H. pylori* filtrates or the CM was added to the 24-well lower chamber (354578, BD Biosciences). *H. pylori* filtrates were prepared as described (Kwon, Won et al. 2012). The cells were placed on 24-well inserts at 1 x 10^5 cells per well in serum-free RPMI 1640 media. After 16 hours, mouse peritoneal macrophages and RAW267.4 cells had migrated toward the insert chamber and attached on the lower side of the membrane. The insert was fixed with 10% formalin for 15 minutes and soaked in hematoxylin for 1 minute. Membrane was cut from the insert and placed on a glass slide and mounted under a coverslip with Permount (Fisher Scientific, Waltham, MA, USA). The number of migrated cells was averaged by counting 3 high power fields (*200x*). As THP-1 cells had migrated completely through the membrane, total media from the lower chamber were collected and the number of migrated cells was counted using typan blue exclusion assay.

Quantitative real-time RT-PCR (QRT-PCR)

Total RNA from both stomach tissues and cell lines was extracted by RNeasy Plus Mini kit (Qiagen) according to the manufacturer's instruction. 0.1 μg of total RNA from each sample was reverse-transcribed using the QuantiTect Reverse Transcription kit (Qiagen) and analyzed by real-time PCR using the Rotor-Gene SYBR Green PCR kit

(Qiagen) with specific primers. Target genes were amplified and quantified using the Rotor-Gene Q and manufacturer's software (Qiagen). The amount of target gene was calculated using mRNA encoding β-actin and GAPDH as a housekeeping gene. QRT-PCR primers for mouse genes were F: 5'-GGA GAA CCA AGC AAC GAC AA-3' and R: 5'-TGG GGA ACT CTG CAG ACT CA-3' for *Il1b,* F: 5'-AGC CCC CAC TCT GAC CCC TTT AC-3' and R: 5'-TGT CCC AGC ATC TTG TGT TTC T-3' for *Tnf,* F: 5'-AGC GGC TGA CTG AAC TCA GAT TGT AG-3' and R: 5'-GTC ACA GTT TTC AGC TGT ATA GGG-3' for *Ifng,* and F: 5'-CAG GAG ATG GCC ACT GCC GCA -3' R: 5'-TCC TTC TGC ATC CTG TCA GCA-3' for *Actb*. QRT-PCR primers for human genes were F: 5'-CCA GTG AAA TGA TGG CTT ATT AC-3' and R: 5'-CTG TAG TGG TGG TGG TCG GAG ATT-3' for *IL1B,* F: 5'-GCT TGT TCC TCA GCC TCT TCT-3' and R: 5'-GGT TTG CTA CAA CAT GGG CTA-3' for *TNF,* and F: 5'-GAG TCA ACG GAT TTG GTC G-3' R: 5'-TGG AAT CAT ATT GGA ACA TGT AAA C-3' for *GAPDH*.

Western blotting (WB)

Both mouse stomach tissues and cell lines were lysed with T-PER Tissue Protein Extraction Reagent (Thermo Fisher Scientific, Hudson, NH, USA) supplemented with protease inhibitor (P3100-001, GenDEPOT, Barker, TX, USA) and phosphatase inhibitor (P3200-001, GenDEPOT) according to manufacturer's instruction. Protein samples

were mixed with 4x Laemmli sample buffer and boiling for 5 minute at 100 °C. Equal amounts of protein were separated on SDS-polyacrylamide gel and transferred onto nitrocellulose membrane by electrophoresis and blotting apparatus (Bio-Rad, Hercules, CA, USA). The proteins were probed with the primary antibodies and horseradish peroxidase (HRP)-conjugated secondary antibodies at the recommended dilutions. The following primary antibodies were used in this study; goat polyclonal anti-mouse OPN antibody (1:100; AF808, R&D systems), goat polyclonal anti-human OPN antibody (1:100; AF808, R&D systems), rabbit polyclonal anti-p21antibody (1:1000; sc-397, Santa Cruz Biotechnology, Santa Cruz, CA, USA), rabbit polyclonal anti-Cyclin E antibody (1:1000; 07-687, Merck Millipore, Billerica, MA, USA), rabbit polyclonal anti phospho-Akt1/2/3 (Thr 308) antibody (1:1000; sc-16646-R, Santa Cruz Biotechnology), rabbit polyclonal anti-Akt 1/2/3 antibody (1:1000; sc-8312, Santa Cruz Biotechnology), mouse monoclonal anti phospho-p44/42 MAPK (pErk1/2) antibody (1:1000; #9106, Cell Signaling Technology, Beverly, MA, USA), rabbit polyclonal anti p44/42 MAPK (Erk1/2) antibody (1:1000; sc-292838, Santa Cruz Biotechnology), and mouse monoclonal anti- β-actin antibody (1:1000; sc-47778, Santa Cruz Biotechnology). Immunodetection were performed by using an enhanced chemiluminescence (ECL) detection kit (Thermo Fisher Scientific).

Statistical analysis

All data are expressed as means ± standard errors (SEMs). Statistical analysis were performed by GrapH. pyloriadPrism4 (version 4.0; GrapH. pyloriad Software, San Diego, CA, USA). The data were analyzed using unpaired two-tailed Student's *t*-test. *P* values of less than 0.05 were considered statistically significant.

Results

Attenuated inflammation in H. pylori-infected OPN KO mice

We confirmed whether *H. pylori* successfully infected WT and OPN KO mice using TaqMan real-time PCR amplification of the 16S rDNA gene of *H. pylori* SS1(Roussel, Harris et al. 2007). *H. pylori* burden between OPN KO and WT was not statistically different, indicating *H. pylori* burden is not directly affected by OPN gene itself (Fig. 1A). We then compared the degree of inflammatory changes between two groups at 8 and 16 weeks after *H. pylori* infection as previously described(Rogers, Taylor et al. 2005). WT mice exhibited gastritis displaying multifocal infiltration of moderate numbers of neutrophils, macrophages, and lymphocytes in the lamina propria and submucosa at 8 weeks (Fig. 1B and 1C). In WT mice at 16 weeks, the inflammatory response expanded and occasionally infiltrated below the submucosa. Meanwhile, OPN KO mice showed an attenuation of the inflammation compared with WT mice at both 8 and 16 weeks (Fig. 1C), which was confirmed by histological grading (Fig. 1B). The numbers of infiltrating macrophages (F4/80-positive cells), T cells (CD3-positive cells) and neutrophils (polymorphonuclear cells) in *H. pylori*-infected OPN KO mice were significantly decreased compared to that of *H. pylori*-infected WT mice (Figs. 1D and 1E). The reduction in infiltrating macrophages was especially prominent in OPN KO mice infected with *H. pylori* ($p<0.0001$).

These results demonstrate that OPN deficiency reduces gastric inflammatory response to *H. pylori* infection. In addition, WT mice occasionally showed epithelial defects such as slightly dilated glands and mild surface erosion both at 8 and 16 weeks, but these lesions were either not detected or mild in OPN KO mice (Fig 2). *H. pylori*–infected WT mice also showed 1.5 to 2–fold increases in the isthmus length compared with uninfected WT mice (Fig 2), but the hyperplastic change was significantly reduced in OPN KO mice at 16 weeks after *H. pylori* infection. TFF2–expressing metaplasia (SPEM) in gastric mucosa was observed in neither WT nor OPN KO mice until 16 weeks after *H. pylori* infection (Fig 3).

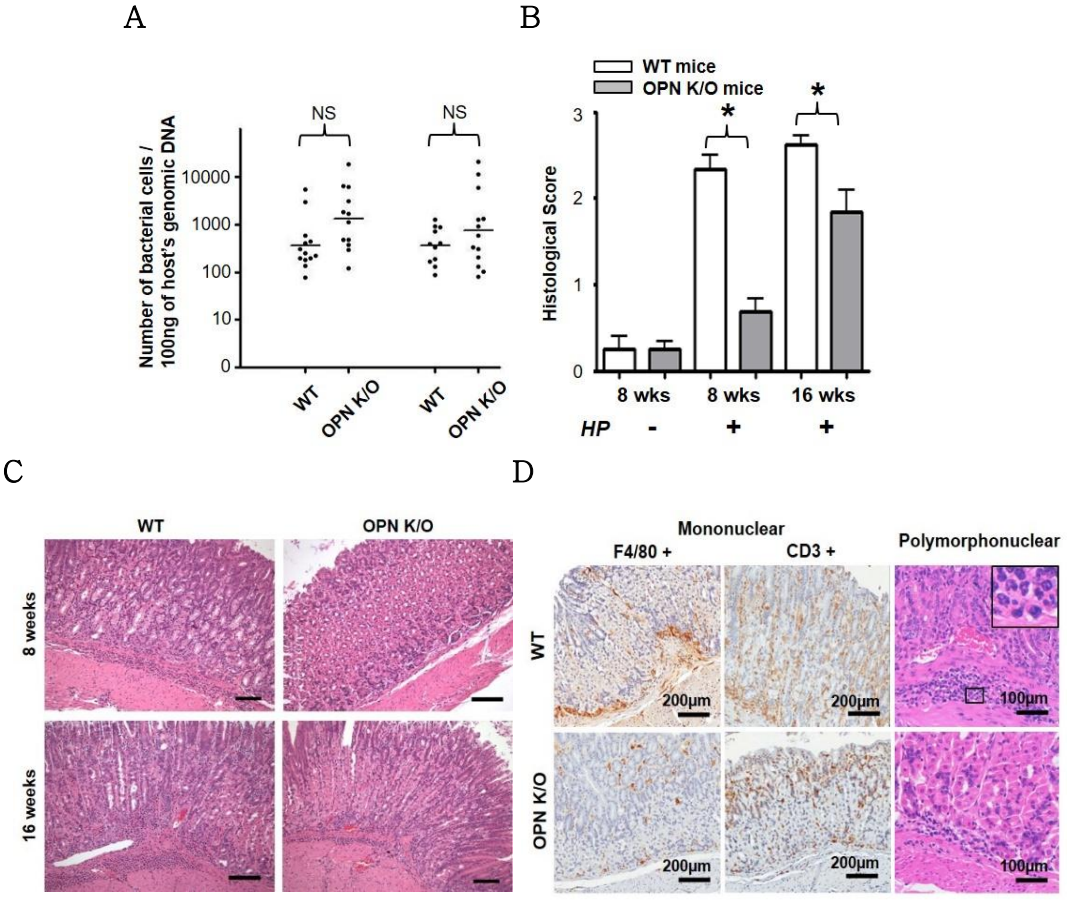

Fig 1. Histopathological and immunohistochemical findings of *H. pylori*–induced gastritis in WT and OPN KO mice. (A) Assessment for bacterial colonization in *H. pylori*–infected stomach tissues. (B) Histopathological scoring for gastritis. Results are presented as means±SEMs (n=10). (C) Representative H&E images of gastric tissues at both 8 and 16 weeks after infection. (D) Representative immunohistochemical images of inflammatory cells infiltrated in stomach tissues. (E) Quantitation of F4/80, CD3 positive cells and polymorphonuclear cells at 8 and 16 weeks after infection. Results are presented as means±SEMs (n=10). $*P < 0.05$.

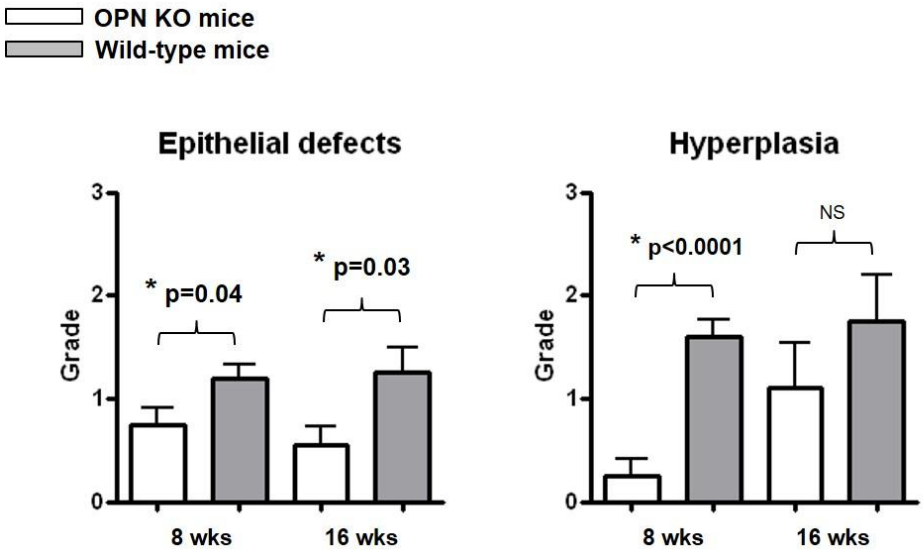

Fig 2. Gastric histopathological grade for WT and OPN KO mice at 8 and 16 weeks after *H. pylori* infection.

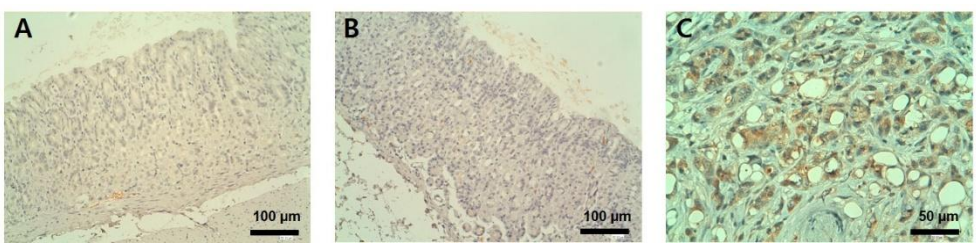

Fig 3. Representative pictures of immunohistochemical staining for TFF2 in WT and OPN KO mice at 16 weeks after *H. pylori* infection. Gastric mucosa from a *H. pylori*–infected WT mouse (A) and OPN KO (B). As previously reported, a gastric cancer tissue from a *Pdx-1-Cre;Smad4*$^{F/F}$*;Trp53*$^{F/F}$*;Cdh1*$^{F/+}$ mice were used for positive control (C).(Park, Jang et al. 2014)

Gastric OPN expression is up-regulated after H. pylori infection, and both gastric epithelial cells and macrophages are the source of OPN

We next examined whether *H. pylori* infection up-regulated OPN expression in murine gastric tissues. In non-infected WT gastric tissues, WB analysis detected minimal OPN expression (Fig. 4A) and IHC showed weak and scattered random OPN expression in the gastric glands (Fig. 4Ba). As expected, OPN expression was not detected in OPN KO mice (Fig. 4Ba). By contrast, WB analysis showed mild increase of OPN in WT mice at 8 weeks after *H. pylori* infection (Fig. 4A). IHC revealed moderate expression of OPN in a small population of infiltrating inflammatory cells, whereas the increased OPN expression was not prominent in the gastric epithelium (Fig. 4Bb). Double immunofluorescence (IF) staining for OPN and F4/80 showed that inflammatory cells expressing OPN were mainly macrophages (Fig. 4C). These results indicate that source of gastric OPN expression at early stage *H. pylori* infection is infiltrating macrophages rather than gastric epithelium. However, there was a marked up-regulation of gastric OPN in WT mice at 16 weeks after *H. pylori* infection compared to 8 week on WB (Fig. 4A). Immunohistochemically, in contrast to 8 weeks response, the major source of OPN expression is gastric glandular epithelial cells rather than infiltrating macrophages (Fig. 4Bb). These results demonstrate a time-dependent increase in gastric OPN expression according to disease progression and implicate OPN in gastric epithelial

responses to the infection

We performed *in vitro* studies to confirm that the increases in OPN expression in response to *H. pylori* infection were attributable to both gastric epithelial cells and macrophages. WB showed that OPN expression did not change in AGS cells at 24 hours after co-culture with *H. pylori* (20 MOI; Fig. 4D). On the other hand, OPN expression was mildly up-regulated in Di-THP-1 at 24 hours after *H. pylori* co-culture (Fig. 4D). By contrast, over 2-fold increase of OPN expression was observed in NCC-S1M cells but not in RAW 264.7 cells, at 24 hours after *H. pylori* co-culture (Fig. 4D). Peritoneal macrophages isolated from WT mice showed over 2-fold increase of OPN expression after *H. pylori* exposure (Fig. 4D). These results suggest that increased expression of OPN in the *H. pylori*-infected stomach originate from both epithelial cells and macrophages in a context-dependent manner.

A

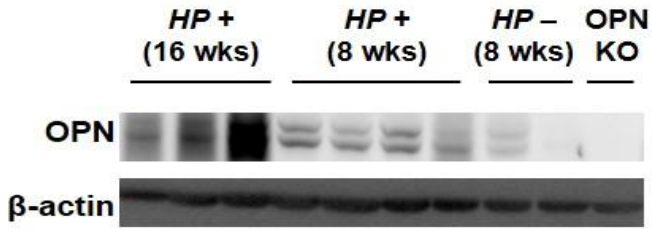

B

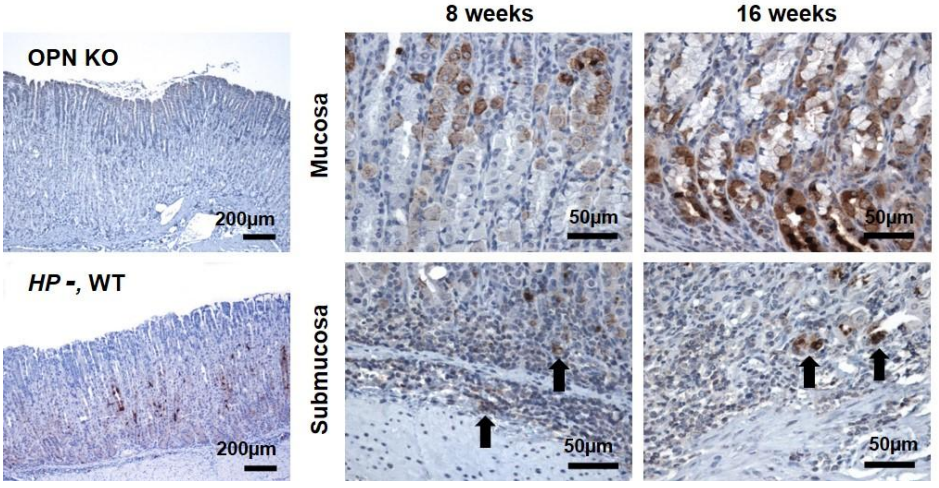

C

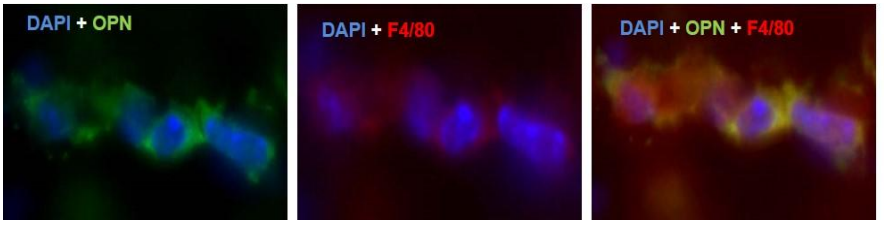

D

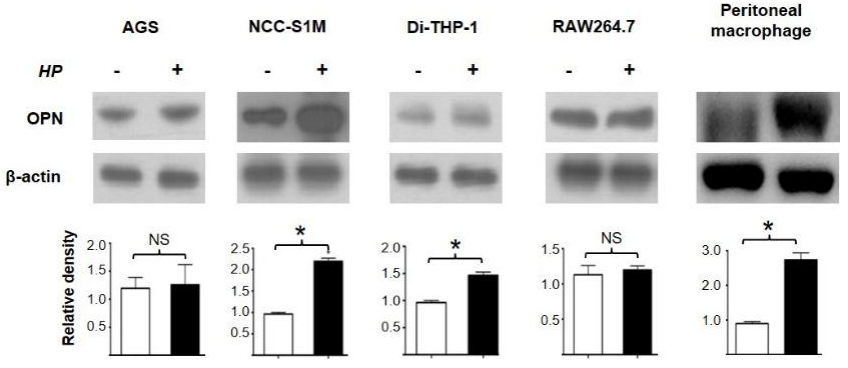

Fig 4. OPN expression in *H. pylori*–infected stomach tissues of WT mice and various cell lines. (A) Western blot analysis for OPN of *H. pylori*–infected or non–infected WT mice. (B) Representative immunohistochemistry for OPN in *H. pylori*–infected WT stomach tissues. (a) OPN KO stomach tissue and non–infected WT stomach tissue. (b) OPN expression was elevated in gastric epithelial cells of mucosal layer at 16 weeks after *H. pylori*–infection compared to 8 weeks. Inflammatory cells in submucosal layer frequently showed OPN immunoreactivity (arrow) during *H. pylori* infection. (C) Double immunofluorescence for F4/80 and OPN. OPN was expressed in F4/80 positive cells. Original magnification x 1000. (D) OPN expression in various cell lines and peritoneal macrophages at 24 hours after *H. pylori* exposure. $*P < 0.05$.

OPN deficiency down-regulates major pro-inflammatory cytokines induced by H. pylori infection

We investigated whether OPN deficiency influenced the expression of cytokines in *H. pylori*-infected stomach tissues. *QRT-PCR* analysis revealed decreased mRNA expression of IL-1β, TNF-α, and IFN-γ in OPN KO mice compared to WT mice at 8 weeks after *H. pylori* infection (Fig. 6A). By 16 weeks after *H. pylori* infection, although IL-1β and TNF-α mRNA levels were not significantly different between WT and OPN KO mice, reduced expression of IFN-γ was observed in OPN KO mice compared with WT mice (Fig. 6A).

We further performed *in vitro* studies to investigate which types of cells might account for the altered expression of these cytokines in *H. pylori*-infected OPN KO mice. Both OPN KD AGS and OPN KD NCC-S1M cells co-cultured with *H. pylori* showed reduced IL-1β and TNF-α mRNA expression compared to shRNA-control cells (Figs. 6B and C). Like *H. pylori*-stimulated OPN KD gastric cancer cells, OPN KD Di-THP-1 cells and OPN KO peritoneal macrophages showed reduced expression of these cytokines compared with shRNA-control Di-THP-1 cells and WT peritoneal macrophages, respectively, following the co-cultured with *H. pylori* (Fig. 6D and E). Taken together, these observations indicate that the altered expression of these cytokines in response to *H. pylori* infection might be attributable to a change in the

production of these cytokines in both gastric epithelial cells and infiltrating macrophages.

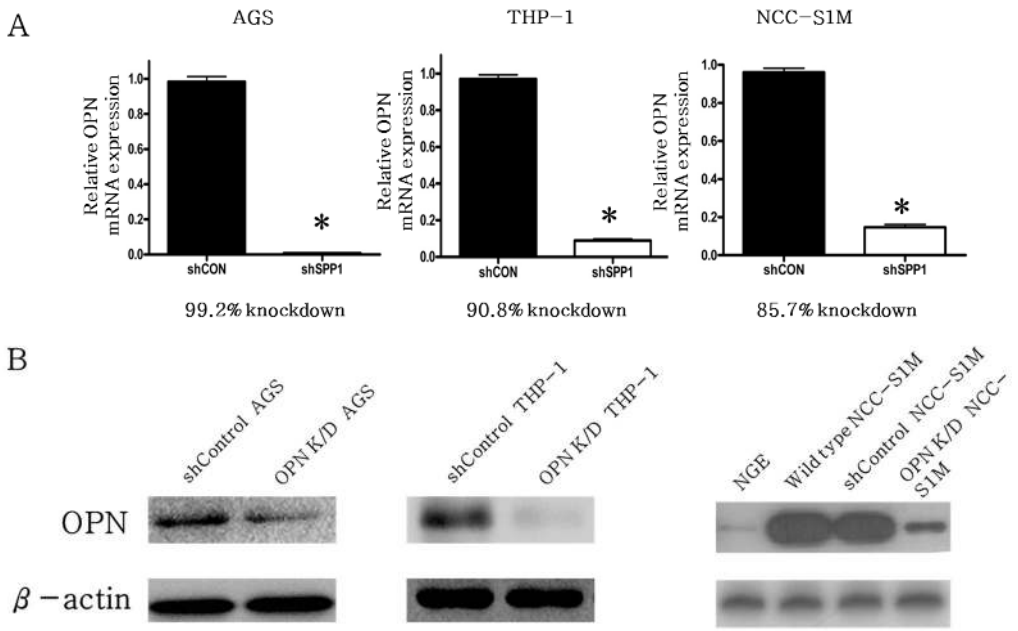

Fig 5. OPN knockdown (KD) efficiency in AGS, THP-1 and NCC-S1M cells. (A) Relative OPN mRNA expression in AGS, THP-1 and NCC-S1M cells. Results are presented as means±SEMs (n=3). (B) Representative blots of OPN protein expression in control and OPN KD cells. $*P < 0.05$.

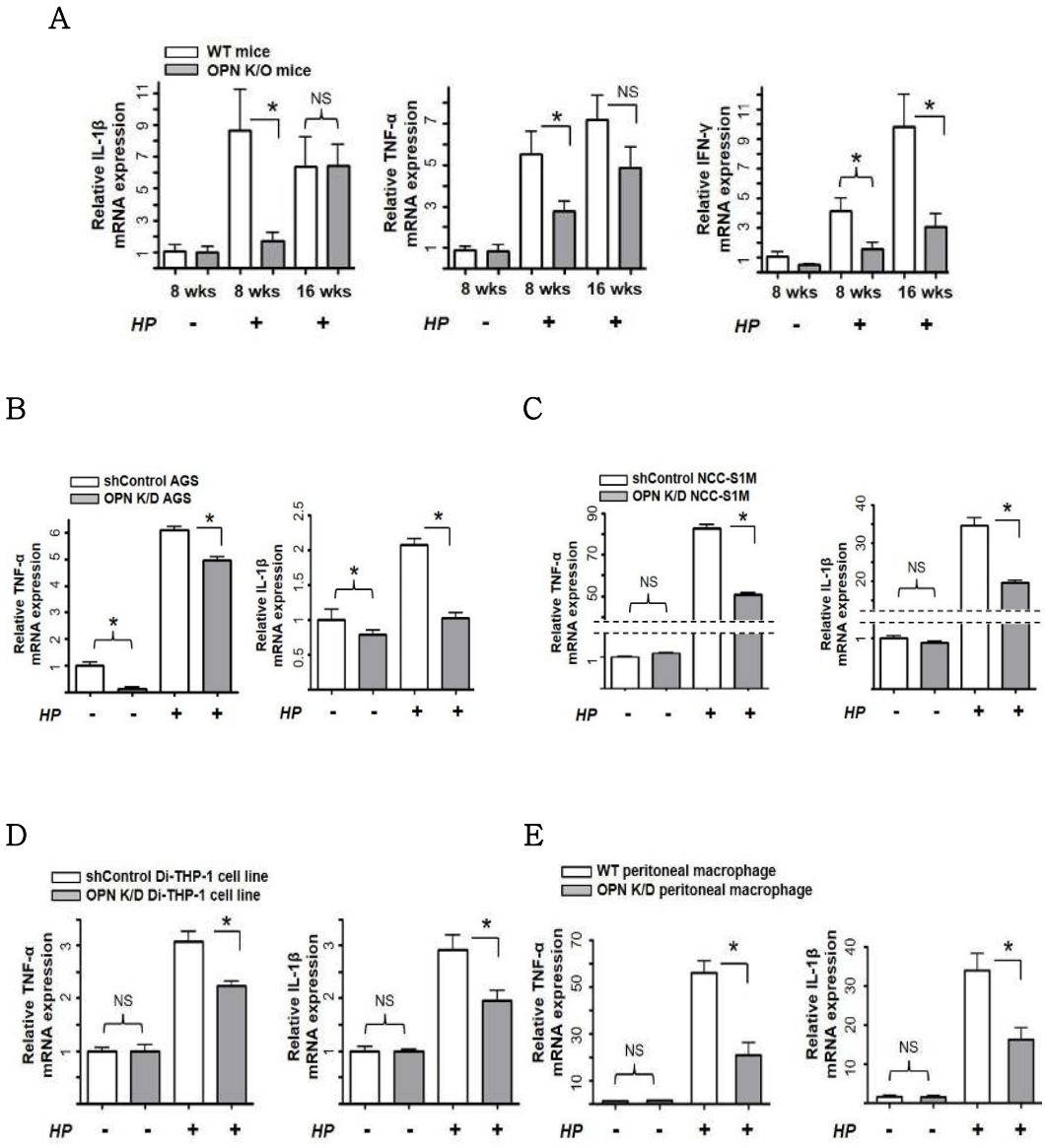

Fig 6. Relative mRNA expression levels of pro-inflammatory cytokines in *H. pylori*-infected OPN KO mice and OPN KD cell lines. (A) Expression level of IL-1ß, TNF-α and IFN-γ in stomach tissues of *H. pylori*-infected WT and OPN KO mice. Results are presented as means±SEMs (n=6). (B-D) Effect of OPN knockdown or knockout on TNF-α and IL-1ß expression in (B) AGS cells, (C) NCC-S1M cells, (D) Di-THP-1 cells, and (E) peritoneal macrophages at 24 hours after *H. pylori* exposure. $*P < 0.05$.

OPN deficiency suppresses the migration of macrophages in response to H. pylori infection

Because *H. pylori*-infected OPN KO mice showed a significant reduction in macrophage infiltration, we investigated the role of OPN in macrophage migration in response to *H. pylori* infection using a modified Boyden chamber. Peritoneal macrophages from OPN KO mice showed reduced migration towards media containing *H. pylori* infiltrates compared to those from WT mice (Fig. 7A). OPN KD THP-1 cells also showed reduced migratory activity towards media containing *H. pylori* infiltrates compared to shRNA-control THP-1 cells (Fig. 7B). In addition, we tested the effects of altered cytokine expression in *H. pylori*-infected OPN KD AGS cells (Fig. 6B) on the migration of inflammatory cells. CM harvested from *H. pylori*-co-cultured OPN KD AGS and OPN KD NCC-S1M cells decreased the migratory behavior of THP-1 and RAW 264.7 cells compared with CM from *H. pylori*-co-cultured shRNA-control cells (Figs. 7C and D). These results show that the reduced infiltration of macrophages in the stomach of *H. pylori*-infected OPN KO mice is due to reduction in the migratory activity of macrophages as well as decreased production by gastric epithelial cells of soluble factors that attract macrophages.

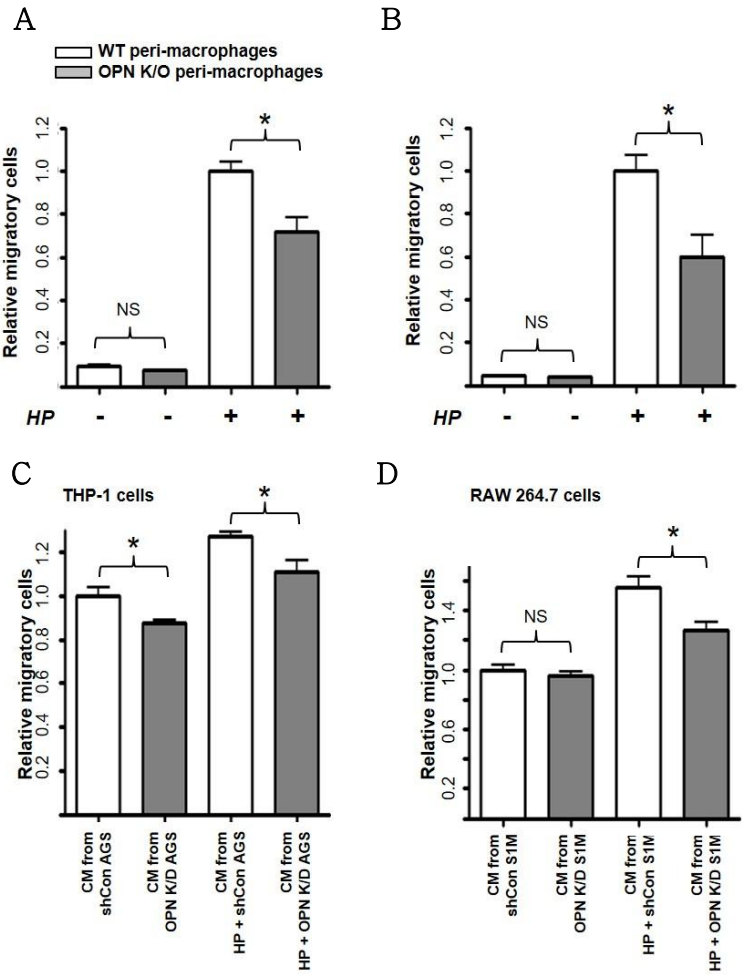

Fig 7. Effect of OPN on migratory activity of inflammatory cells in response to *H. pylori*. Migratory activities of (A) OPN KO mouse peritoneal macrophages and (B) OPN KD THP-1 cells toward *H. pylori* infiltrates-containing media. Migratory activities of (C) THP-1 cells and (D) RAW 264.7 cells toward CMs harvested from OPN KD AGS cells or S1M cells co-cultured with *H. pylori*. $*P < 0.05$

OPN deficiency inhibits the proliferation of gastric epithelial cells in response to H. pylori infection

H. pylori infection can modulate gastric epithelial cell proliferation and apoptosis contributing the development of gastric cancer (Fan, Kelleher et al. 1996, de Freitas, Urbano et al. 2004). Based on the low degree of mucosal hyperplasia in OPN KO mice compared with WT mice after *H. pylori* infection (Fig. 2), we performed IHC for Ki-67 on stomach tissues of *H. pylori*-infected mice to investigate the impact of the lack of OPN on gastric epithelial proliferation in response to *H. pylori* infection. We found out that the number of Ki-67 positive gastric epithelial cells in *H. pylori*-infected WT mice at 8 and 16 weeks after *H. pylori* infection was significantly higher than that of uninfected WT mice (Fig. 8A). Notably, *H. pylori*-infected OPN KO mice showed lower numbers of proliferative gastric epithelial cells than *H. pylori*-infected WT mice at both 8 and 16 weeks after *H. pylori* infection (Fig. 8A). In addition, IHC for PNCA, a specific marker of cell division, also demonstrated that *H. pylori*-infected OPN KO mice showed a lower number of PCNA-positive gastric epithelial cells than WT mice at 8 weeks after *H. pylori* infection (Fig. 8B). These results indicate that the lack of OPN led to decreased proliferation of gastric epithelial cells in response to *H. pylori* infection.

Similar results were obtained *in vitro*, where OPN KD AGS cells showed reduced cell viability compared to shRNA-control AGS cells at 24 hours after *H. pylori* co-culture (Fig. 8C). This result might be

attributable to suppression of the G1/S cell-cycle checkpoint in OPN KD AGS cells (Fig. 8C), which was accompanied by increased induction of cyclin-dependent kinase inhibitor p21 and decreased expression of Cyclin E (Fig. 8C). OPN KD S1M cells also exhibited reduced cell viability compared to shRNA-control cells after *H. pylori* co-culture for 24 hours, showing results similar to those of the cell cycle analysis and molecular changes observed in OPN KD AGS cells (Fig. 8D). Thus, these results demonstrate that OPN is involved in cycle regulation of gastric epithelial cells by controlling the G1/S transition during *H. pylori* infection.

We investigated the effects of OPN on IL-1β and TNF-α-induced gastric epithelial proliferation, because IL-1β and TNF-α were important mediators that could be responsible for gastric epithelial changes in response to *H. pylori* infection(Houghton, Macera-Bloch et al. 2000, Luo, Shin et al. 2005, Shigematsu, Niwa et al. 2013). OPN KD AGS and NCC-S1M cells showed decreased cell proliferation compared with shRNA control cells following exposure to IL-1β and TNF-α for 24 hours (Fig. 9A). In addition, compared to shRNA-control cells, OPN KD AGS and S1M cells showed an attenuation of the increase in the mitogen-activated protein kinase (MAPK)-related molecule, phosphorylated Akt and Erk following exposure to IL-1β and TNF-α treatment (Fig. 9B-E). The induction of MAPK-related molecules induced by *H. pylori* infection also decreased in OPN KO mice than in WT

mice (Fig. 9F).

A

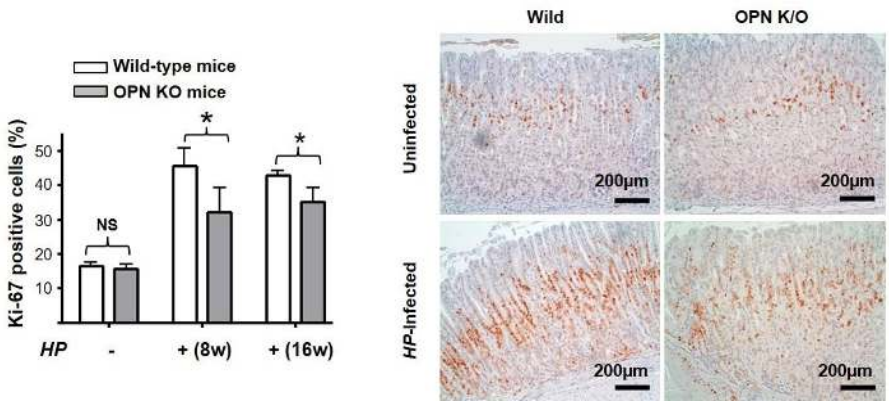

B

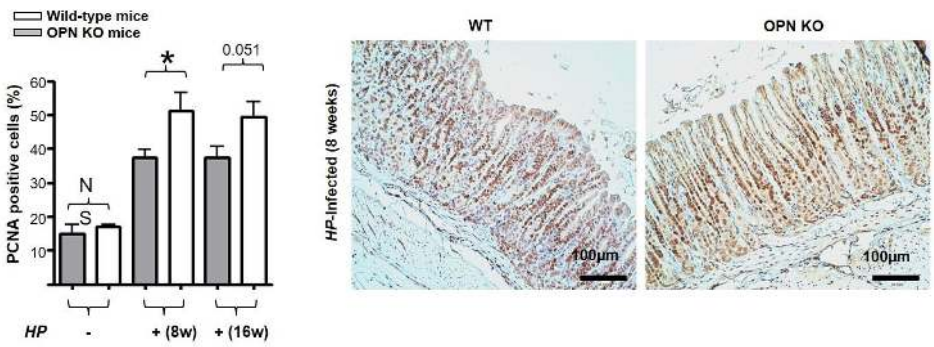

C

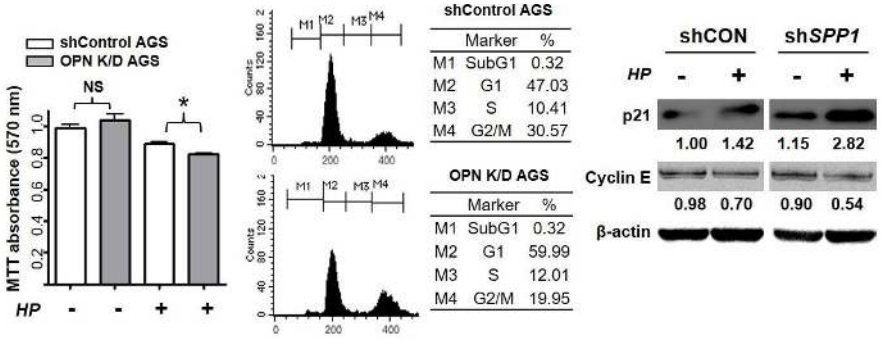

D

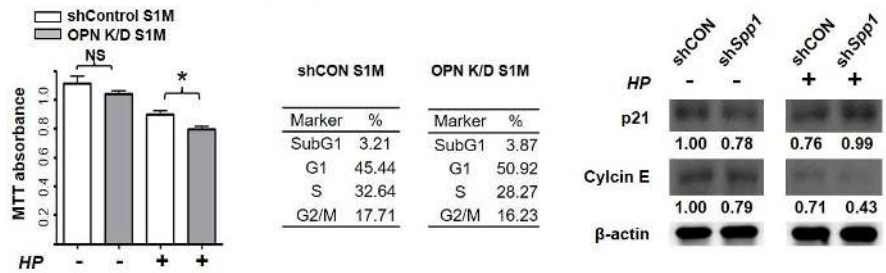

Fig 8. Effect of OPN on gastric epithelial proliferation during *H. pylori* infection. (A) Quantitation of Ki-67 positive cells in stomach tissues of WT and OPN KO mice. Results are presented as means±SEMs (n=10). (B) Representative images of immunohistochemistry for Ki-67 in stomach tissues at 8 weeks after infection. (C) Effect of OPN knockdown in AGS cells on cell viability and cell cycle after *H. pylori* co-culture. In addition, Western blotting for cell cycle regulatory proteins in *H. pylori*-infected OPN KD AGS cells. (D) Effect of OPN knockdown in S1M cells on cell viability, cell cycle, and cell cycle regulatory proteins after *H. pylori* co-culture. $*P < 0.05$.

A

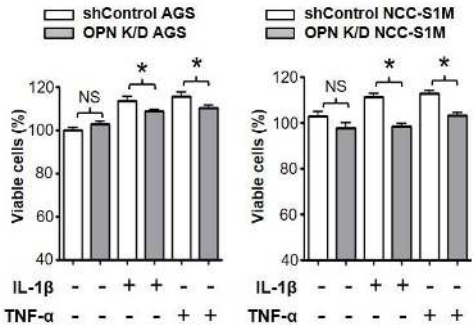

B

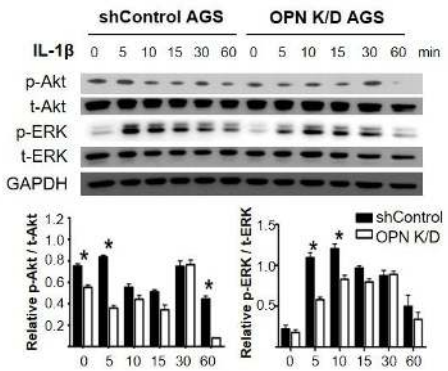

C

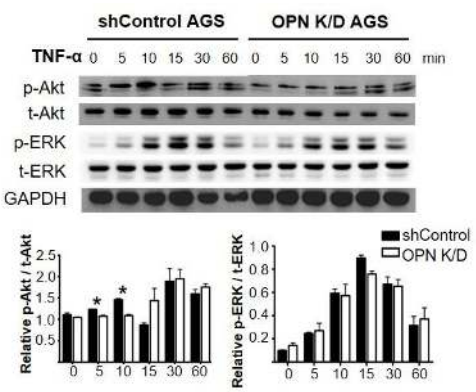

D

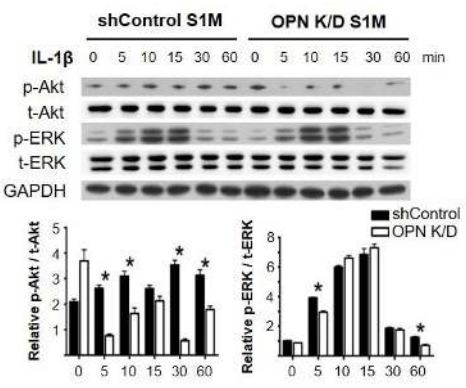

E

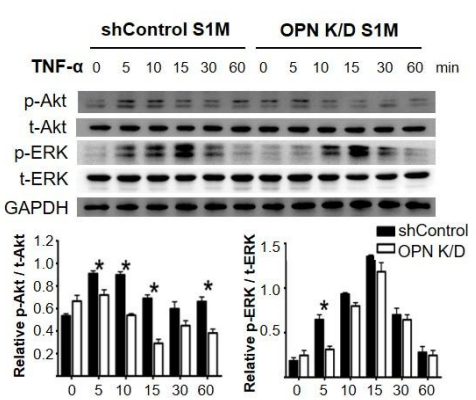

F

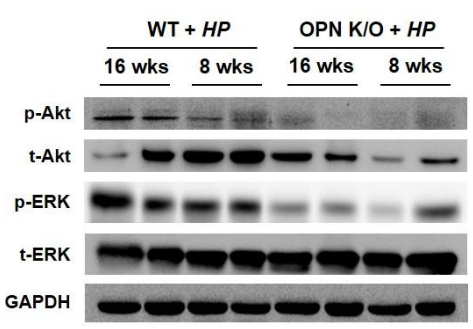

Fig 9. Effect of OPN on the activation of MAPK pathway in gastric cancer cells and mouse gastric tissues during *H. pylori* infection. (A) MTT assays for cell viability at 24 hours after IL-1β or TNF-α treatment in OPN KD gastric cancer cells. MAPK-related protein expression in OPN KD AGS cells treated with (B) IL-1β and (C) TNF-α at the respective time points. Expression levels of MAPK-related proteins in OPN KD S1M cell treated with (D) IL-1β and (E) TNF-α. (F) MAPK-related protein expression in OPN KO mouse gastric tissues infected with *H. pylori.* Results are presented as means±SEMs (n=2). $*P < 0.05$ *versus* shControl-transfected cell. p-Akt, phosphorylated Akt; t-Akt, total Akt; p-ERK, phosphorylated ERK; t-ERK, total ERK.

Discussion

In this study, we investigated the roles and mechanism of OPN in *H. pylori*–induced gastritis in mice. The degree of inflammation of OPN KO mice was weak compared to that of WT mice, with a significant reduction in infiltrating macrophages and the expression of IL-1β, TNF-α, and IFN-γ. Similar with these results, mRNA expression of these pro-inflammatory cytokines was reduced in OPN KD gastric cancer cell lines exposed to *H. pylori*, and the CM from these cells had a decreased capacity on the migration of monocytic and macrophage-like cell lines. Furthermore, *H. pylori*–infected OPN KO mice showed a lower number of proliferative gastric epithelial cells than WT mice, in association with a reduction in MAPK pathway activation. OPN KD gastric cancer cell lines also showed the suppression of the G1/S cell-cycle after *H. pylori* co-culture and reduced MAPK activation after IL-1β and TNF-α treatment. To our knowledge, this is the first study to explore the functional roles of OPN during *H. pylori* infection.

The immune response of the host during *H. pylori* infection is considered to be a key event in the development of gastric cancer. It has consistently been reported that gastric mucosal levels of the pro-inflammatory cytokines IL-1β, IL-6, IL-8, IFN-γ, and TNF-α increased in *H. pylori*–infected individuals (Rahn, Redline et al. 2004, Yamamoto, Kita et al. 2004). Notably, there is considerable evidence that

elevated expression of IL−1β, IFN−γ, and TNF−α are associated with chronic gastritis and gastric cancer development following *H. pylori* infection (Yamamoto, Kita et al. 2004, Chan, Chu et al. 2007, Santos, Ladeira et al. 2012, Syu, El−Zaatari et al. 2012, Shigematsu, Niwa et al. 2013). Our study revealed that OPN expression was elevated in response to *H. pylori* infection, and OPN depletion decreased production of these cytokines in both gastric epithelial cells and macrophages during *H. pylori* infection. These results suggest that OPN is an important mediator of pro−inflammatory cytokine production during *H. pylori* infection. Previous studies have focused on the role of OPN in inflammatory cells and have reported that OPN induces the expression of these cytokines in inflammatory cells, such as macrophages, dendritic cells, and T cells (Lund, Giachelli et al. 2009, Uede 2011). However, the effect of OPN on epithelial cell in the development of inflammatory conditions has not yet been studied. For the first time, we demonstrate the involvement of OPN in the production of pro−inflammatory cytokines by gastric epithelial cells in the immune response against *H. pylori* in addition to inflammatory cells.

Macrophage infiltration is a characteristic feature of *H. pylori* infection that may promote progression or resolution of chronic gastritis following *H. pylori* infection (Whitney, Emory et al. 2000). Indeed, we found that the number of infiltrated macrophages was positively correlated with the grade of gastritis in *H. pylori*−infected WT mice (*data not shown*).

Importantly, OPN KO mice showed a significant reduction in the number of infiltrating macrophages following *H. pylori* infection compared with WT mice. This reduction could result from the down-regulated expression of chemoattractants, such as IL-1β, IFN-γ and TNF-α, in OPN-deficient gastric epithelial and inflammatory cells as well as the decrease in the migratory ability of monocytes and macrophages lacking OPN. The demonstration that CM from *H. pylori*-infected OPN KD gastric cancer cell lines had a reduced ability to recruit monocytic and macrophage-like cells provides support for this hypothesis.

H. pylori infection enhances the proliferative activity of gastric epithelial cells (Brenes, Ruiz et al. 1993, Fan, Kelleher et al. 1996, Jones, Shannon et al. 1997, Xia, Lam et al. 2005). The gastric epithelial cell proliferation results from both the direct effects of *H. pylori* pathogenic factor, such as CagA (Rokkas, Ladas et al. 1999), and the indirect effects of inflammatory environment enriched with cytokines, such as TNF-α and IL-1β, induced by *H. pylori* infection (Houghton, Macera-Bloch et al. 2000, Beales 2002), which could activate the MAPK cascades. As expected, *H. pylori*-infected WT mice showed elevated gastric epithelial proliferation in association with enhanced MAPK pathway activation. In contrast, epithelial proliferation and MAPK pathway activation induced by *H. pylori* infection was suppressed in OPN KO mice, suggesting that OPN is associated with MAPK-mediated epithelial proliferative activity in response to *H. pylori* infection. This conclusion is supported by the

demonstration that *H. pylori*-stimulated OPN KD gastric cancer cell lines showed the suppression of the G1/S cell-cycle transition, of which the MAPK pathway is a master regulator (Meloche and Pouyssegur 2007). In addition to gastric epithelial proliferation via a direct interaction between *H. pylori* and gastric epithelial cells, our results also showed that IL-1β and TNF-α increased the proliferation of gastric cancer cells, in association with up-regulated expression of MAPK pathway-related proteins. These effects were attenuated in OPN KD gastric cancer cells. Taken together, our findings suggest that OPN depletion suppresses *H. pylori*-induced gastric epithelial proliferation via suppression of the MAPK pathway.

Our study definitely proved OPN deficiency suppressed *H. pylori*-induced gastritis and gastric epithelial proliferation, and we focused on the roles of OPN in gastric epithelial cells and macrophages during *H. pylori* infection. Although OPN is not essential for normal mouse development and physiology (Rittling, Matsumoto et al. 1998), it is a multifunctional protein which is upregulated in various types of cells in variety of diseases, where it mediates diverse cellular functions including regulating inflammatory response of macrophages, T-cells, and dendritic cells (Lund, Giachelli et al. 2009). However, OPN-KO mice used in this study was deficient in OPN expression of whole tissues and cells. In this respect, it is need to consider the possibilities that OPN in other stromal cells, such as neutrophils, dendritic cells and lymphocytes, was involved

in *H. pylori*–induced gastritis. Actually, as shown in Fig. 1D, the numbers of infiltrating T cells and neutrophils in *H. pylori*–infected OPN KO mice were significantly decreased compared to those of *H. pylori*–infected WT mice. Also, OPN could be involved in monocytes migration and differentiation into macrophages during infection, because OPN is strongly induced when human monocytic cell lines were treated with PMA (Rittling 2011). In addition, other activated or inactivated pathways in OPN KO mice during mouse development might be concerned in immunosuppressive effect to *H. pylori*–induced gastritis. To specify the role of OPN and clearly elucidate which types of cells play important roles in *H. pylori*–induced gastritis, further studies using cell– or tissue–specific OPN knockout mice may be helpful.

In summary, the present study has demonstrated that OPN depletion decreased inflammation and gastric epithelial proliferation in *H. pylori*–infected mice, establishing the importance of OPN as a mediator of the gastritis induced by *H. pylori* infection. In addition, our results suggest that targeting OPN might be an appropriate therapeutic strategy for limiting inflammation and mucosal pathology during *H. pylori* infection.

CHAPTER II.

ABLATION OF OSTEOPONTIN SUPPRESSES *N*-METHYL-*N*-NITROSOUREA AND *HELICOBACTER pylori*-INDUCED GASTRIC CANCER DEVELOPMENT IN MICE

Abstract

Several clinical studies have reported increased expression of osteopontin (OPN) in various types of human cancer, including gastric cancer. However, the precise mechanisms underlying tumor development remain unclear. In the present study, we investigated the pathogenic roles of OPN in *Helicobacter pylori*–induced gastric cancer development. Wild-type (WT) and OPN knockout (KO) mice were treated with *N*-methyl-*N*-nitrosourea (MNU) and infected with *H. pylori*. Mice were sacrificed 50 weeks after treatment, and stomach tissues were assessed by histopathological examination, immunohistochemistry, quantitative real-time RT-PCR and Western blotting. To clarify the carcinogenic effects of OPN, we also conducted an *in vitro* study using AGS human gastric cancer cell line and THP-1 human monocytic cell line. The overall incidence of gastric tumors was significantly decreased in OPN KO mice compared to WT mice. Apoptotic cell death was significantly enhanced in OPN KO mice, and was accompanied by upregulation of signal transducer and activator of transcription 1 (STAT1) and inducible nitric oxide synthase (iNOS). *In vitro* study, OPN suppression also caused STAT1 upregulation and iNOS overexpression in AGS and THP-1 cells, which resulted in apoptosis of AGS cells. In addition, a negative correlation was clearly identified between expression of OPN and iNOS in human gastric cancer tissues. Our data demonstrate that loss of OPN decreases *H. pylori*–induced gastric carcinogenesis by suppressing

proinflammatory immune response and augmenting STAT1 and iNOS-mediated apoptosis of gastric epithelial cells. An important implication of these findings is that OPN actually contributes to the development of gastric cancer.

Introduction

Gastric cancer is one of the most prevalent malignant cancers in the world, particularly in Eastern Asia, including Korea and Japan (Ferlay, Shin et al. 2013, Jung, Won et al. 2014). Although the etiology of gastric cancer is thought to be multifactorial, *Helicobacter pylori* infection has been recognized as a major risk factor. *H. pylori* infection induces chronic gastric inflammation, which can progress via chronic atrophic gastritis, intestinal metaplasia and dysplasia towards gastric cancer (Parsonnet, Friedman et al. 1991, Correa 1992, Eslick, Lim et al. 1999). Host responses that mediate *H pylori*–associated gastric cancer development include disruption of the balance between gastric epithelial cell proliferation and apoptosis. Increased compensatory proliferation that is not balanced by a rise in apoptosis during advanced stage of infection may increase the risk of gastric carcinogenesis (Murakami, Fujioka et al. 1997, Osman, Bloom et al. 2013).

Nitric oxide (NO) has diverse functions in many pathophysiological conditions including vasodilation, cell migration, immune response and apoptosis (Muntane and la Mata 2010). Numerous reports have provided convincing evidences that NO is associated with gastric cancer. Increased inducible nitric oxide synthase (iNOS), a key enzyme to produce NO, has been observed in patients with chronic gastritis and gastric cancer, and iNOS expression in the gastric mucosa is significantly higher in *H. pylori*–positive gastric cancer patients than in *H. pylori*–

negative patients (Mannick, Bravo et al. 1996, Rieder, Hofmann et al. 2003). However, the precise role of NO in gastric carcinogenesis is still a matter of controversy, with both tumor-promoting and -inhibitory effects ascribed to NO. These contradicting effects are attributable to concentration-dependent NO activity: low concentrations of NO activate oncogenic pathways, cell proliferation and angiogenesis, whereas high concentrations of NO can cause cytostasis and apoptosis (Edwards, Cendan et al. 1996, Ambs and Glynn 2011).

Osteopontin (OPN) is a multifunctional secreted glyco-phosphoprotein that is expressed in various tissues and plays important roles in a wide range of biological processes including inflammation (Ashka, Weber et al. 2000, Cho and Kim 2009). During the past decade, emerging evidences have refined the significance of OPN as a candidate biomarker and even possible target for cancer therapy (Ahmed, Behera et al. 2011). OPN binds to receptors, including integrins and CD44, which potentially allow it to stimulate various signaling pathways that ultimately lead to tumor progression (Ue, Yokozaki et al. 1998, Lee, Wang et al. 2007). Several studies have indicated that OPN activates phosphoinositide 3-kinase (PI3K)/Akt signaling through the $\alpha v \beta 3$ integrin-mediated pathway and promotes cell survival and migration (Song, Ouyang et al. 2009, Luo, Ruhland et al. 2011). A few studies also have explored the effects of OPN on iNOS expression using *in vivo* and *in vitro* models. These studies showed that iNOS expression in epithelial tumor cells or macrophages is

negatively regulated by OPN, thereby decreasing the extent of NO production (Gao, Guo et al. 2007, Patouraux, Rousseau et al. 2014). Because upregulated or downregulated NO production affects tumor cell survival and proliferation, it is conceivable that the role of OPN in tumor cell biology partially involves modulation of iNOS expression.

Previous studies have shown increased expression of OPN in human gastric cancer, and demonstrated that the level of OPN is correlated with more advanced tumor stages and poor prognosis (Dai, Bao et al. 2007, Higashiyama, Ito et al. 2007). Elevated expression of OPN and its receptor, CD44v9, have been shown to correlate with the degree of lymphatic vessel invasion and lymph node metastasis in gastric cancer (Kim, Bae et al. 2009). However, the roles of OPN in human gastric cancer and the precise mechanism underlying its contribution to tumor development remain unclear. In the present study, we mechanistically addressed the role of OPN during gastric carcinogenesis *in vivo* using an *H pylori*–induced mouse gastric tumor model and *in vitro* using human cell lines. We found out that OPN deficiency suppresses the development and progression of *H. pylori*–induced gastric cancer by attenuating chronic gastritis and protecting tumor cells from iNOS mediated–apoptosis. Based on these findings, we further found OPN was negatively correlated with iNOS expression, and OPN expression had a positive correlation with tumor progression in human gastric cancer using tissue microarray.

Materials and Methods

Chemical and bacteria

N-methyl-*N*-nitrosourea (MNU; Sigma Chemical Co., St. Louis, MO) solutions were prepared twice a week by dissolving 200 mg/L MNU in distilled water. Mouse-adapted *H. pylori* Sydney strain 1 was inoculated onto Brain Heart Infusion agar plates (Difco, Detroit, MI) containing 10% sheep blood. The plates were kept at 37 ° C under microaerobic conditions produced by GasPak jars (Difco) and Campy-Paks (Becton Dickinson, Cockeysville, MD). After 24 hours of fasting, mice were orally administered a 0.1 mL suspension of H pylori containing 1×10^9 colony-forming units/mL.

Induction of gastric tumor in mouse

Mouse gastric tumor was induced with MNU and *H. pylori* as described previously (Han, Kim et al. 2002, Nam, Oh et al. 2004). Five week-old male C57BL/6-Spp1^{tm1Blh} (OPN$^{-/-}$) (OPN KO) mice, purchased from Jackson Laboratory (Bar Harbor, ME), and wild-type (WT) were divided into four groups. WT (n=32) and OPN KO (n=27) mice were administered drinking water containing MNU (200mg/L) biweekly for 10 weeks. One week after termination of MNU treatment, mice were inoculated with *H. pylori* three times on alternate days. Mice in each control group (n=10) were given a standard pellet chow diet. All mice were sacrificed 50 weeks after the first administration of MNU solutions.

In vivo study was approved by the Institutional Animal Care and Use committee of Seoul National University (approval number: SNU-100729-1), and all experiments were carried out in compliance with the Guide for Care and Use of Laboratory Animals, Institute for Laboratory Animal Research (Washington, DC).

Analysis of the gastric colonization of mice by H. pylori

To identify *H. pylori* infection, some of stomach tissues were used to carry out the rapid urease test when all mice were sacrificed. Furthermore, the quantification of *H.pylori* was performed through DNA extracted from stomach tissues. Protocol for quantification of *H. pylori* was described previously (Mikula, Dzwonek et al. 2003). Total DNA was extracted from mouse stomachs using QIAamp DNA mini kit (Qiagen) according to the manufacturer's instructions. Ten nanograms of each DNA sample were amplified using specific primer used to detect the 16S rDNA gene of *H. pylori* SS1 with TaqMan probe, and the quantity of target gene was normalized using β-actin as a housekeeping gene.

Gross and histopathological examination

Mice were sacrificed 24 hours after starvation, and stomachs were opened along the great curvature. The number and sizes of nodules in each stomach were measured, and then half the stomach was fixed in neutral-buffered 10% formalin. After 24 hours of fixation, each stomach

was cut into three strips, processed by routine method, embedded in paraffin, and stained with hematoxylin and eosin (H&E) for diagnosis (Leininger, Jokinen et al. 1994). The other half of the stomach was stored at −70° C freezer until analysis. The grades of mucosal inflammation, various preneoplastic changes, as well as tumor incidence and type were also graded as previously described (Rogers, Taylor et al. 2005).

Immunohistochemical staining for Ki−67, iNOS, OPN and F4/80, and TUNEL assay

For immunohistochemical staining, serial sections of paraffin−embedded stomach tissues were mounted on silicon−coated slides, deparaffinized, rehydrated, and then antigen retrieval was carried out by heating at 100° C for 20 minutes in 0.01M citrate buffer (pH 6.0). Endogenous peroxidase activity and non−specific protein binding were quenched using hydrogen peroxide and serum−free protein block (DakoCytomation, Glostrup, Denmark). The slides were incubated with one of the following antibodies at room temperature for 15 minutes: anti−iNOS (1:500; Abcam, Cambridge, MA); anti−OPN (1:100; R&D Systems, Minneapolis, MN); anti−Ki−67 (1:200; Abcam), used to measure proliferative activity of gastric epithelial cells; and anti−F4/80 (1:200; Abcam), used to quantify macrophage infiltration. After incubation with each primary antibody, slides were stained using the

indirect labeling streptavidin avidin-biotin technique using DAB as a substrate. The extent of each staining was analyzed using an H-scoring system, where scores are calculated based on the intensity and number of positive cells according to equation, Score= (3 × % intensely positive) + (2 × % moderately positive) + (1 × % weakly positive). A total score and/or regional score were assigned to each animal. Apoptosis of gastric epithelial cells was examined using the terminal deoxynucleotidyl transferase dUTP nick end labeling (TUNEL) assay employing the Fluorecein FragEL DNA Fragmentation Detection kit (Calbiochem, Darmstadt, Germany) according to the manufacturer's instructions

Generation of OPN knock down cell lines

Human gastric cancer cell line AGS, derived from fragments of a human gastric adenocarcinoma, and human monocyte cell line THP-1, derived from human infant patient with acute monocytic leukemia, were purchased from American Type Culture Collection (ATCC; Manassas, VA). Both cell lines, certified and characterized by ATCC, were cultured in RPMI-1640 medium (Gibco, Grand Island, NY) containing 10 % fetal bovine serum (Gibco), 1% penicillin and streptomycin (Invitrogen Biotechnology, Grand Island, NY); mercaptoethanol was also included as a supplement in THP-1 cell cultures. To stably knockdown spp1 gene of AGS and THP-1 cell lines, lentiviral vector-mediated short-hairpin RNA (shRNA) construct targeting the human SPP1 gene (Sigma-Aldrich,

St. Louis, MO) with pLKO.1-puro eGFP control vector (Sigma) were purchased, and the target construct was generated from accession number NM_000582. Lentivirus was created by co-transfecting shRNA-expressing vector and packaging vectors (Addgene) into 293T cell through lipofectamine 2000 (Invitrogen Biotechnology). Virus-containing supernatant were harvested 48 hours after transfection, filtered using a 0.45 μm filter, titered and used for viral transduction with 10 μg/mL polybrene. Cells were treated by 2 μg/ml puromycin at 48 hours after viral transduction and selected for 3 days. Knockdown efficiency was determined by quantitative real-time RT-PCR and Western blotting.

Recombinant human OPN and anti-OPN antibody treatment

After seeded on 6-well plates at 1×10^6 for 24 hours, control (Con) or OPN knockdown (KD) AGS cells were treated with various concentrations (0, 0.1, 0.5, 1.0 and 5.0 μg/ml) of recombinant human OPN (rhOPN; R&D Systems) for 15 minutes, and OPN KD AGS cells were incubated with 1.0 μg/ml of rhOPN for 0, 5, 15, 30 and 60 minutes. Furthermore, various concentrations (0, 0.1, 0.2, 0.5 and 1.0 μg/ml) of anti-OPN antibody (R&D Systems) were used to block secreted OPN in control AGS cells for 6 hours. Similarly, control THP-1 cells seeded on 6-well plates with 40 nM phorbol 12-myristate 13-acetate (PMA) were incubated with same concentrations of anti-OPN antibody for 6 hours. All cells were harvested for western blotting after incubation with rhOPN

or anti-OPN antibody.

AGS co-cultured with THP-1 or H. pylori

For co-culture experiments, control (Con) or OPN knockdown (KD) AGS cells were seeded on 6-well plates at 1×10^6 for 24 hours. Control or OPN KD THP-1 cells were seeded on 6-well Trans-well inserts (Corning, Cambridge, MA) at 1×10^6 with 40 nM PMA for 12 hours, and then incubated with or without 100 ng/mL of LPS. After incubating each cell separately, AGS cells were co-cultured with THP-1 cells or with 10 multiplicity of infection (MOI) of *H. pylori* for 24 hours, yielding the following experimental groups: group A: single-cultured cells (A1, Con AGS cells and Con THP-1 cells; A2, OPN KD AGS and OPN KD THP-1 cells); group B: AGS cells co-cultured with *H. pylori* (B1, Con AGS cells; B2, OPN KD AGS cells); group C: AGS cells co-cultured with unstimulated THP-1 cell (C1, Con AGS cells and Con THP-1 cells; C2, OPN KD AGS and OPN KD THP-1 cells); and group D: AGS cells co-cultured with LPS-stimulated THP-1 cell (D1, Con AGS and Con THP-1 cells; D2, OPN KD AGS and OPN KD THP-1 cells) (Fig. 7A). Co-cultured AGS and THP-1 cells were harvested separately for Western blotting.

RNA extraction and quantitative real-time RT-PCR

Total RNA from stomach tissue or cells was extracted using an

RNeasy Plus Mini kit (Qiagen, Hilden, Germany) according to the manufacturer's instruction. One microgram of total RNA from each sample was reverse-transcribed using the QuantiTect Reverse Transcription kit (Qiagen) and analyzed by real-time RT-PCR using the Rotor-Gene SYBR Green PCR kit (Qiagen) with specific primers. Target genes were amplified and quantified using the Rotor-Gene Q and manufacturer's software (Qiagen). The amount of target gene was calculated using mRNA encoding β-actin as a housekeeping gene. Quantitative real-time RT-PCR primer pairs for mouse genes were F: 5'-CTT CTG GGC CTG CTG TTC A-3' and R: 5'-CCA GCC TAC TCA TTG GGA TCA-3' for MCP-1, F: 5'-AGA TAT TCG AGC AGG GTC TA-3' and R: 5'-GGG ATA TCA GTC AGA AAG GT-3' for GM-CSF and F: 5' - CAG GAG ATG GCC ACT GCC GCA-3' and 5' - TCC TTC TGC ATC CTG TCA GCA-3' for β-actin.

Western blotting

Total protein was extracted using PRO-PREP™ protein extraction solution (Intron Biotechnology, Seongnam, Korea). AGS and THP-1 cells were lysed using Cytobuster™ protein extraction reagent (Novagen, Madison, WI, USA) supplemented with protease inhibitor cocktail (GenDEPOT, Barker, TX, USA) and phosphatase inhibitor cocktail (GenDEPOT). Equal amounts of protein (30 μg) from mouse tissue or cell pellets were separated by sodium dodecyl sulfate-polyacrylamide

gel electrophoresis (SDS-PAGE) on 12% gels and transferred to a 0.2-μm membrane (BioRad, Hercules, CA, USA). The membranes were blocked with freshly prepared 1×Tris-buffered saline/Tween-20 containing 10% nonfat milk (Difco, Sparks, MD, USA). The blocked membranes were probed with anti-OPN (1:500; R&D Systems), anti-iNOS (1:200; Santa Cruz Biotechnology, Santa Cruz, CA, USA), anti-STAT1 (1:500; Santa Cruz Biotechnology), anti-phosphorylated STAT1 (1:250; Santa Cruz Biotechnology), anti-Caspase3 (1:500; Cell Signaling Technology, Danvers, MA, USA), anti-Bcl-2 (1:1000; Santa Cruz Biotechnology) or PARP-1 (1:1000; Santa Cruz Biotechnology) antibody. Membranes were incubated with horseradish peroxidase-conjugated rabbit anti-goat IgG antibody (GenDEPOT) or goat anti-rabbit IgG antibody (Millipore, Billerica, MA, USA), as appropriate. β-actin (Cell Signaling Technology) was used as internal control.

Tissue microarray-based immunohistochemical staining of OPN and iNOS in human gastric cancer tissues

Tissue-arrayed slides containing 51 patient-matched human gastric cancer and normal gastric tissues were purchased from SuperBioChips Laboratories (Seoul, Korea, www.tissue-array.com) and slides containing 41 human gastric cancer tissues (eight of which were paired with normal gastric tissues) were purchased from ISU ABXIS Co., Ltd. (Seoul, Korea, tma.abxis.com). Each cancer tissue was classified based

on the TNM classification scheme. Immunohistochemistry (IHC) was carried out using an ImmPress™ Reagent kit (Vector Laboratories, Burlingame, CA) and an ImmPACT™ DAB peroxidase substrate kit (Vector Laboratories), as described by the manufacturers. Anti-OPN antibody (1:100; R&D Systems) or anti-iNOS antibody (1:100; Abcam) were employed as a primary antibody. Each staining was assessed according to the intensity (negative, 0; weak, 1; moderate, 2; intense, 3) and area (none, 0; focal, 1; multifocal, 2; diffuse, 3) of positive cells. The grade of each staining was scored as 0 to 3, obtained by multiplying area by intensity (negative, 0; weak, 1 or 2; moderate, 3 or 4; intense, 6 or 9).

Statistical analysis

All data are expressed as means ± standard errors (SEMs). Statistical analyses were performed using SPSS Statistics (version 19.0; SPSS Inc., Chicago, IL) and GrapH. pyloriadPrism4 (version 4.0; GrapH. pyloriad Software, San Diego, CA). Correlations between OPN expression and clinicopathological features or iNOS expression were analyzed using the Chi-squared test or the Spearman's correlation test. The relationship between OPN genotype and the incidence of gastric cancer was analyzed using the Chi-squared test. Other data were analyzed using the unpaired two-tailed Student's *t*-test or the Mann-Whitney U-test. *P*-values less than 0.05 were considered statistically significant.

Results

OPN depletion suppresses development of H. pylori-induced gastric cancer

Macroscopically and microscopically, the tumors were formed mainly in the pyloric region, and they exhibited protruding single-to-multiple polypoid-to-sessile growth patterns in both the WT and OPN KO mice (Fig. 1A-B). The properties of the tumors in the WT and OPN KO mice are summarized in Table 1. The tumors in the OPN KO mice (3.9 ± 0.5 mm) were significantly smaller than the tumors in the WT mice (5.1 ± 0.9 mm). In addition, tumor multiplicity was lower in the OPN KO mice (0.89 ± 1.33) than in the WT mice (2.09 ± 1.31; $P<0.01$). A histological assessment showed a significantly lower incidence rate of gastric tumors in the OPN KO mice (33.3%) than in the WT mice (85.2%; $P<0.001$). Although the incidence rate of benign tumors did not differ significantly between the two genotypes, the frequency of malignant tumors was markedly lower in the OPN KO mice (8.3%) compared to the WT mice (44.4%; $P<0.01$). As shown in Fig. 1C, neoplastic nodules from the WT mice were composed of pleomorphic neoplastic cells exhibiting moderate to poor differentiation that formed irregular tubules or solid nests and occasional submucosal invasion. Unlike the neoplastic nodules from the WT mice, the nodules from the OPN KO mice consisted of small acini and tubules composed of well-differentiated neoplastic cells. These

results indicate that the lack of OPN suppresses the development and progression of *H. pylori*–induced gastric cancer, implying that OPN acts as an important tumor–promoting factor in this model.

In addition to tumor classification, we also investigated preneoplastic lesions. Varying degrees of preneoplastic lesions, such as foveolar hyperplasia, intestinal metaplasia and dysplasia, were observed in mice exposed to MNU and *H. pylori* (Fig. 2A). Evaluations of the preneoplastic lesions showed that all of the lesions in the OPN KO mice were significantly milder than the lesions in the WT mice (Fig. 2B). These results suggest that OPN depletion suppresses the progression of multistep carcinogenesis of gastric cancer.

Groups	OPN genotype	*H. pylori* infection	Total mice (n)	Dead mice (n)	Remaining mice (n)	Tumor-bearing mice n(%)	Gastric adenoma n(%)	Gastric adenocarcinoma n(%)	Tumor multiplicity	Tumor size diameter (mm)
1	WT	Yes	32	5	27	23(85.2)	11(40.7)	12(44.4)	2.09±1.31	5.1±0.9
2	KO	Yes	27	3	24	8(33.3)***	6(25.0)	2(8.3)**	0.89±1.33*	3.9±0.5*
3	WT	No	10	0	10	0	0	0	0	0
4	KO	No	10	0	10	0	0	0	0	0

Table 1. Incidence and multiplicity of MNU and *H. pylori*-associated gastric tumor

Data are presented as means ± SEMs. $*P < 0.05$, $**P < 0.01$ and $***P < 0.001$ *versus* WT mice

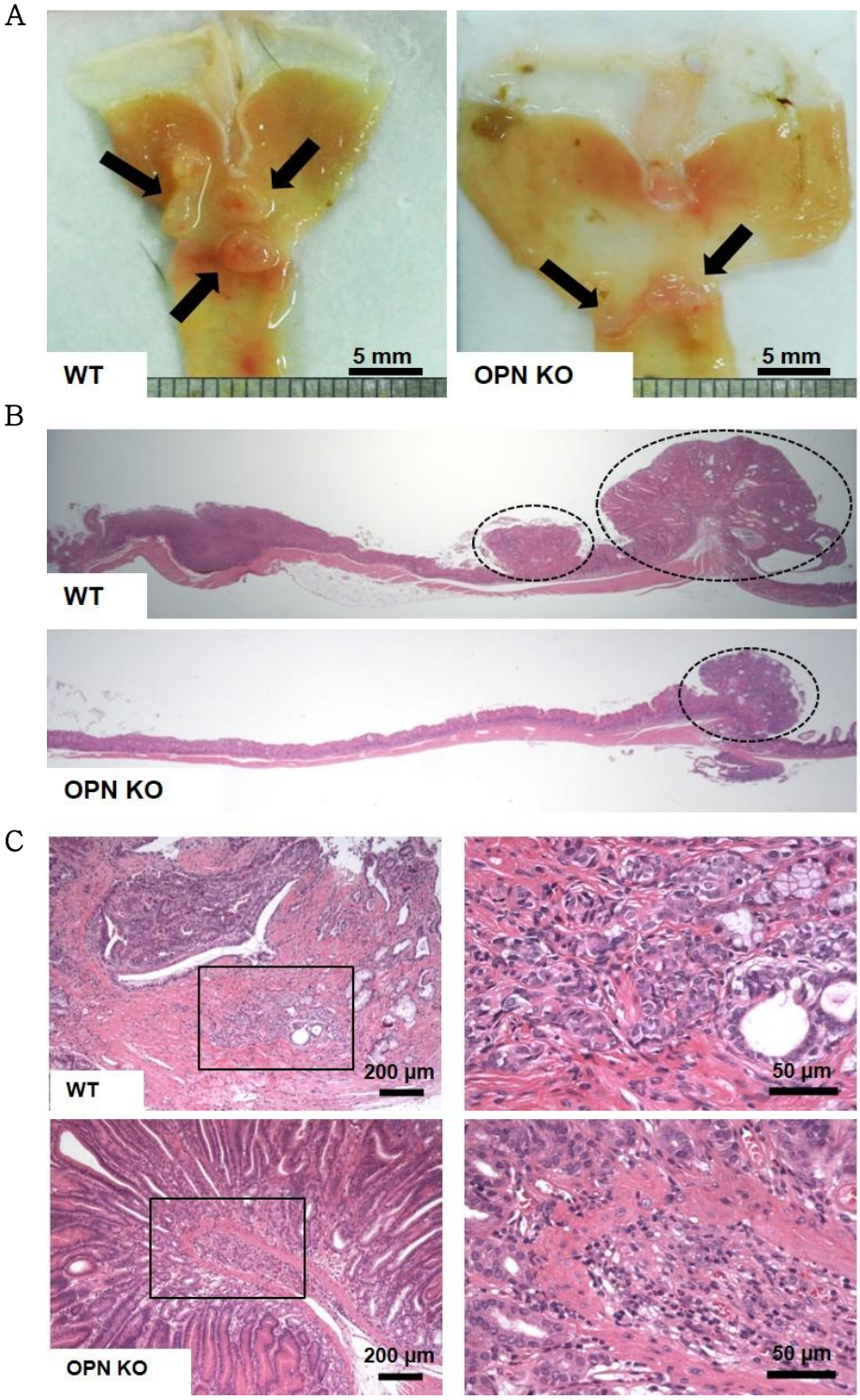

Fig 1. Gross morphology and histopathology of gastric cancer. (A) Gross morphology of wild-type (WT) and osteopontin knockout (OPN KO) mice stomachs. Note markedly decreased size of neoplastic nodules (arrows) in the antrum of OPN KO mice compared with those of WT mice. (B) H&E staining of WT and OPN KO mice stomachs. Neoplastic nodules (circles) showed a polypoid appearance in the antrum. Original magnification = 12.5× (C) Magnification of neoplastic nodules. Boxed regions of left panels are shown at higher magnification in the right panels. Nodules in the WT mouse stomach consisted of pleomorphic tumor cells showing a sessile growth pattern with invasion to submucosa. Nodules in the OPN KO mice stomach showed glandular and tubular growth patterns composed of well-differentiated tumor cells. Note an intact basement membrane and submucosa in OPN KO mice.

A

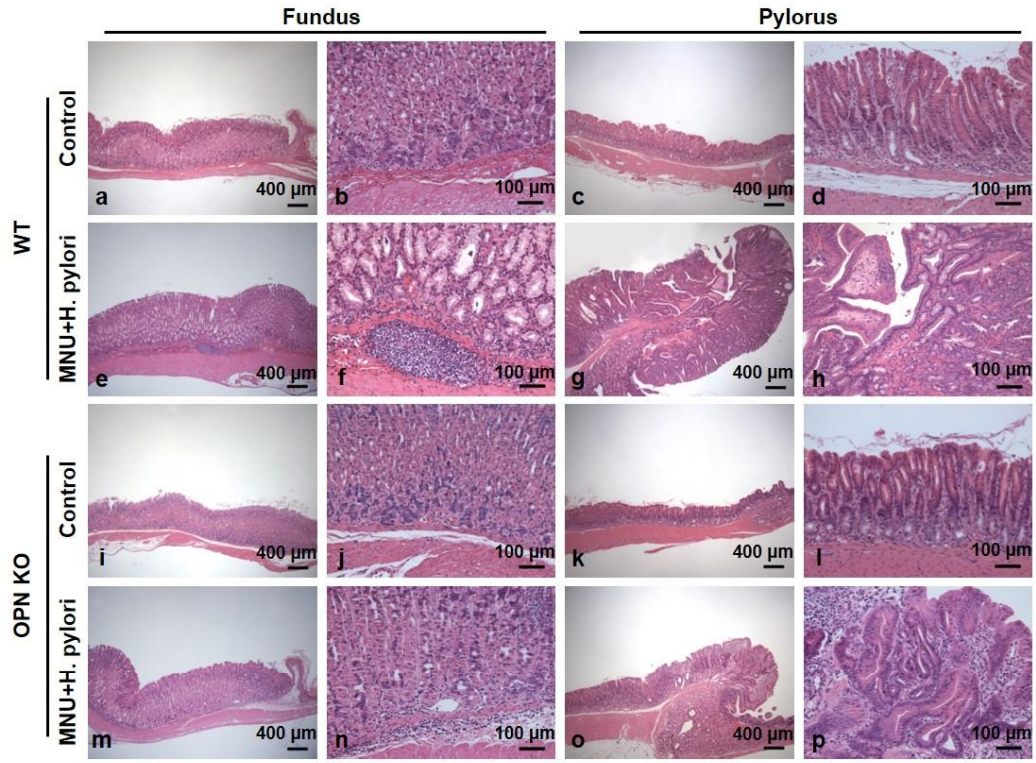

B

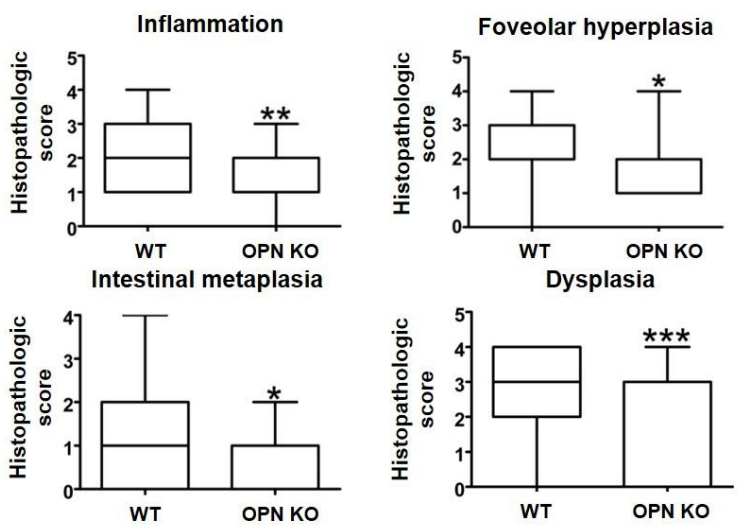

Fig 2. Gastric histopathology of the fundus and pylorus on H&E staining. Boxed regions of left panels are shown at higher magnification in the right panels. (A) Wild-type (WT) (a, b, c and d) and osteopontin knockout (OPN KO) (i, j, k and l) control mice stomachs exhibited a normal structure. (e and f) WT mice exposed to *N*-methyl-*N*-nitrosourea (MNU) and *H. pylori* showed severe inflammation and mucous metaplasia of parietal cells (foamy change) in the fundus. (m and n) In OPN KO mice exposed to MNU and *H. pylori*, gastritis, hyperplasia and metaplasia in the fundus were attenuated compared with WT mice. (g and h) Furthermore, WT mice exposed to MNU and *H. pylori* showed a severe loss of pyloric gland organization and orientation (dysplasia), intestinal metaplasia characterized by heightening and foamy change of foveolar cell. (o and p) Note the markedly decreased levels of dysplasia and metaplasia in OPN KO mice stomachs. (B) Histopathological scoring for inflammation, foveolar hyperplasia, intestinal metaplasia and dysplasia in wild-type (WT) and osteopontin knockout (OPN KO) mice exposed to MNU and *H. pylori*. Results are presented as means±SEMs (examined all the mice for each groups). $*P < 0.05$, $**P < 0.01$ and $***P < 0.001$.

OPN depletion decreases gastric cancer-related macrophage infiltration

As the infiltration of macrophages in *H. pylori* infection-induced chronic gastritis is related to gastric carcinogenesis, we carried out immunohistochemistry for the macrophage marker F4/80 and quantified F4/80-positive cells. Macrophage infiltration was detected primarily in the mucosa and submucosa of both WT and OPN KO mice exposed to MNU and *H. pylori*; however, the number of infiltrating macrophages was much lower in the OPN KO mice than in the WT mice (Fig. 3A). Real-time RT-PCR results indicated that expression of the macrophage-chemoattractant molecules MCP-1 and GM-CSF was significantly lower in both cancerous and non-cancerous tissues from OPN KO mice exposed to MNU and *H. pylori* compared to those of WT mice (Fig. 3B). These results suggest that OPN depletion suppresses macrophage infiltration, an important factor in gastric carcinogenesis, through the downregulation of chemoattractant factor expression.

A

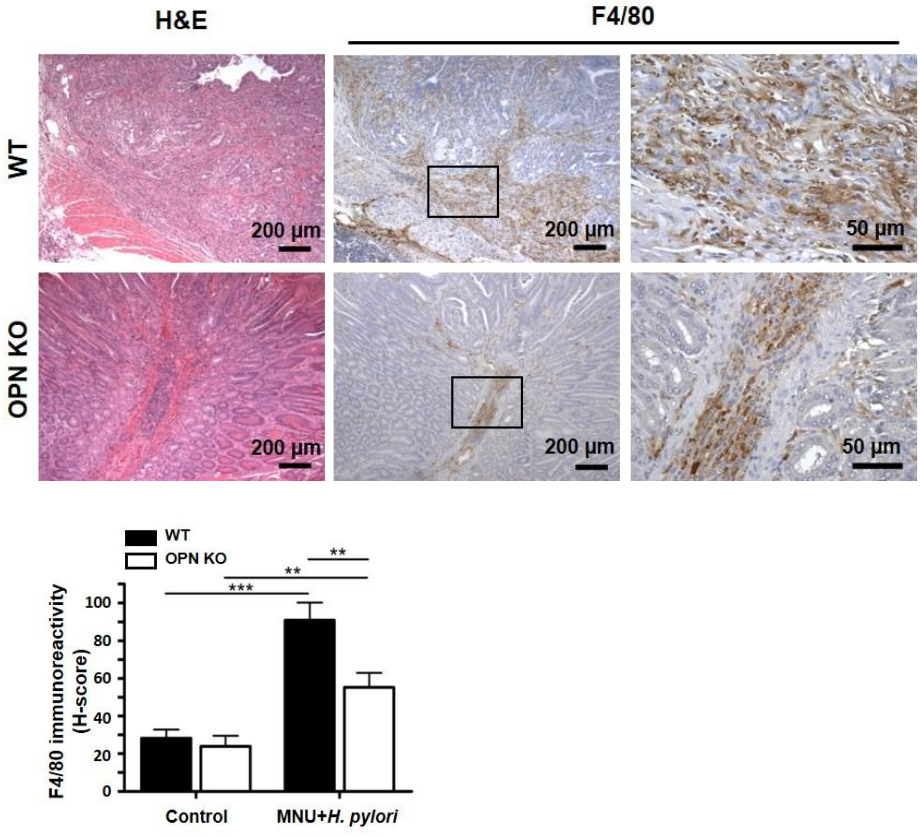

B

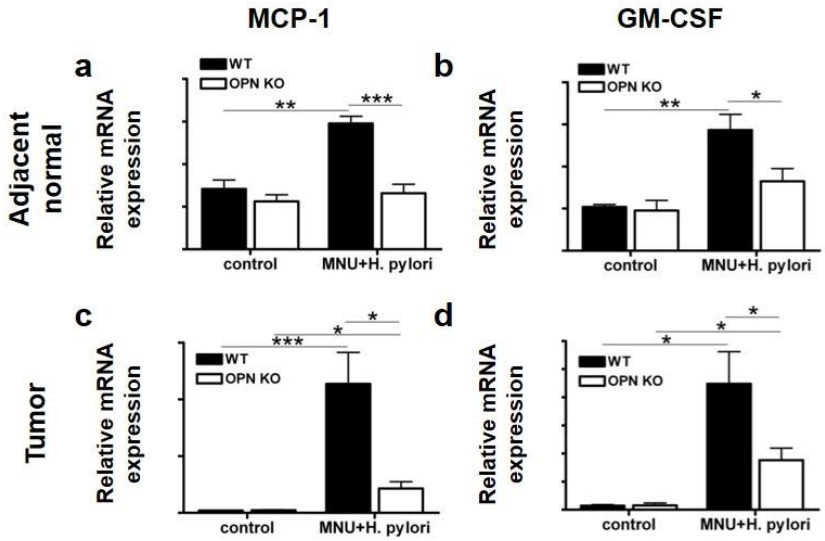

Fig 3. Macrophage infiltration and inflammatory chemokine expression. (A) H&E staining and immunohistochemical staining for F4/80 in serial sections of wild-type (WT) (a-c) and osteopontin knockout (OPN KO) mice stomachs (d-f). WT mice exposed to MNU and *H. pylori* showed greater macrophage infiltration compared with OPN KO mice. Boxed regions of the panels b and e are shown at higher magnification in the panels c and f. Results are presented as means±SEMs (n=4-5 for each group). $*P < 0.05$, $**P < 0.01$ and $***P < 0.001$. (B) The mRNA expression levels of MCP-1 and GM-CSF in adjacent normal (a-b) and tumor (c-d) tissues were determined using real-time RT-PCR. Note significantly decreased expression levels of chemokines in both adjacent normal and tumor tissues in OPN KO mice compared to WT mice. Results are presented as means±SEMs (n=4-5 for each group). $*P < 0.05$, $**P < 0.01$ and $***P < 0.001$.

OPN depletion promotes apoptosis of gastric epithelial cells

Next, we analyzed the proliferation and apoptosis of gastric epithelial cells. A comparison of adjacent normal tissues in the WT and OPN KO mice exposed to MNU and *H. pylori* showed that the OPN KO mice had higher numbers of TUNEL-positive, apoptotic gastric epithelial cells (P=0.09). In tumor tissues, the apoptotic index was significantly higher in the OPN KO mice than in the WT mice (Fig. 4A). Consistent with the TUNEL assay, the expression levels of caspase3 and cleaved caspase3 protein in gastric tissues, including tumor and adjacent normal tissues, were higher in the OPN KO mice than in the WT mice (Fig. 4B).

Compared with untreated control mice, the WT mice and OPN KO mice exposed to MNU and *H. pylori* had a high number of Ki-67-positive cells in tumor tissues. WT mice exposed to MNU and *H. pylori* showed a trend toward increased proliferation compared with OPN KO mice, although this difference did not reach statistical significance (Fig. 5).

A

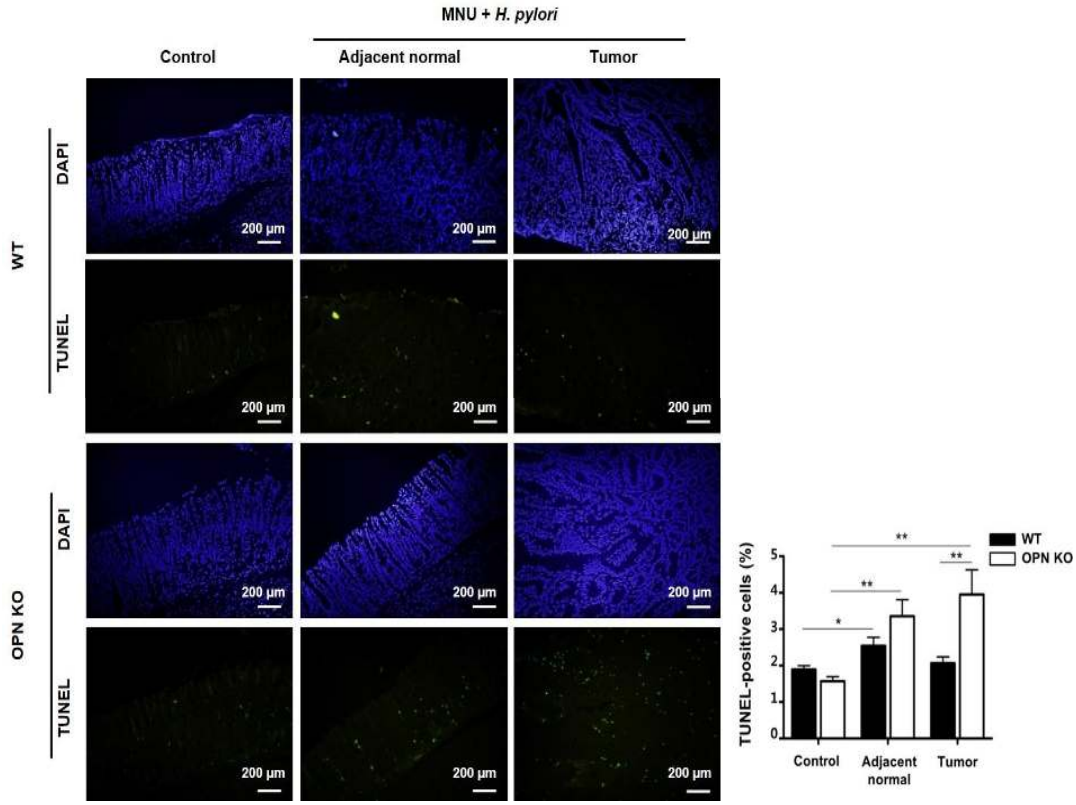

B

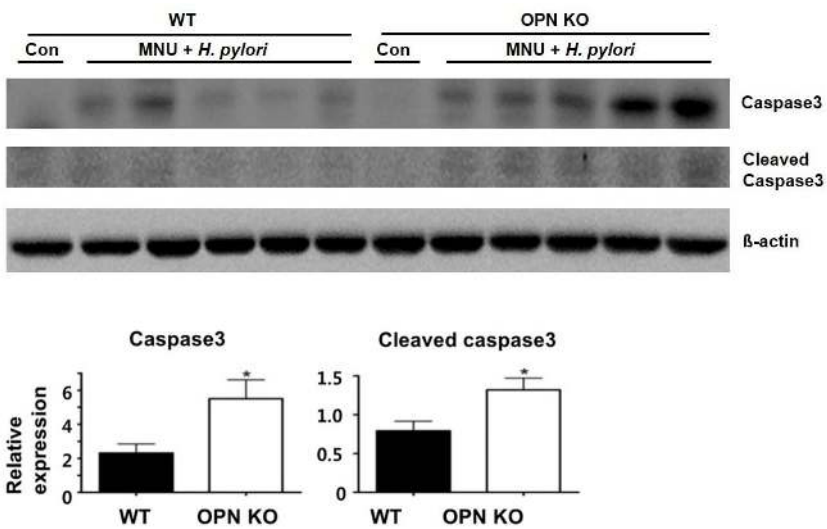

Fig 4. Apoptotic cell death in the gastric mucosa. (A) Representative photomicrographs of total cells in the stomach tissue of wild-type (WT) (a-c) and osteopontin knockout (OPN KO) (g-i) mice. (d-f and j-l) Representative photomicrographs of apoptotic cells in stomach tissue corresponding the panels a-c and g-i. The apoptotic index in adjacent normal tissue of WT mice (e) was slightly lower than that in OPN mice (k). The apoptotic index of mucosal epithelium in tumor tissue was significantly higher in OPN KO mice (l) than in WT mice (f). Results are presented as means±SEMs (n=5 for control groups and n=6-10 for MNU and *H. pylori*-treated groups). $*P < 0.05$ and $**P < 0.01$. (B) Western blotting for caspase3 and cleaved caspase3 protein in WT and OPN KO mouse stomachs. Results are presented as means±SEMs (n = 4-6 for each group). $*P < 0.05$ *versus* WT mice.

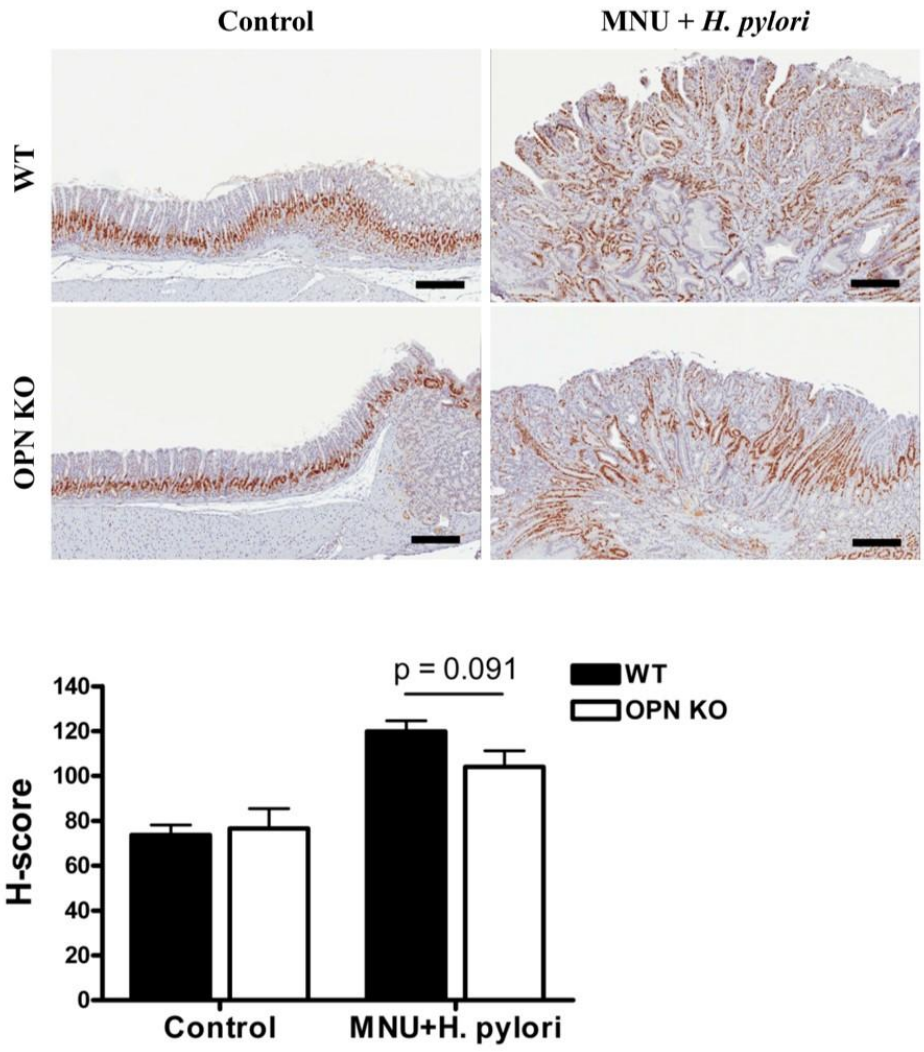

Fig 5. Proliferative activity in the gastric mucosa. Wild-type (WT) and osteopontin knockout (OPN KO) mice exposed to MNU and *H. pylori* showed higher proliferative index of gastric epithelial cells compared with WT and OPN KO control mice. OPN KO mice exposed to MNU and *H. pylori* showed a trend toward decreased proliferation compared with WT mice ($P = 0.091$). *Bar* = 200 μm

OPN suppresses H pylori-induced activation of STAT1/ iNOS signaling

We then investigated the pattern and intensity of iNOS expression using serial sectioned stomach tissues of the WT and OPN KO mice. Almost all of the cells in the stomachs of the control mice were negative for iNOS expression, with the exception of a few chief cells and epithelial cells of the pyloric gland, which exhibited weakly positive iNOS staining. Tumor tissues from the WT mice exposed to MNU and *H. pylori* showed moderate expression of iNOS in the cytoplasm of a few tumor cells, and weakly positive signals in a small number of macrophages (Fig. 6A). By contrast, in the OPN KO mice exposed to MNU and *H. pylori*, iNOS expression was clearly detected in the epithelial and stromal cells of tumor tissues (Fig. 6A). In tumor tissues from these mice, large numbers of tumor cells and inflammatory cells, especially macrophages, exhibited moderate to intense positive signals (Fig. 6A). Western blotting confirmed these results, showing significantly higher expression levels of iNOS in the OPN KO mice compared to the WT mice exposed to MNU and *H. pylori* (Fig. 6B).

The expression of iNOS is transcriptionally and post-transcriptionally regulated by a signal transducer and activator of the transcription 1 (STAT 1) pathway (de Vera, Shapiro et al. 1996). Consistent with this relationship, expressions of STAT1 and phosphorylated STAT1 in the gastric mucosa were significantly higher in the OPN KO mice exposed to MNU and *H. pylori* than in the WT mice (Fig. 6B).

A

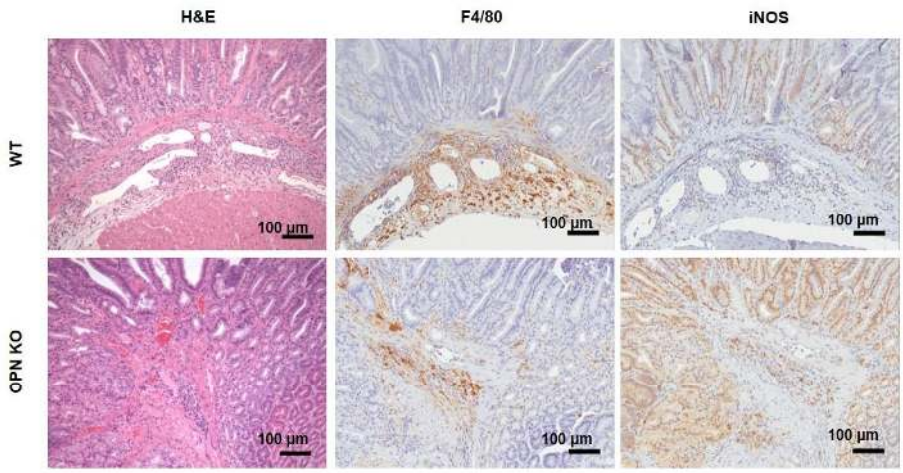

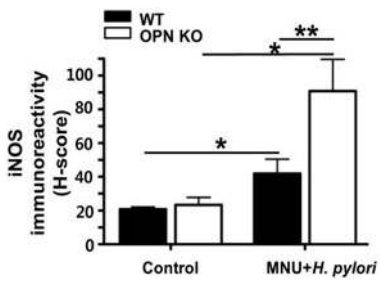

B

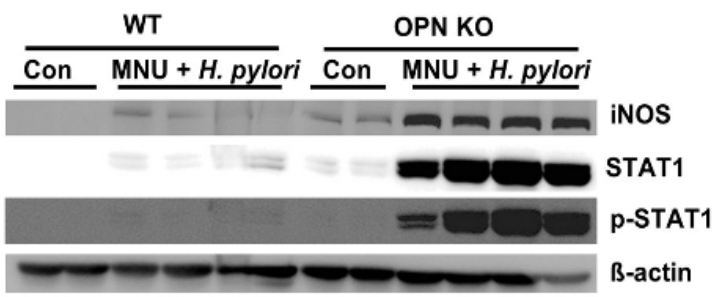

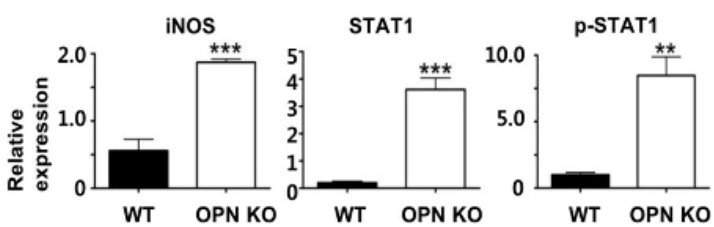

Fig 6. Expression of inducible nitric oxide synthase (iNOS) in tumor cells and macrophages (A) H&E staining and immunohistochemical staining for F4/80 and iNOS in serial stomach sections from wild-type (WT) and osteopontin knockout (OPN KO) mice. WT mice exposed to MNU and *H. pylori* showed lower level of iNOS expression in tumor cells and macrophages compared with OPN KO mice. Results are presented as means±SEMs (n=4-6 for each group). $*P < 0.05$ and $**P < 0.01$. (B) Western blotting for iNOS, STAT1 and p-STAT1 protein in the stomach of WT and OPN KO mice. Results are presented as means±SEMs (n=4-5 for each group). $*P < 0.05$, $**P < 0.01$ and $***P < 0.001$.

Secreted OPN downregulates the expressions of iNOS and STAT1

To investigate whether the suppressive effects of OPN on iNOS and STAT1 are due to intracellular or secreted OPN, treatment of recombinant human OPN (rhOPN) or neutralization of OPN by anti-OPN antibody was performed. In the various concentrations of rhOPN, OPN KD AGS cells exhibited significantly lower expression levels of iNOS and STAT1, in a concentration-dependent manner, compared to control AGS cells (Fig. 7A). Furthermore, rhOPN treatment on OPN KD AGS cells caused the downregulation of iNOS, STAT1, and p-STAT1 in a time-dependent manner (Fig. 7B). In line with these findings, the neutralization of secreted OPN in control AGS cells for six hours resulted in the upregulation of iNOS, STAT1, and p-STAT1 in a concentration-dependent manner (Fig 7C). Similar to AGS cells, control THP-1 cells displayed increasing expression patterns of iNOS, STAT1, and p-STAT1, dependent on concentrations of anti-OPN antibodies (Fig. 7D).

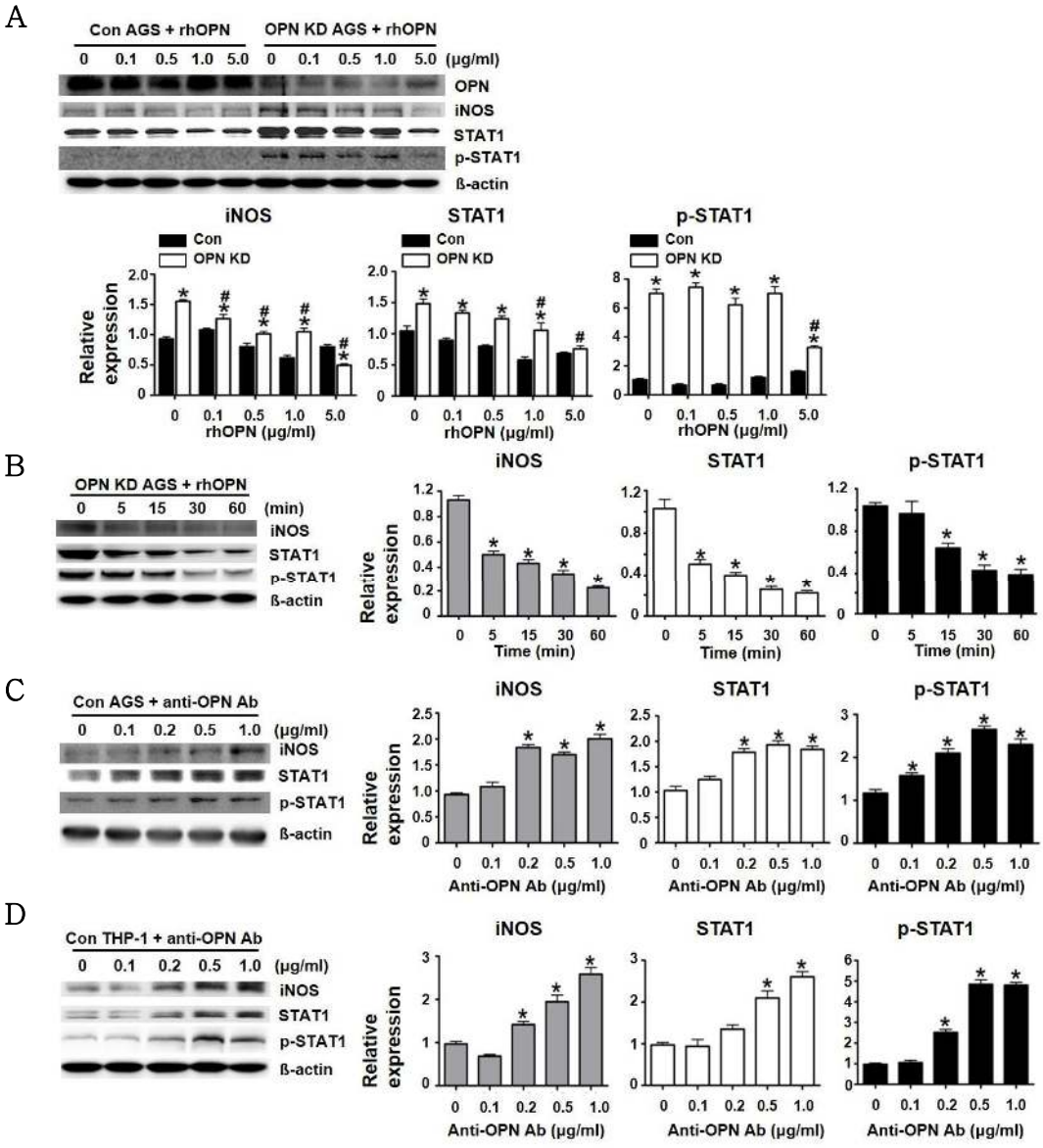

Fig 7. Regulation of inducible nitric oxide synthase (iNOS) and signal transducer and activator of transcription 1 (STAT1) expressions by secreted osteopontin (OPN). (A–D) Western blotting for iNOS, STAT1 and p–STAT1 proteins. (A) Various concentrations of recombinant human OPN (rhOPN) treatment on control (Con) or OPN knockdown (OPN KD) AGS cells. Results are presented as means±SEMs (n = 3 for each concentration). * $P < 0.05$ *versus* control vector–transfected (Con) cells under the respective concentration. # $P < 0.05$ *versus* 0 μg/ml of rhOPN under the respective concentration. (B) Various time points of rhOPN treatment on OPN KD AGS cells. Results are presented as means±SEMs (n = 3 for each time point). * $P < 0.05$ *versus* 0 minutes under the respective time point. (C–D) Various concentrations of anti–OPN antibody treatment on control AGS (C) and THP–1 cells (D). Results are presented as means±SEMs (n = 3 for each concentration). * $P < 0.05$ *versus* 0 μg/ml of anti–OPN antibody under the respective concentration.

OPN suppression promotes apoptosis of AGS cells in the co-culture condition

To extend the mouse study results and clarify the relationships among OPN, STAT1, and iNOS expression in macrophages and tumor cells, we examined the effects of OPN suppression in AGS cells and THP-1 cells co-cultured under various conditions (Fig. 8A-D). shRNA-mediated OPN knockdown considerably upregulated STAT1 and p-STAT1 expression levels in unstimulated THP-1 cells cultured alone (group A2) and LPS-stimulated THP-1 cells co-cultured with AGS cells (group D2). Similarly, iNOS expression was enhanced significantly in LPS-stimulated OPN KD THP-1 cells (group D2) compared with LPS-stimulated control THP-1 cells co-cultured with control AGS cells (group D1). In line with the expression pattern observed in THP-1 cells, STAT1 and p-STAT1 protein levels were higher in OPN KD AGS cells than in control AGS cells (groups A, C, and D). The suppressive effect of OPN on iNOS expression was most prominent in AGS cells co-cultured with LPS-stimulated THP-1 cells (group D).

To determine the effect of *H. pylori* infection on epithelial cells, we also co-cultured AGS cells with *H. pylori*. In these co-cultures, STAT1 and p-STAT1 expression levels were higher in OPN KD AGS cells (group B2) than in control AGS cells (group B1), and iNOS expression in AGS cells exposed to *H. pylori* was increased considerably by OPN suppression (Fig. 8C). Furthermore, the expression levels of cleaved

caspase3 were higher in OPN KD AGS cells than in control AGS cells; these differences were more prominent in co-culture conditions (groups B-D) than in single-cultured conditions (group A; Fig. 8D). In line with the expression of cleaved caspase3, OPN KD promoted PARP-1 cleavage and suppressed Bcl-2 expression (Fig. 8D).

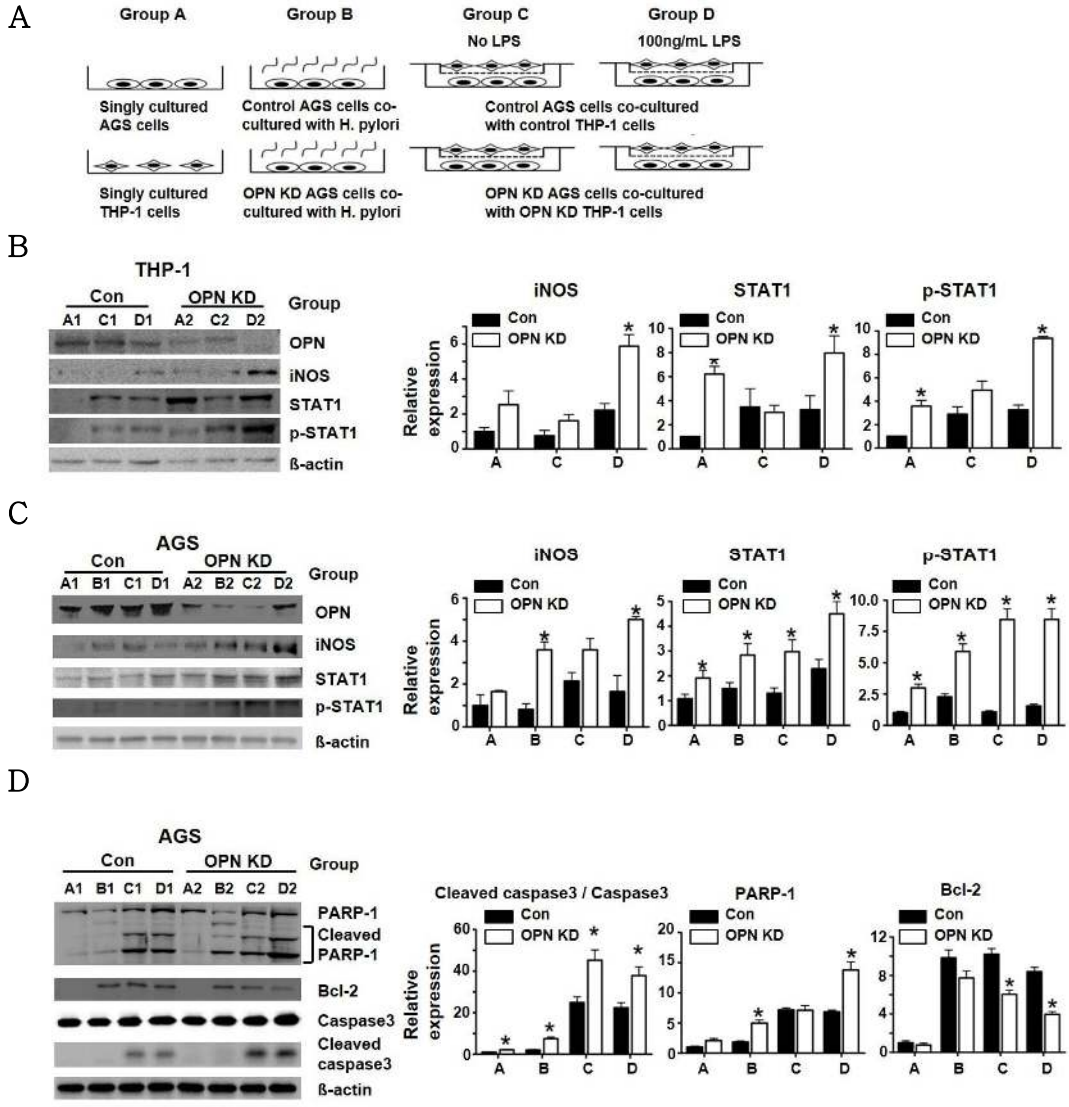

Fig 8. Effect of osteopontin (OPN) downregulation on apoptosis in relation to signal transducer and activator of transcription 1 (STAT1) mediated-inducible nitric oxide synthase (iNOS) protein expression in the various co-culture conditions. (A) A schematic illustration of the co-culture system: Group A; singly cultured AGS cells and THP-1 cells; group B, control (Con) or OPN knockdown (KD) AGS cells co-cultured with *H. pylori*; group C, AGS cells co-cultured with unstimulated THP-1 cells with same OPN phenotype (control or OPN KD); group D, AGS cells co-cultured with LPS-stimulated THP-1 cells with same OPN phenotype (control or OPN KD). (B) Western blotting for iNOS, STAT1 and p-STAT1 proteins and relative expression levels in THP-1 cells under each culture condition. Results are presented as means±SEMs (n = 3 for each culture condition). * $P < 0.05$ *versus* control vector-transfected (con) cells under the respective culture condition. (C) Western blotting for iNOS, STAT1 and p-STAT1 and relative expression levels in AGS cells under each culture condition. Results are presented as means±SEMs (n = 3 for each culture condition). * $P < 0.05$ *versus* control vector-transfected (con) cells under the respective culture condition. (D) Western blotting for pro-apoptotic proteins, PARP-1, caspase3 and cleaved caspase3 and anti-apoptotic protein, Bcl-2, under each culture condition. Relative expression levels of apoptosis-related proteins in AGS cells co-cultured with THP-1 cells (upper panels) or *H. pylori* (lower panels). Results are presented as

means±SEMs (n = 3 for each culture condition). * $P < 0.05$ *versus* control vector-transfected (con) cells under the respective culture condition.

OPN negatively regulates iNOS expression in human gastric cancer tissues

Using human microarray slides, we compared degrees of OPN expression in gastric cancer tissues (tumor) and adjacent normal tissues (non-tumor) and analyzed the correlation between OPN expression and TNM stage. Similar to the results of a previous study, we found that OPN expression was significantly higher in gastric cancer tissues than in paired normal tissues (P<0.001; Fig. 9B). In cancer tissues, 49.1% of the samples showed moderate to intense OPN expression in the cytoplasm of cancer cells, whereas 89.9% of adjacent normal tissues displayed negative to weak expression (Fig. 9A). Degree of OPN expression in human gastric cancer tissues was also positively correlated with TMN stage (P<0.001; Fig. 9B). In cancer tissues from stage I or II patients, more than half of the samples showed negative to weak positive expression of OPN (Fig. 9A); however, moderate to intense positive expression levels were detected in 64% and 66.7% of stage III and IV samples, respectively (Fig. 9A).

Finally, we examined the correlation between OPN and iNOS expression. Similar to results obtained in mice, OPN expression was strongly negatively correlated with iNOS expression in gastric cancer tissues (P<0.001, r=-0.5843; Fig. 9B). In 54 cases exhibiting negative or weak positive expression of OPN, moderate to intense expression of iNOS was observed in 31 cases (57.4%) (Fig. 9A). Conversely, in cases

where OPN expression was moderate or intense, 93.8% (30/32) displayed negative or weak positive expression of iNOS (Fig. 9A).

A

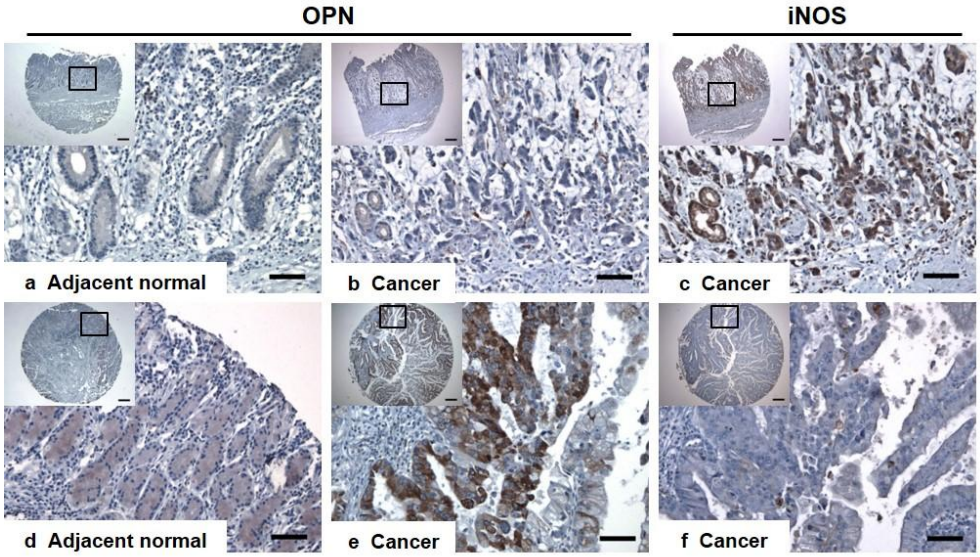

B

	OPN expression				
	Number of case (%)				p-value
	Negative	Weak	Moderate	Strong	
Tissue					
Cancer (n=59)	10 (16.9)	20 (33.9)	15 (25.4)	14 (23.7)	p<0.001
Normal (n=59)	26 (44.1)	27 (45.8)	6 (10.2)	0 (0)	
pTNM stage					
I (n=24)	14 (58.3)	9 (37.5)	1 (4.2)	0 (0)	
II (n=25)	6 (24)	12 (48)	4 (16)	3 (12)	p<0.001
III (n=25)	1 (4)	8 (32)	9 (36)	7 (28)	
IV (n=12)	1 (8.3)	3 (25)	3 (25)	5 (41.7)	
iNOS expression					
Negative (n=32)	0 (0)	8 (25)	13 (76.5)	11 (73.3)	Spearman
Weak (n=21)	9 (40.9)	6 (18.8)	2 (11.8)	4 (26.7)	r = -0.5843
Moderate (n=17)	7 (31.8)	9 (28.1)	1 (5.9)	0 (0)	p<0.001
Strong (n=16)	6 (27.3)	9 (28.1)	1 (5.9)	0 (0)	

Fig 9. Immunohistochemical staining (IHC) for osteopontin (OPN) and inducible nitric oxide synthase (iNOS) in human gastric cancer tissue and adjacent normal tissue. (A) Representative photomicrographs of IHC for OPN and iNOS. (a) Normal gastric tissue adjacent to cancer tissue shown in panel b. (b–c) serial sectioned gastric cancer samples (pTNM stage I). Weakly positive OPN staining (b) and moderate–to–strong positive iNOS expression (c). (d) Normal gastric tissue adjacent to cancer tissue shown in panel e. (e–f) serial sectioned gastric cancer samples (pTNM stage III). Moderate–to–strong positive OPN expression (e) and negative or weakly positive iNOS staining (f). (B) Correlation between OPN expression and tissue types, pTNM stages and iNOS expression. *Bar* = 400 μm (inserts) and 50 μm

A

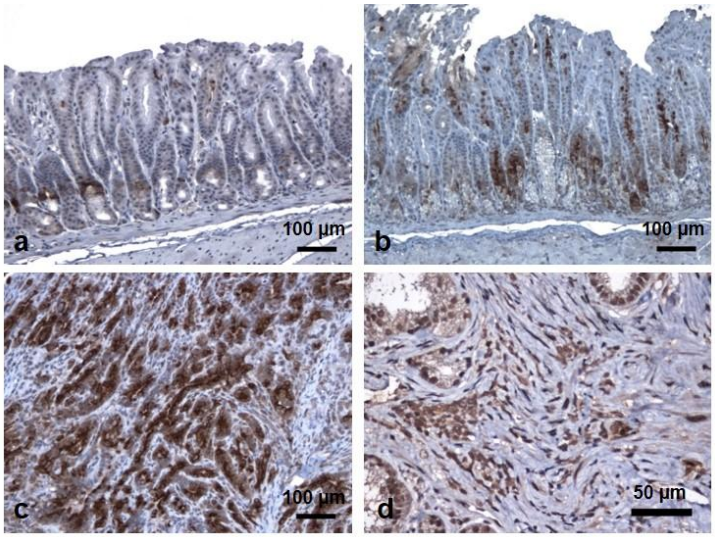

B

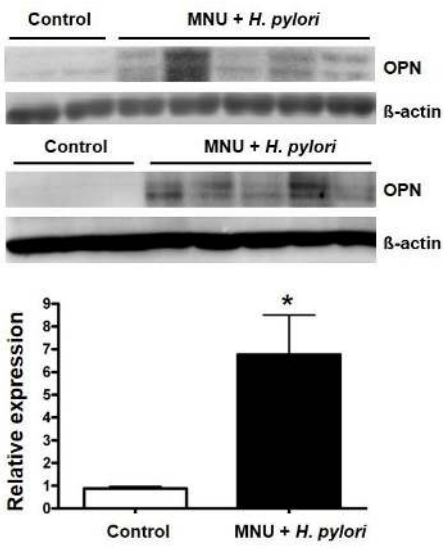

C

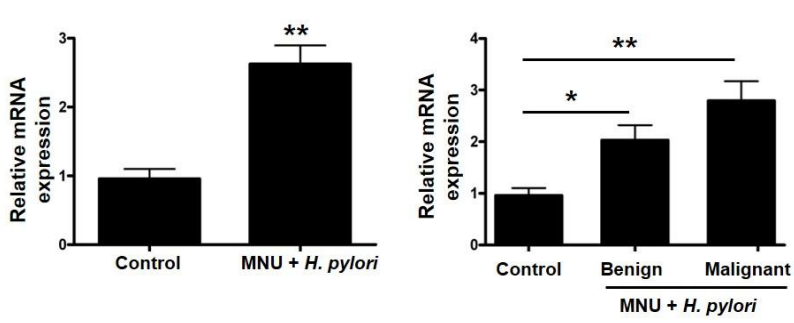

Fig 10. Immunohistochemical staining, Western blotting and real-time RT-PCR for osteopontin (OPN). (A) A representative photomicrograph of OPN staining in the stomach tissue of wild-type (WT) mice. (a) Scattered, weak positive staining for OPN in the cytoplasm of pyloric gland epithelium, but not in foveolar cells in the gastric mucosa of control mouse. (b) Moderate to intense positive staining for OPN in dysplastic mucosa, showing cytoplasmic and luminal expression patterns. (c) Intense positive staining for OPN in tumor tissue from a mouse exposed to *N*-methyl-*N*-nitrosourea (MNU) and *H. pylori*. (d) Moderate positive staining for OPN in inflammatory cells infiltrated in the gastric submucosa in a mouse exposed to MNU and *H. pylori*. (B) Evaluation of OPN protein expression in WT mice using Western blotting. In WT mice exposed to MNU and *H. pylori*, the expression of OPN protein was variably increased compared with control WT mice (2.5-20-fold change). Results are presented as means±SEMs (n = 5 for the control group and n = 10 for MNU + *H. pylori* group). $*P < 0.05$ *versus* control mice. (C) Evaluation of OPN mRNA expression in mice using real-time RT-PCR. Note considerably increased expression levels of OPN protein and mRNA in mice exposed to MNU and *H. pylori*. Results are presented as means±SEMs (n = 5 for the control group and n = 10 for MNU + *H. pylori* group). $*P < 0.05$ and $**P < 0.01$ *versus* control mice.

Discussion

In this study, we showed that gastric cancer development induced by MNU and *H. pylori* infection was significantly suppressed by lack of OPN. OPN depletion also attenuated the degrees of chronic gastritis and preneoplastic lesions such as foveolar hyperplasia and intestinal metaplasia and dysplasia. Furthermore, increased OPN expression was noted in both preneoplastic and neoplastic lesions in WT mice (Fig. 10A). The degree of OPN protein expression was statistically higher in WT mice exposed to MNU and *H. pylori* than in the control group (P=0.035; Fig. 10B). Similarly, the mRNA expression level of the cancer group was also higher than that of the control group, although the difference between adenoma and adenocarcinoma was not significant (Fig. 10C). Importantly, these observations are in line with previous studies that reported that high-level OPN expression was positively associated with progression of human gastric cancer (Dai, Bao et al. 2007, Higashiyama, Ito et al. 2007).

Human clinical studies have established a relationship between OPN and chronic inflammation. Chang *et al.* showed that OPN expression levels are correlated positively with severity of chronic gastritis and intestinal metaplasia in *H. pylori*-positive patients. They also reported that persistent OPN expression originated from inflammatory cells, especially macrophages, as well as gastric epithelial cells (Chang, Yang et al. 2011). In addition, Sato *et al.* demonstrated in a mouse TNBS

model that higher plasma OPN levels, seen in human inflammatory bowel disease and OPN ablation, resulted in attenuation of the progression of colitis (Sato, Nakai et al. 2005, Mishima, Takeshima et al. 2007, Oz, Zhong et al. 2012). We previously showed that lack of OPN caused a decreased proinflammatory response to *H. pylori* infection, including attenuated expression of cytokines and inflammatory cell infiltration, such as macrophages, lymphocytes, and polymorphonuclear leukocytes (Park, Lee et al. 2015). In line with previous studies, we found that OPN KO mice exhibiting lower levels of MCP-1 and GM-CSF expression displayed a diminished degree of macrophage infiltration. Some reports support the idea that inflammatory chemokines, such as MCP-1 and GM-CSF, play an integral role in linking macrophage migration with cancer (Kuroda, Kitadai et al. 2005, Lin, Wu et al. 2006, Popivanova, Kostadinova et al. 2009). These results suggest that OPN plays a crucial role in chronic inflammatory disease by promoting inflammatory cell migration, which could allow for the creation of an environment favorable to cancer development.

We also elucidated that OPN promotes chronic gastritis and gastric epithelial hyperplasia through TNF-α- and IL-1β-dependent activation of the MAPK pathway during *H. pylori* infection (Park, Lee et al. 2015). Not only is complementary proliferation of gastric epithelia infected with *H. pylori* significant for gastric carcinogenesis, but evasion of tumor cell death is also required for tumor promotion and progression

(Yanai, Hirata et al. 2003). It is well known that OPN plays an important role in the promotion and progression of carcinogenesis by acting as an antiapoptotic protein (Zhao, Dong et al. 2008, Matusan-Ilijas, Damante et al. 2011). Our results indicate that the decreased incidence and progression of gastric cancer in OPN KO mice was correlated with increased apoptosis of gastric epithelial cells. The antiapoptotic function of OPN is mediated by CD44 or integrin receptors, and OPN interactions with CD44 variants exert important inhibitory effects on cancer cell apoptosis through the PI3K/Akt pathway-associated translocation of ß-catenin to the nucleus (Ue, Yokozaki et al. 1998, Robertson and Chellaiah 2010).

We further investigated the mechanism by which OPN suppresses apoptosis by examining NO signaling. Some studies showed that *H. pylori* infection could induce overexpression of iNOS in gastric mucosa, and increased iNOS expression in stomach was positively correlated with gastritis and gastric cancer (Chen, Hsieh et al. 2006, Cho, Lim et al. 2010). In line with these studies, we found WT mice treated with MNU and *H. pylori* showed high expression level of iNOS compared to the control WT mice. These results imply iNOS and NO may play an oncogenic role. However, it has been definitively proved that NO has bimodal effects on carcinogenesis, and high concentrations of NO originating from macrophages or cancer cells exert cytotoxic effects (Edwards, Cendan et al. 1996, Weigert and Brune 2008, Ambs and Glynn

2011). In addition, it is generally accepted that OPN suppresses NO-mediated cytotoxicity by negatively regulating iNOS expression (Rollo, Laskin et al. 1996, Wai, Guo et al. 2006). Our observation that OPN KO mice treated with MNU and *H. pylori* showed significantly higher expression levels of iNOS compared to WT mice may offer evidence that these are both side-effects of iNOS. To elucidate the mechanism by which OPN suppresses iNOS expression, we took note of the transcription factor STAT1, which Kusmartsev *et al.* demonstrated is important in regulating iNOS expression, using a STAT1-/- mouse model (Kusmartsev and Gabrilovich 2013). In the current study, we found that OPN KO mice that maintained high levels of STAT1 expression exhibited higher expression levels of iNOS that WT mice following exposure to MNU and *H. pylori*. In an *in vitro* study, we found that secreted OPN has a main role in the downregulation of STAT1 and iNOS. In a co-culture study, we further found that shRNA-mediated OPN suppression in human gastric cancer cells and macrophages upregulated STAT1 and iNOS. Our results are consistent with those of previous studies that reported that OPN suppresses iNOS expression in murine macrophages and mammary tumor cells through ubiquitin-dependent STAT1 degradation (Gao, Mi et al. 2007, Guo, Wai et al. 2008, Guo, Mi et al. 2010).

OPN suppression also increased considerably the degree of apoptosis in gastric epithelia, especially in tumor cells, a finding that parallels the

observed increase in iNOS expression levels. Our *in vitro* study supports the interpretation that secreted OPN suppresses tumor cell apoptosis, as well as iNOS expression in tumor cells and macrophages. OPN KD AGS cells co-cultured with OPN KD THP-1 cells or *H. pylori* displayed increased expression levels of apoptotic proteins, accompanied by decreased expression levels of Bcl-2, compared with control AGS cells co-cultured with control THP-1 cells or *H. pylori*. Taken together with previous studies, our results suggest that secreted OPN mainly downregulates STAT1 to suppress iNOS expression and tumor cell apoptosis, thereby promoting tumor promotion and progression.

Interestingly, tissue microarrays of human stomach cancer samples clearly revealed a negative correlation between OPN and iNOS expression in gastric cancer. Although several clinical studies have shown a relationship between OPN expression and cancer stage in various types of human cancer, few studies have addressed the underlying mechanism (Dai, Bao et al. 2007, Li, Li et al. 2014, Zhu, Guo et al. 2014). In the present study, we not only confirmed that OPN expression levels were positively correlated with the stage of human gastric cancer, as reported in previous studies, but we also identified a candidate mechanism regulated by OPN that is involved in gastric carcinogenesis.

In conclusion, we demonstrated that ablation of OPN suppresses *H. pylori* infection-associated gastric carcinogenesis in a mouse model. In

addition to suppressing the inflammatory response to *H. pylori*, which can result in the development of gastric cancer, OPN deficiency promotes the apoptotic cell death of tumor cells through upregulation of STAT1-mediated iNOS expression. Our clinicopathological study also provided the first demonstration of a negative correlation between OPN and iNOS expression in human gastric cancer. In the present study, we focused on the role of OPN expressed in tumor cells and macrophages in terms of their apoptotic effect on tumor cells. However, it is well known that OPN expressed in the tumor microenvironment (i.e., fibroblasts, dendritic cells, lymphocytes, etc.) was also involved in tumor growth, invasion, and metastasis in H. pylori-induced gastric carcinogenesis (Anborgh, Mutrie et al. 2010). Further studies using cell- or tissue-specific OPN knockout mice rather than whole tissues-OPN KO mice may be helpful to elucidate the specific roles OPN in various types of cells. Despite these limitations in the present study, our findings indicate that OPN may contribute to the development and progression of gastric cancer by suppressing proinflammatory immune responses and reducing STAT1 and iNOS-mediated apoptosis of gastric epithelial cells. Consequently, OPN might be a good target for the prevention and treatment of human gastric cancer.

CHAPTER III.

SUPPRESSION OF OSTEOPONTIN INHIBITS CHEMICALLY INDUCED HEPATOCARCINOGENESIS BY INDUCTION OF APOPTOSIS

Abstract

Previous clinical reports have found elevated osteopontin (OPN) levels in tumor tissues to be indicative of greater malignancy in human hepatocellular carcinoma (HCC). However, the role of OPN on carcinogenesis and its underlying mechanism remain unclear. In the present study, we investigated the oncogenic role of OPN in diethylnitrosamine (DEN)-induced hepatic carcinogenesis in mice. The overall incidence of hepatic tumors at 36 weeks was significantly lower in OPN knockout (KO) mice than in wild-type (WT) mice. Apoptosis was significantly enhanced in OPN KO mice, and was accompanied by the downregulation of epidermal growth factor receptor (EGFR). In the *in vitro* study, OPN suppression also led to lower mRNA and protein levels of EGFR associated with the downregulation of c-Jun in Hep3B and Huh7 human HCC cells lines, which resulted in increased apoptotic cell death in both cell lines. Moreover, a positive correlation was clearly identified between the expression of OPN and EGFR in human HCC tissues. These data demonstrate that the OPN deficiency reduced the incidence of chemically induced HCC by suppressing EGFR-mediated anti-apoptotic signaling. An important implication of our findings is that OPN positively contributes to hepatic carcinogenesis.

Introduction

Liver cancer is the second most common cause of cancer-related death, and its incidence and mortality are prominent in East Asia, including Korea, Japan, and China (Ferlay, Shin et al. 2013). Many studies have determined that various etiologies, including chronic hepatitis B or C viral infection and cirrhosis are important risk factors for HCC (Davila, Morgan et al. 2004, Yang, Harmsen et al. 2011). Each factor or combination of these factors can give rise to an inflammatory response and DNA damage, which progress through chronic hepatitis, cirrhosis, and eventually HCC (Baffy, Brunt et al. 2012, Ringelhan and Protzer 2015, Sukowati, El-Khobar et al. 2016). Nagoshi established that HCC-associated liver disease were strongly associated with the expression of OPN in various cells, including hepatocytes, Kupffer cells, and stellate cells (Nagoshi 2014).

OPN is a secreted glycophosphoprotein that acts a ligand for its receptors, including integrins and CD44 variants, and the interactions between OPN and its receptors promote a variety of signaling pathways that eventually result in tumor progression (Lee, Wang et al. 2007). Clinical reports have found that a range of tumor tissues showed higher OPN expression than adjacent normal tissue (Dai, Bao et al. 2007, Kumar, Behera et al. 2010). Likewise, it is accepted that OPN plays a crucial role in the oncogenesis of HCC, and that OPN overexpression is positively correlated with tumor progression (Nagoshi 2014). Zhang *et al.*

established that the binding of OPN to integrin and CD44 activated MMP-2, resulting in greater invasiveness (Zhang, Pan et al. 2011). In addition, HCC patients displaying the elevated expression of OPN mRNA in tumor tissues had a higher risk of intrahepatic metastasis and early recurrence (Pan, Ou et al. 2003). Based on above findings, it is reasonable to conclude that OPN is a candidate biomarker and target for HCC therapy.

EGFR is a transmembrane growth factor which is regulated by receptor dimerization, which could be transactivated by OPN. The binding then promotes the activation of the intracellular tyrosine kinase domain of EGFR, and this cascade principally activates the mitogen-activated protein kinase (MAPK), signal transducer and activator of transcription (STAT) 3 and phosphoinositide 3-kinase/Akt pathway pathways (Liu, Tian et al. 2016, Wang 2016). Although EGFR is essential in the regulation of normal development and cell differentiation, it has been proposed that EGFR activation may be tightly linked with the carcinogenesis of solid tumors (Nuciforo, Radosevic-Robin et al. 2015, Russo, Franchina et al. 2015, Yiu and Yiu 2016). Moreover, Harada *et al.* found that cirrhotic liver tissue and HCC tumor tissue tended to show EGFR overexpression (Harada, Shiota et al. 1999).

Over the past decades, several reports have demonstrated that OPN overexpression in tumor tissues indicate more advanced tumor stages in human HCC, and that OPN is a viable marker for determining the

prognosis, in combination with other factors (Hua, Chen et al. 2011, Yoo, Gredler et al. 2011, Cheng, Wang et al. 2014). However, the role of OPN on tumor development and the underlying mechanism remain poorly understood. In this study, we assessed how OPN deficiency affected liver carcinogenesis *in vivo* through a DEN-induced mouse HCC model and *in vitro* using human HCC cell lines, with the result that OPN was overexpressed in the tumor tissue in human HCC samples. We found that OPN played an oncogenic role in DEN-induced hepatic carcinogenesis, accompanied by the upregulation of EGFR.

Materials and Methods

Induction of hepatocellular carcinoma in mouse

Male C57BL/6-Spp1^{tm1Blh} (OPN$^{-/-}$) (OPN KO) mice, purchased from Jackson Laboratory (Bar Harbor, ME, USA), and WT mice were divided into four groups (26 and 36 weeks with either OPN KO or WT) with seven mice in each group as controls. The mice at 2 weeks old were injected with 25 mg/kg of DEN (Sigma Chemical Co., St. Louis, MO, USA) or vehicle intraperitoneally once to induce hepatic carcinogenesis. Mice in the control groups were not subjected to DEN injection. All mice were sacrificed 26 and 36 weeks after the injection of DEN. This study was approved by the Institutional Animal Care and Use Committee of Seoul National University, and all experiments were performed according to the Guide for Care and Use of Laboratory Animals published by the Institute for Laboratory Animal Research (Washington, DC, USA).

Gross and histopathological examination

The mice were sacrificed after 24 hours of fasting. The liver was excised from each mouse and the number and size of nodules were measured. All liver tissue samples containing adjacent normal tissue were fixed in neutral-buffered 10% formalin. After 24 hours of fixation, the liver tissue samples were processed using a routine method, embedded in paraffin, and stained with hematoxylin and eosin for

diagnosis.

Immunohistochemical staining for OPN and TUNEL assay

In order to perform immunohistochemical staining for OPN in human and mouse tissue, replicate sections of paraffin-embedded liver tissue were mounted on silicon-coated slides, dewaxed, and rehydrated, and antigen retrieval was then performed by heating at 100° C for 20 minutes in a 0.01 M citrate buffer (pH 6.0). The inactivation of endogenous peroxidase and blocking of non-specific protein binding were relieved utilizing hydrogen peroxide and serum-free protein block solution (DakoCytomation, Glostrup, Denmark). The slides were incubated with anti-mouse or-human OPN antibody (1:100; R&D Systems, Minneapolis, MN, USA). After incubation with the primary antibody, slides were stained using the indirect labeling streptavidin avidin-biotin technique with 3-3' -diaminobenzene as a substrate.

We also performed IHC for proliferating cell nuclear antigen (PCNA) using anti-PCNA antibody (1:100; Santa Cruz Biotechnology, Santa Cruz, CA) in order to investigate whether OPN depletion affected cell proliferation.

Quantitation of immunoreactivity was performed using an H-scoring system, in which scores were calculated based on the intensity and number of positive cells according to the equation: Score = (3 × % intensely positive) + (2 × % moderately positive) + (1 × % weakly

positive).

Apoptotic cell death in mouse tissue samples and human HCC cell lines was determined through the terminal deoxynucleotidyl transferase dUTP nick-end labeling (TUNEL) assay using the Fluorecein FragEL DNA Fragmentation Detection kit (Calbiochem, Darmstadt, Germany).

Generation of OPN knock down cell lines

The human HCC cell lines Hep3B and Huh7 were purchased from the Korean Cell Line Bank (KCLB; Seoul, Korea). Hep3B and Huh7 cells were separately cultured in Dulbecco's modified Eagle medium (Gibco, Grand Island, NY, USA) or RPMI-1640 medium (Gibco) containing 10% FBS (Gibco), 1% penicillin, and streptomycin (Invitrogen Biotechnology, Grand Island, NY, USA). For the stable knockdown of the Spp1 gene in the Hep3B and Huh7 cell lines, a lentiviral vector-mediated short-hairpin RNA (shRNA) construct targeting the human Spp1 gene (Sigma-Aldrich, St. Louis, MO, USA) with the pLKO.1-puro enhanced green fluorescent protein control vector (Sigma) were produced from accession number NM_000582. The lentivirus was generated by the cotransfection of the shRNA-expressing vector and packaging vectors (Addgene) into 293Ts cell through lipofectamine 2000 (Invitrogen Biotechnology). After transfection for 48 hours, virus-containing supernatant was collected, filtered using a 0.45-μm filter, assessed for titer values, and used for viral transduction with 10 μg/mL of polybrene.

Cells were selected over the course of three days through treatment with 2 μg/mL of puromycin after viral transduction. Knockdown efficiency and OPN-related molecular changes were confirmed by quantitative real-time reverse transcription polymerase chain reaction (RT-PCR) and western blotting.

OPN transfection

cDNA containing the coding region of human OPN-a, which was subcloned into the expression vector pDest-490, was a gift from Xin Wang (Addgene plasmid # 17590) [1]. Hep3B or Huh7 cells were transfected with 500 ng of pDest490-OPN-a or pDest490 control vector using Lipofectamine 2000 (Invitrogen Biotechnology) according to the manufacturer's instructions. At the appropriate time point after transfection, the cells were harvested to perform an Annexin V assay or a western blot analysis.

Analysis of cell viability and flow cytometry for the apoptosis and cell cycle

To identify the effect of OPN on cell viability, a trypan blue exclusion assay was performed. After seeding on six-well plates at 1×10^5 cells/well and incubation for 12, 24, and 48 hours with 1% fetal bovine serum (FBS), control and short-hairpin RNA (shRNA)-mediated-OPN knockdown (KD) Hep3B and Huh7 cells were harvested, stained with

trypan blue solution, and then counted using an inverted microscope.

Next, we performed anti-human OPN antibody (R&D Systems) or recombinant human OPN (rhOPN; R&D Systems) treatment on control and OPN KD Hep3B and Huh7 to investigate the effect of secreted OPN on cell viability. Before incubation with rhOPN or anti-human OPN antibody, the minimal cytotoxic concentrations were determined. After seeding on six-well plates at 1×10^5 cells/well for 12 hours with 1% FBS, control Hep3B and Huh7 were incubated with 1 μg/mL of anti-human OPN antibody, and OPN KD Hep3B and Huh7 were incubated with 2 μg/mL of rhOPN for 12 hours. These cells were subjected to the trypan blue exclusion assay after being harvested.

For analysis of the apoptosis, control and OPN KD Hep3B and Huh7 treated with 2 μg/mL of rhOPN from the Hep3B and Huh7 lines were cultured at 2×10^5 cells/well for 24 hours with 1% FBS, and harvested, washed, and re-suspended with cold phosphate-buffered saline. Apoptotic cell death was determined using an Annexin V Apoptosis Detection Kit FITC (eBioscience, San Diego, CA, USA). Cell-associated fluorescence was measured using a FACSCalibur apparatus (BD Bioscience). We also performed a TUNEL assay and a western blot for apoptosis-related proteins. After seeding on Lab-Tek Chamber slides (Thermo Fisher Scientific, Hudson, NH) at 5×10^4 cells/well and incubation with 2 μg/mL of rhOPN for 24 hours, the TUNEL assay was performed on control, non-treated OPN KD and rhOPN-treated OPN KD

Hep3B and Huh7. Similarly, control and OPN KD Hep3B and Huh7 incubated with 2 μg/mL of rhOPN from both cells were harvested and lysed at appropriate time points for western blotting.

RNA extraction, RT-PCR and quantitative real-time RT-PCR

The total RNA from Hep3B and Huh7 cells was extracted using the RNeasy Plus Mini kit (Qiagen, Hilden, Germany), and 500 ng of total RNA from each sample was reverse-transcribed using the QuantiTect Reverse Transcription kit (Qiagen) and analyzed by quantitative real-time RT-PCR using the Rotor-Gene SYBR Green PCR kit (Qiagen) with specific primers. The amplification and quantitation of target genes were performed using the Rotor-Gene Q and the manufacturer-provided software (Qiagen). The amount of the target gene was calculated using mRNA encoding glyceraldehyde 3-phosphate dehydrogenase (GAPDH) as a housekeeping gene. The amplified target genes were also loaded on 2% agarose gel. The primer pairs for human genes were F: 5'-GCC AAG GCA CGA GTA ACA AGC-3' and R: 5'-AGG GCA ATG AGG ACA TAA CC-3' for EGFR, F: 5'-TGA AAC GAG TCA GCT GGA TGA CCA-3' and R: 5'-GCT CTC ATC ATT GGC TTT CCG CTT-3' for OPN and F: 5'-GAG TCA ACG GAT TTG GTC G-3' and R: 5'-TGG AAT CAT ATT GGA ACA TGT AAA C-3' for GAPDH.

Western blotting

The total protein of the cells was extracted using the RIPA II Cell Lysis Buffer (GenDEPOT, Barker, TX, USA) supplemented with a protease inhibitor cocktail (GenDEPOT) and phosphatase inhibitor cocktail (GenDEPOT). The cell fraction for extracting nuclear proteins was performed using the Qproteome Cell Compartment Kit (Qiagen). Equal amounts of protein (25 μg) from cell pellets were loaded by sodium dodecyl sulfate-polyacrylamide gel electrophoresis (SDS-PAGE) on 10% or 12% gels and transferred onto 0.2-μm nitrocellulose membranes (GE Healthcare, Buckinghamshire, UK). Proteins were detected with one of the following antibodies: anti-human OPN (1:500; R&D Systems), anti-EGFR (1:1000; Santa Cruz Biotechnology), anti-ERK1/2 (1:1000; Cell Signaling Technology, Danvers, MA), anti-phosphorylated ERK1/2 (1:1000; Cell Signaling Technology), anti-caspase 3 (1:1000; Santa Cruz Biotechnology), anti-caspase9 (1:1000; Santa Cruz Biotechnology), anti-Bcl-2 (1:1000; Cell Signaling Technology), anti-Bcl-xL (1:1000; Cell Signaling Technology), anti-c-Jun (1:500; Santa Cruz Biotechnology), anti-lamin A (1:1000; Abcam, Cambridge, MA), or anti-PARP-1 (1:1000; Santa Cruz Biotechnology) antibody. The membranes were then incubated with horseradish peroxidase-conjugated rabbit anti-goat IgG antibody (GenDEPOT) or goat anti-rabbit IgG antibody (Millipore, Billerica, MA, USA), as appropriate. GAPDH (Cell Signaling Technology) was used as an internal

control.

Tissue microarray-based immunohistochemical staining of OPN and EGFR in human hepatocellular carcinoma tissues

Tissue-microarray (TMA) slides containing 58 HCC samples were purchased from SuperBioChips Laboratories (Seoul, Korea, www.tissue-array.com). Immunohistochemistry (IHC) for OPN and EGFR on serially sectioned TMA slides was carried out using the BOND-MAX automated immunostainer (Leica Microsystems, Bannockburn, IL, USA) with the Bond Polymer Refine detection kit (Leica). Anti-OPN antibody (1:50; R&D Systems) or anti-EGFR antibody (1:100; Ventana Medical Systems, Oro Valley, AZ, USA) were employed as the primary antibody. Each stain was assessed according to the intensity (negative, 0; weak, 1; moderate, 2; intense, 3) and area (none, 0; focal, 1; multifocal, 2; diffuse, 3) of positive cells. The overall grade of each stain was obtained by multiplying the area score by the intensity score (negative, 0; weak, 1 or 2; moderate, 3 or 4; intense, 6 or 9).

Statistical analysis

All data are expressed as means ± standard errors (SEMs). Statistical analyses were performed using GrapH. pyloriadPrism6 (version 6.0; GraphPad Software, San Diego, CA). The comparison between OPN expression in tumor tissues and non-tumor tissues of

mouse and human liver tissues was analyzed using paired two-tailed Student's *t*-test. The relationship between OPN genotype and the incidence of hepatocellular adenoma or carcinoma was analyzed using the Chi-squared test. Correlations between OPN expression and clinicopathological features or EGFR expression were analyzed using the Spearman's correlation test. Other data were analyzed using the unpaired two-tailed Student's *t*-test. *P*-values less than 0.05 were regarded statistically significant.

Results

Lack of OPN suppresses DEN-induced hepatocarcinogenesis

Macroscopically, the nodules displayed protruding single-to-multiple polypoid patterns in both the WT and OPN KO mice at 36 weeks after DEN injection. The properties of the nodules are summarized in Table 1. The size of the nodules in the OPN KO mice (1.2 ± 0.2 mm) was significantly smaller than that of WT mice (7.3 ± 1.8 mm; $P<0.01$), although the multiplicity was not significantly different between OPN KO mice (3.9 ± 0.9) and the WT mice (4.9 ± 1.3).

A histological analysis at 36 weeks after DEN injection showed a significantly lower prevalence of liver tumors in the OPN KO mice (14.3%) than in the WT mice (61.5%; $P<0.05$), and two of the eight tumor-bearing WT mice exhibited HCC (15.4%). Microscopically, the neoplastic nodules from the OPN KO mice at 36 weeks were sharply demarcated and consisted of well-differentiated neoplastic cells exhibiting trabecular patterns (Figure. 1A). WT mice at 36 weeks showed similar histologic pattern but larger neoplastic nodules bulging from the capsular surface (Figure 1A). Meanwhile, HCC from WT mice at 36 weeks consisted of poorly differentiated neoplastic cells showing solid growth pattern with irregular border (Figure 1A). In contrast, OPN KO mice at 26 weeks after DEN injection showed a 13.3% incidence rate of hepatocellular adenoma, whereas WT mice did not have liver tumors at

this time point, although this tendency was not found to be statistically significant. The neoplastic nodules from the OPN KO mice at 26 weeks showed similar histopathological features to nodules from the OPN KO mice at 36 weeks (Figure 1A).

Table 1. Incidence and multiplicity of DEN-induced liver tumors in mice.

OPN genotype	DEN treat	Weeks after DEN	Mice (n)	Tumor-bearing mice (%)	Hepatocellular adenoma (%)	Hepatocellular carcinoma (%)	Tumor multiplicity	Tumor size diameter (mm)
WT	Yes	26	14	0	0	0	0	0
KO	Yes	26	15	2/15 (13.3)	2/15 (13.3)	0	1.7 ± 0.5	0.8 ± 0.3
WT	No	26	7	0	0	0	0	0
KO	No	26	7	0	0	0	0	0
WT	Yes	36	13	8/13 (61.5)	8/13 (61.5)	2/13 (15.4)	4.9 ± 1.3	7.3 ± 1.8
KO	Yes	36	14	2/14 (14.3) *	2/14 (14.3)	0	3.9 ± 0.9	1.2 ± 0.2 **
WT	No	36	7	0	0	0	0	0
KO	No	36	7	0	0	0	0	0

Data are presented as means±SEMs. * $P < 0.05$ and ** $P < 0.01$ versus WT mice.

OPN, osteopontin; DEN, diethylnitrosamine; WT, wild-type; KO, knockout

OPN expression is increased in tumor tissues of human hepatocellular carcinoma

Based on our results, we performed IHC for OPN in tumor-bearing WT mice, and six of the eight WT mice demonstrated a significantly higher degree of OPN expression in the cytoplasm of tumor cells compared to adjacent normal areas (P<0.01; Figure 1Ba-b and C). Although this observation was based on only two cases, the degree of OPN expression was stronger in carcinomas than in adenomas (Figure 1Ba-b).

We also carried out IHC for OPN in eight cases of human HCC. Similarly to the mouse results, seven of the eight cases showed higher OPN expression (Figure 1Bc-d). Tumor tissue from those seven cases showed diffuse and moderate to strong OPN expression in the cytoplasm of tumor cells, whereas OPN expression was rarely or weakly observed in the paired non-tumor tissue (P<0.001; Figure 1Bc-d and C). In particular, tumor cells located on the boundary of tumor tissue prominently expressed OPN in all eight cases (Figure 1Bd).

A

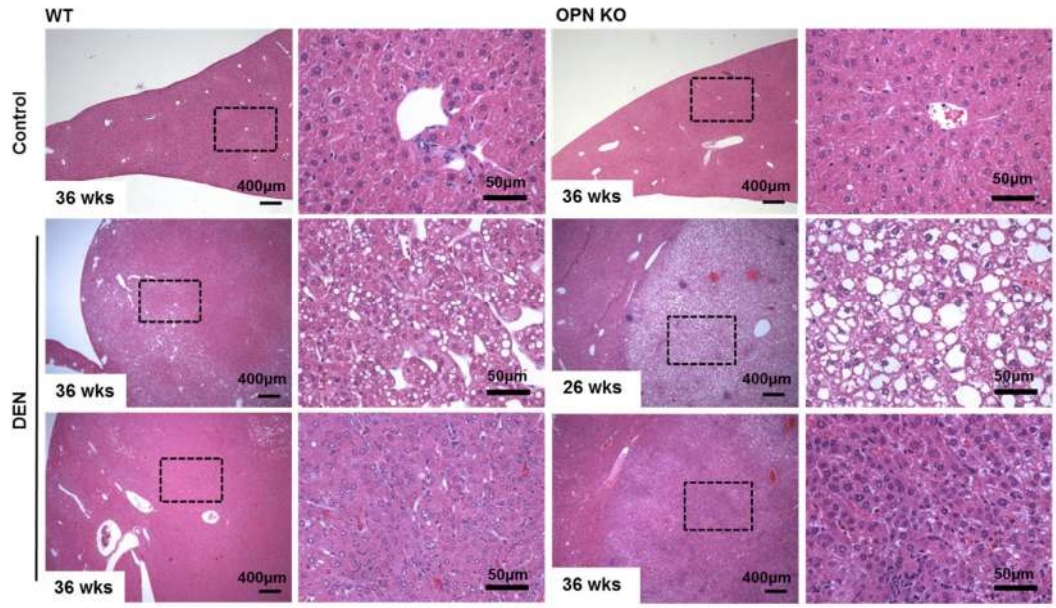

B

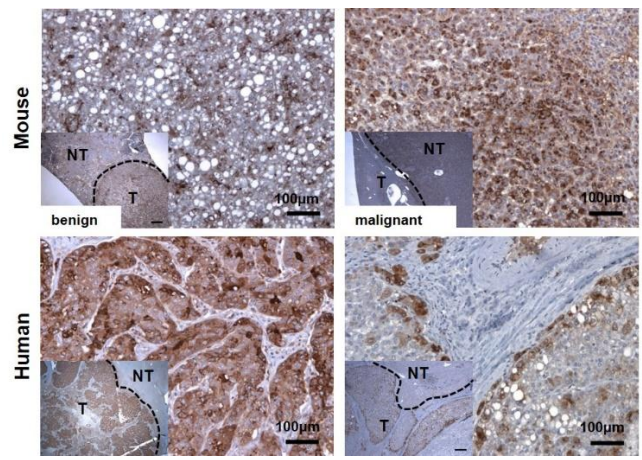

C

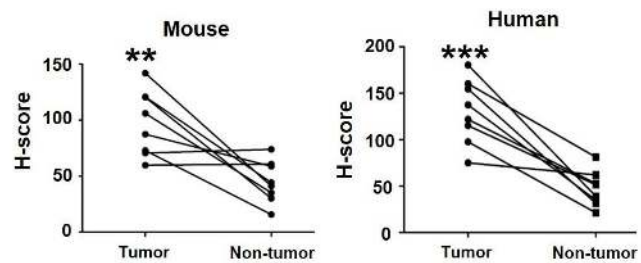

Fig 1. The histopathology and immunohistochemistry (IHC) for OPN (A) H&E staining in liver tissues from tumor-bearing WT and OPN KO mice. Boxed regions of left panels in WT and OPN KO are shown at higher magnification in the right panels. The nodules from the OPN KO mice at 26 and 36 weeks were sharply circumscribed, and composed of well differentiated tumor cells or vacuolated cells that formed trabeculae or nest, whereas the nodules from the WT mice at 36 weeks showed sessile and solid growth pattern. (B, C) IHC and quantitation for OPN in mouse and human liver tissues. The tumor tissues showed higher cytoplasmic expression of OPN compared with non-tumor tissues in both mouse (a, b) and human (c, d) samples. In mouse, hepatocellular carcinoma (b) displayed more prominent OPN expression compared with hepatocellular adenoma (a). $^{**}P < 0.01$ or $^{***}P < 0.001$ *versus* non-tumor tissues.

OPN depletion promotes apoptotic cell death in mouse liver

Next, we characterized the effect of OPN on apoptotic cell death in mouse liver tissue. Compared with WT mice at 26 weeks after DEN injection, non-tumor tissue from OPN KO mice showed a greater number of TUNEL-positive apoptotic hepatocytes (Figure 2A and B). In tumor tissue from mice at 36 weeks after DEN injection, the apoptotic index was considerably higher in the OPN KO mice than WT mice (Figure 2A and B). The extent of apoptotic cell death in non-tumor tissue from OPN KO mice was also greater than in the corresponding samples obtained from WT mice (Figure 2A and B). These results suggest that increased apoptosis in normal hepatocytes and in tumor cells of OPN KO mice may inhibit hepatic carcinogenesis.

Meanwhile, we also performed IHC for PCNA to investigate whether OPN depletion affects cell proliferation. At 26 and 36 weeks after DEN injection, WT mice displayed higher frequency of PCNA-positive hepatocytes in non-tumor tissues compared with OPN KO mice, however, statistical significance was not detected (Fig. 3).

A

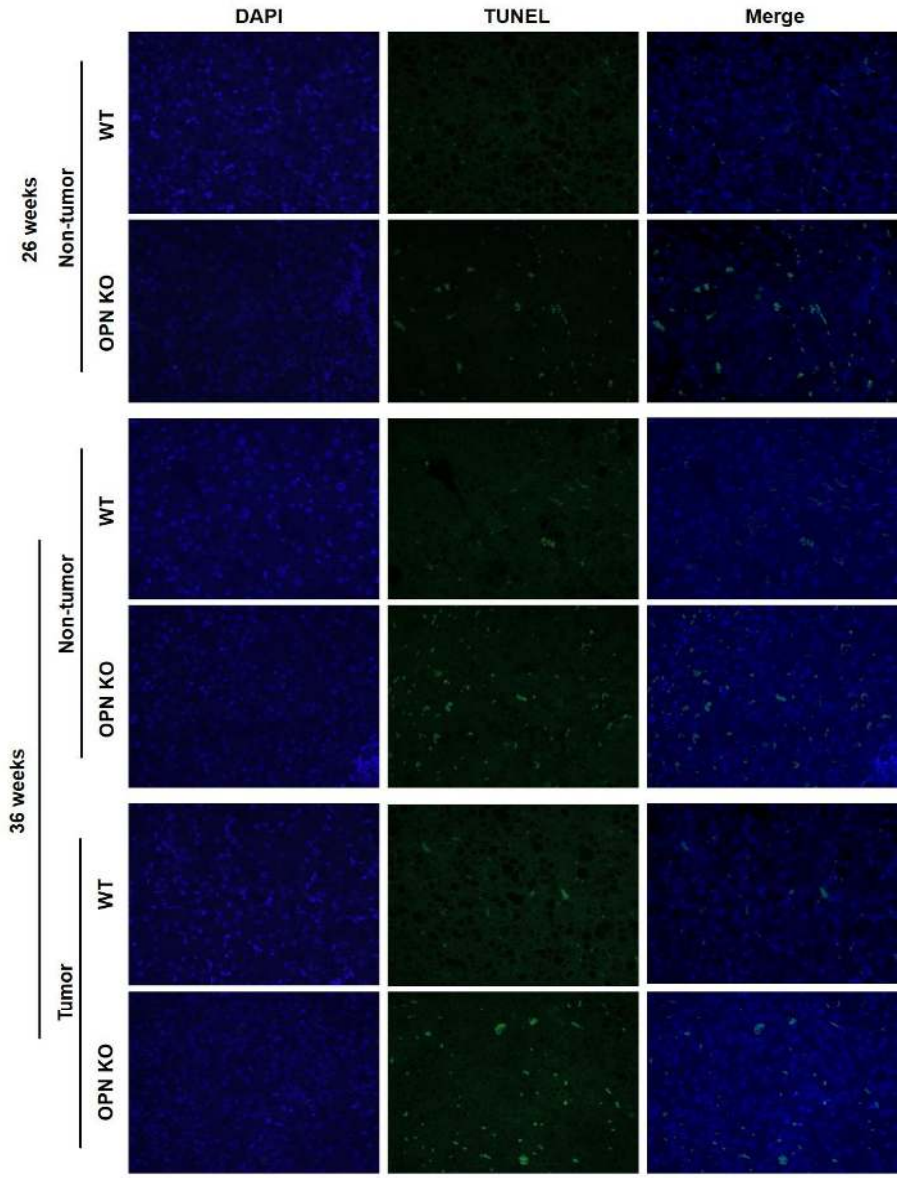

B

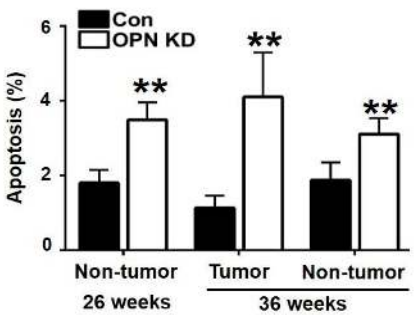

Fig 2. Apoptotic cell death in the mouse liver tissues. (A) Representative photomicrographs of total cells and TUNEL-positive cells in the liver tissues of wild-type (WT) and osteopontin knockout (OPN KO) mice exposed to DEN. The apoptotic index in non-tumor tissues of OPN KO mice at 26 weeks was considerably higher than that in WT mice. At 36 weeks, OPN KO mice also showed significantly larger numbers of apoptotic cell in non-tumor and tumor tissues compared with WT mice. (B) Results are presented as means±SEMs (n=3-4 for non-tumor tissues of WT and OPN KO mice, n=3-4 for tumor tissues of WT mice and n=2 for tumor tissues of OPN KO mice). $^{**}P < 0.01$ *versus* WT mice.

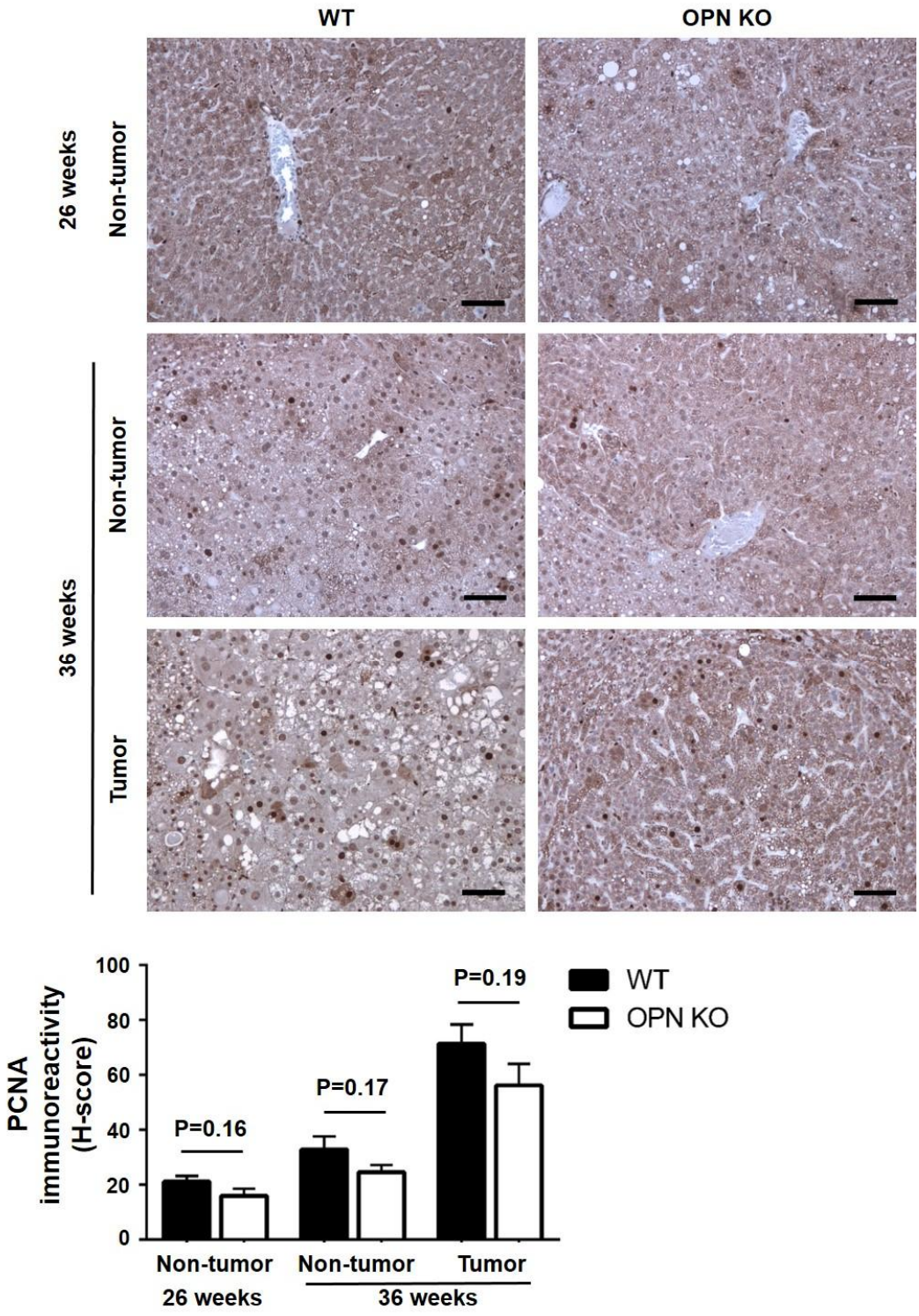

Fig 3. Proliferation in the mouse liver tissues. At 26 and 36 weeks after DEN injection, WT mice displayed more PCNA-positive hepatocytes in non-tumor and tumor tissue samples than did OPN KO mice; however, this tendency was not found to be statistically significant. Results are presented as means±SEMs (n=3-4 for non-tumor tissues of WT and OPN KO mice, n=3-4 for tumor tissues of WT mice and n=2 for tumor tissues of OPN KO mice).

OPN increases cell viability through the inhibition of apoptotic cell death

As observed in mouse liver tissue, OPN is hypothesized to have a negative effect on apoptotic cell death. In order to investigate the effect of OPN on cell viability and apoptosis in human HCC, we compared growth rates between control and OPN KD Hep3B and Huh7. After incubation for 24 hours, the OPN KD Hep3B and Huh7 showed a lower number of cells than the control cells did, and the growth rate differential was more prominent at 48 hours in the Hep3B cells (Fig. 4A).

Furthermore, rhOPN treatment of OPN KD Hep3B and Huh7 at 12 hours after seeding restored cell viability to a similar degree as observed in control cells (Fig. 4B). Accordingly, treatment of OPN antibody on control Hep3B and Huh7 decreased cell viability, but not to a significant extent (Fig. 4B). In order to clarify the role of OPN in cell viability, we also carried out an annexin V assay and a TUNEL assay. The increased proportion of early apoptotic cells in OPN KD Hep3B and Huh7 diminished in rhOPN-treated OPN KD Hep3B and Huh7 (Fig. 4C). The TUNEL assay results also indicated that rhOPN treatment reduced apoptotic cell death in OPN KD Hep3B and Huh7 (Fig. 5A). However, supplemental OPN antibody to control Hep3B and Huh7 had relatively minimal effect on early and late apoptosis in the annexin V assay (Fig. 6A)

Consistent with the TUNEL assay results, OPN KD Hep3B and Huh7 showed lower expression levels of anti-apoptotic proteins (Bcl-xL and

Bcl-2) and higher expression levels of pro-apoptotic proteins (cleaved PARP-1, caspase 9, and caspase 3) than control cells (Fig. 5B). However, the expression levels of these proteins in the OPN KD Hep3B and Huh7 were similar to those observed in control cells following rhOPN treatment (Fig. 5B). Although the changes of apoptotic cell death in the annexin V assay were not remarkable, the expression levels of pro-apoptotic proteins (cleaved PARP-1 and caspase 3) in Hep3B and Huh7 were increased by the incubation with the OPN antibody (Fig. 6B).

A

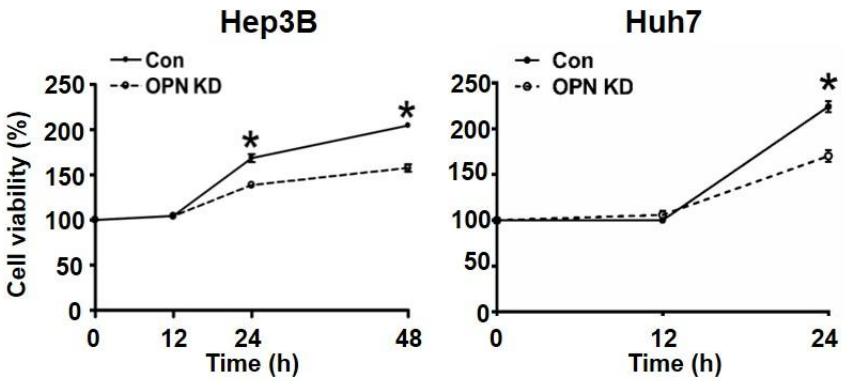

B

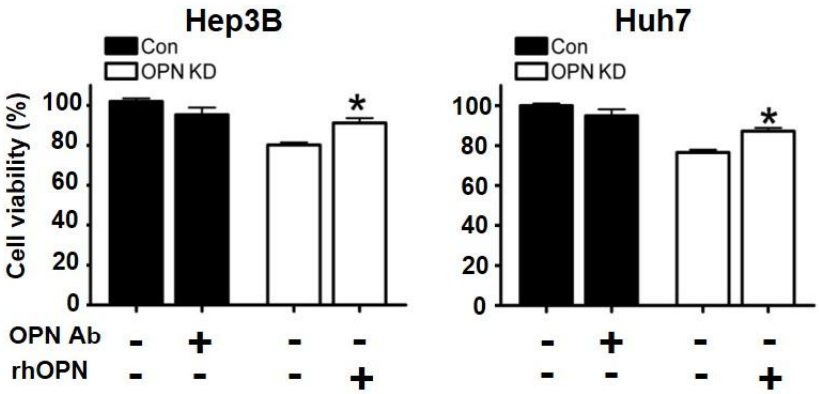

C

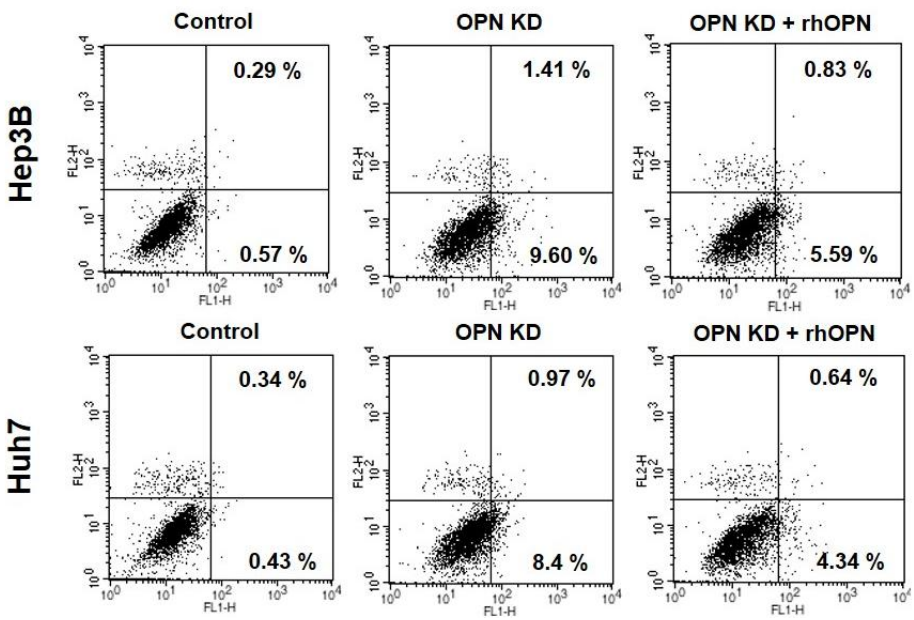

Fig 4. Effect of OPN downreguation on cell viability. (A) Cell viability of Hep3B and Huh7 cell lines at each time point. OPN knockdown (OPN KD) cells of both cell lines at 24 hours showed lower cell viability compared with control cells, and cell viability of Hep3B was also decreased by OPN suppression at 48 hours. # Cell viability of Huh7 at 48 hours was not assessed due to saturation. Results are presented as means±SEMs (n=6 for each time point, three independent experiments). (B) Change of cell viability according to the treatment of OPN antibody (Ab) or recombinant human OPN (rhOPN). The blockade of secreted OPN by OPN Ab in control cells caused to the decrease of cell viability though statistical significance was not observed. The supplement of rhOPN on OPN KD cells considerably increased cell viability in both cell lines. Results are presented as means±SEMs (n=6 for each condition, three independent experiments). (C) Assessment for apoptotic cell death. Early and late apoptosis (lower and upper right quadrants) were more frequently observed in OPN KD cells of both cell lines. The supplement of rhOPN on OPN KD cells caused the decreases of apoptosis.

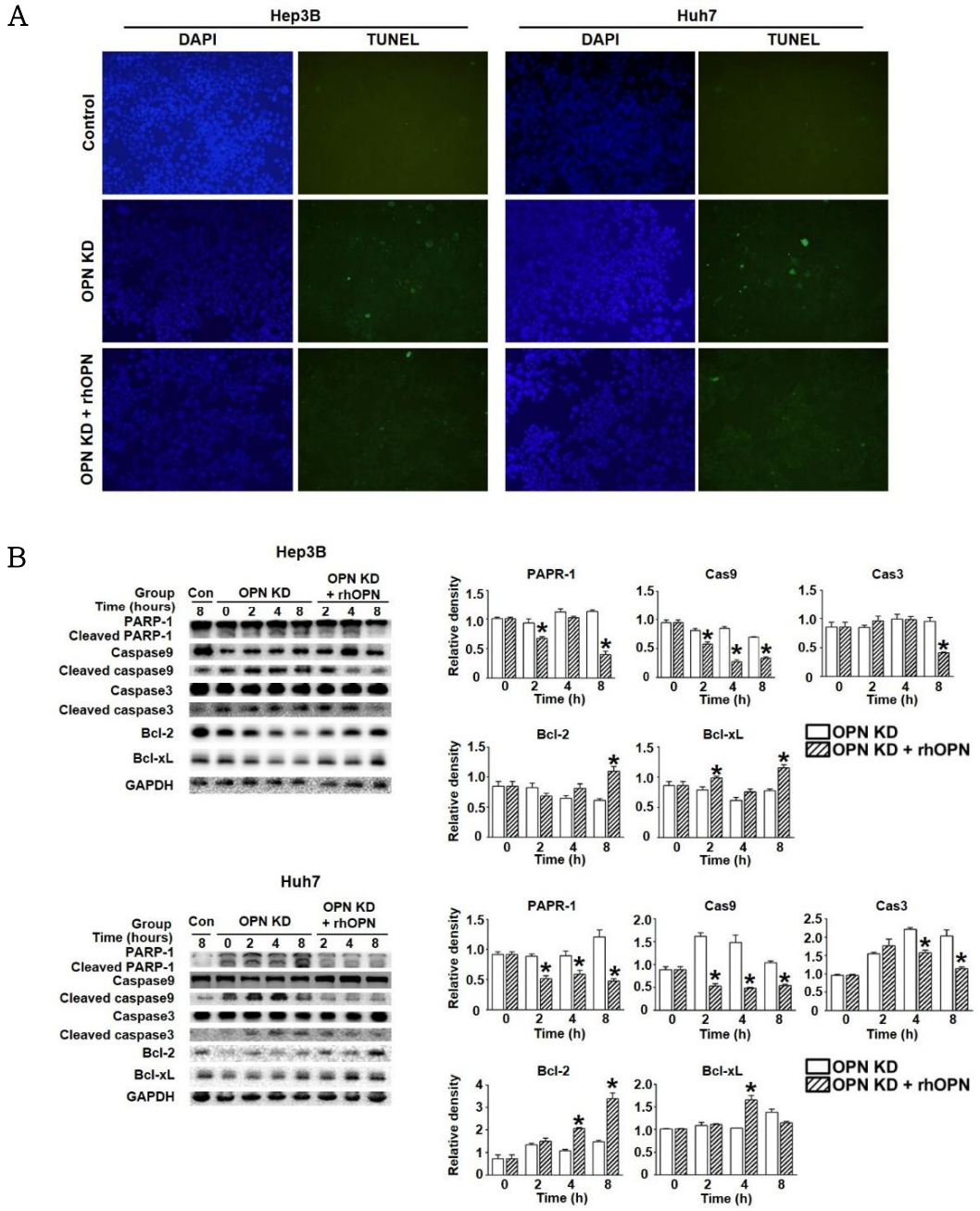

Fig 5. Change of apoptosis in relation to OPN suppression. (A) TUNEL assay in Hep3B and Huh7 cell lines. OPN KD cells of both cell lines showed higher frequency of TUNEL-positive cells compared with control cells, and rhOPN treatment on OPN KD cells decreased apoptotic cell death. (B) Western blotting for pro-apoptotic proteins, PARP-1, caspase9 and caspase3 and anti-apoptotic protein, Bcl-2 and Bcl-xL. Relative expression levels of apoptosis-related proteins in Hep3B (upper panels) or Huh7 cells (lower panels). The cleavages of PARP-1, caspase9 and caspase3 in OPN KD cells of both cell lines were suppressed by the supplement of rhOPN, while the expressions of anti-apoptotic proteins were upregulated. Results are presented as means±SEMs (n=3 for each condition). * $P < 0.05$ *versus* OPN KD cells under the respective culture condition.

A

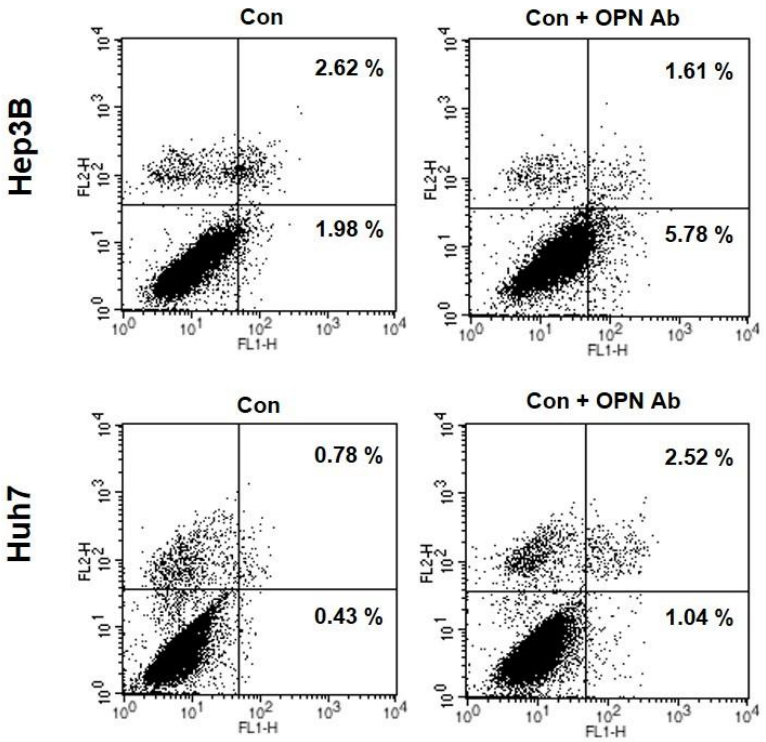

B

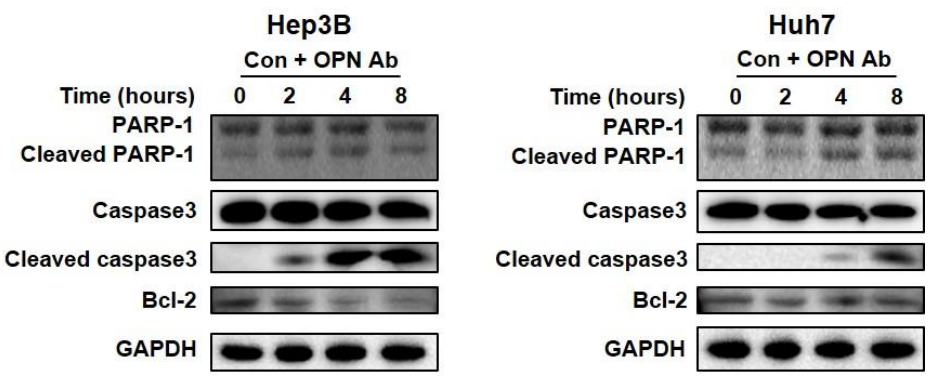

Fig 6. Annexin V assay and western blot for apoptosis. (A) There were observed that a slightly increased proportion of early or late apoptosis in Hep3B and Huh7 cells incubated with anti-OPN antibody. (B) Control shRNA-transfected Hep3B and Huh7 cells showed increased expressions of cleaved PARP-1 and caspase3 depending on the incubation with anti-OPN antibody in a time-dependent manner.

OPN upregulates EGFR expression and related signaling pathway

We then investigated the mRNA and protein levels of EGFR and related molecules depending on OPN expression. IHC demonstrated that WT mice at 36 weeks after DEN injection showed extensive EGFR expression in the cellular membranes, while weakly positive expression was observed in OPN KO mice (Fig. 7A). *In vitro*, the mRNA level of EGFR and the protein level of nuclear c-Jun were significantly decreased by OPN suppression in the Hep3B and Huh7 (Fig. 7B). Likewise, EGFR, phosphorylated ERK1 expression in OPN KD Hep3B and Huh7 were lower than was observed in control cells (Fig. 7C). The expression levels of EGFR and phosphorylated ERK in OPN KD Hep3B and Huh7 were increased by supplemental rhOPN in a time-dependent manner (Fig. 7D).

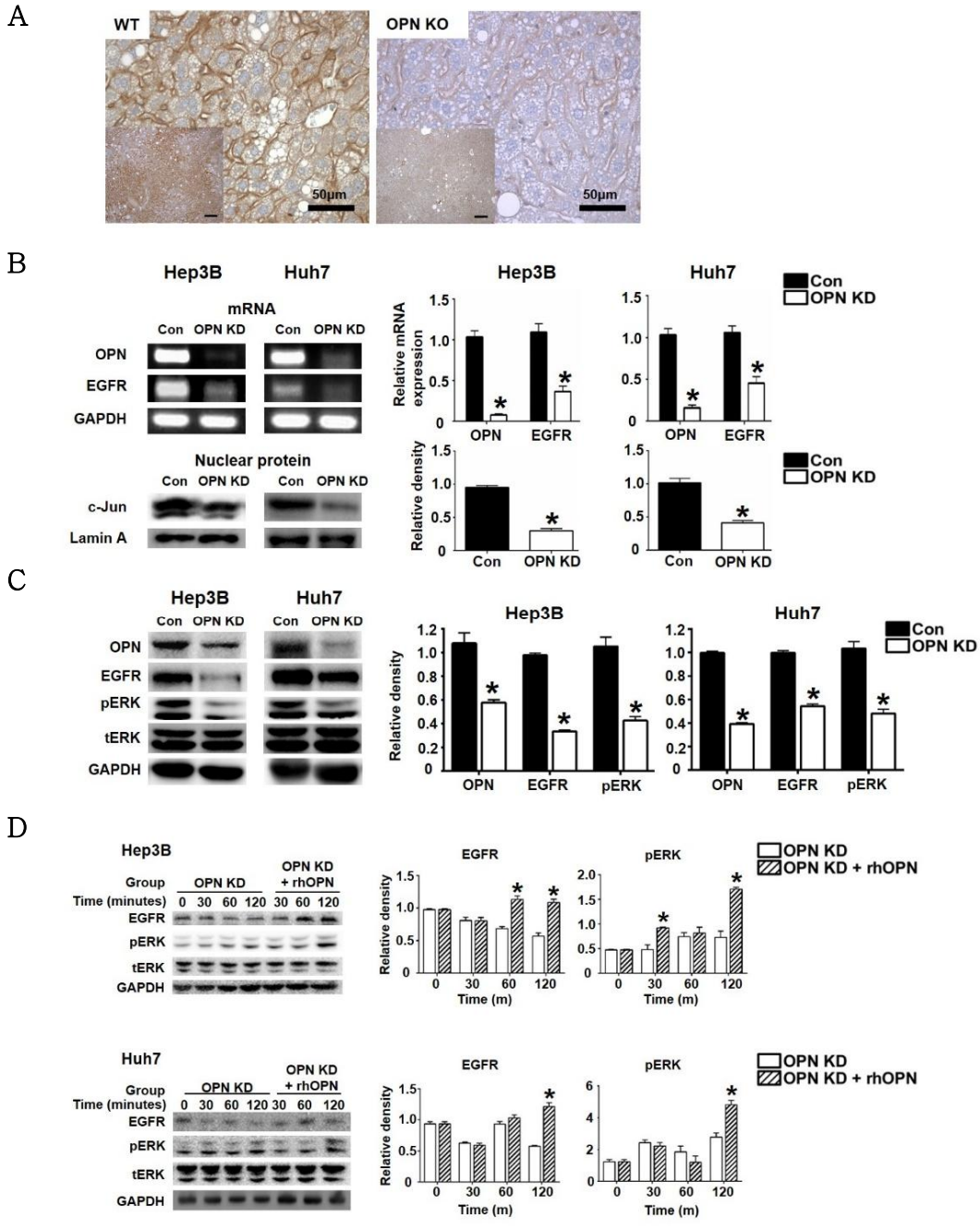

Fig 7. The regulatory effect of OPN on EGFR expression (A) Representative photomicrographs of IHC for EGFR in liver tissues of WT and OPN KO mice at 36 weeks after DEN injection. EGFR expression in cellular membrane of hepatocytes was stronger in WT mice compared with OPN KO mice. *Bar* = 400 μm (inserts) (B) RT-PCR and western blot for EGFR and c-Jun. OPN suppression caused the decrease of EGFR transcription, accompanied by the downregulation of nuclear c-Jun expression in Hep3B and Huh7 cell lines. Results are presented as means±SEMs (n=4). * $P < 0.05$ *versus* control cells. (C) Western blot for EGFR and ERK. OPN KD cells of both cell lines showed decreased expression levels of EGFR and phosphorylated ERK1. Results are presented as means±SEMs (n=4). * $P < 0.05$ *versus* control cells. (D) Western blot for EGFR and ERK according to the supplement of rhOPN on OPN KD cells. The expression of EGFR and phosphorylated ERK were increased by rhOPN treatment in a time-dependent manner. Results are presented as means±SEMs (n=3 for each condition). * $P <$ 0.05 *versus* OPN KD cells.

OPN expression is positively correlated with EGFR expression in human hepatocellular carcinoma tissues.

EGFR expression showed significantly positive correlation with OPN expression in HCC tissues (P<0.01, r=0.3567; Fig 8B). In cases where OPN expression was moderate or strong positive, 85.3% (29/34) exhibited moderate or strong positive expression of EGFR (Fig. 8A and B). Conversely, in the 24 cases showing negative or weakly positive expression of OPN, negative or weak positive expression of EGFR was observed in 15 cases (62.5%) (Fig. 8A and B).

We also found that the degree of OPN expression was correlated with the pTNM stage (P<0.05; Fig. 8B). More than half of the samples displayed a negative or weakly positive expression of OPN in stage I or II patients (Fig. 8B); however, moderate to strongly positive expression of OPN was observed in 66.7% and 80% of stage III and IV samples, respectively (Fig. 8B).

A

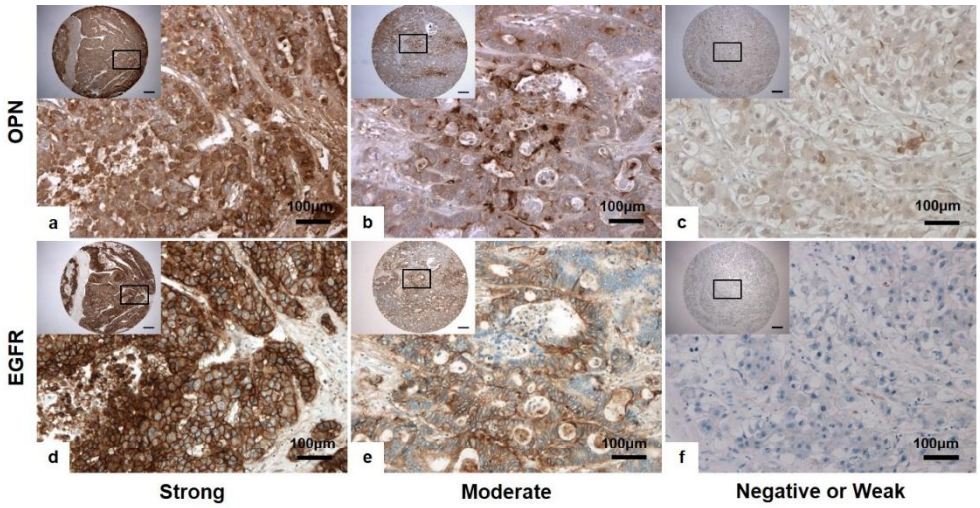

B

	OPN Expression				P-value
	Negative (n=4)	Weak (n=20)	Moderate (n=28)	Strong (n=6)	
pTNM stage					
Ⅰ (n=13)	3	6	3	1	Spearman r=0.3307 p<0.05
Ⅱ (n=18)	1	7	7	3	
Ⅲ (n=12)	0	4	8	0	
Ⅳ (n=15)	0	3	10	2	
EGFR expression					
Negative	0	1	0	0	Spearman r=0.3567 p<0.01
Weak	3	11	5	0	
Moderate	0	2	16	2	
Strong	1	6	7	4	

Fig 8. Immunohistochemistry (IHC) for OPN and EGFR in human HCC tissues. (A) Representative photomicrographs of IHC for OPN and EGFR. Serial sectioned human HCC samples showing strong (a, e), moderate (b, e) and weak expression of OPN and EGFR (c, f). *Bar* = 400 μm (inserts). (B) Correlation between OPN expression and pTNM stages and iNOS expression.

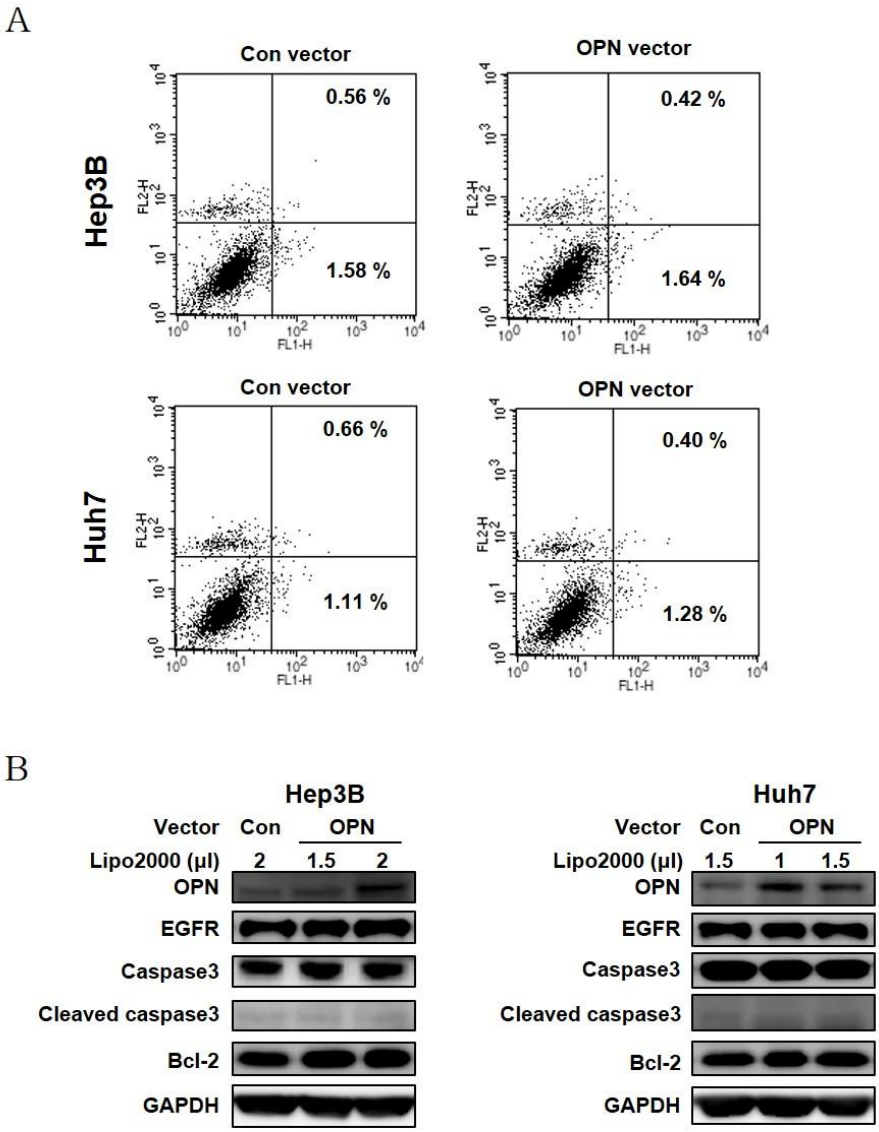

Fig 9. Annexin V assay and western blot for apoptosis in OPN overexpression. pDest-490-OPN-a vector transfection for OPN overexpression neither cause decreased apoptotic cell death (A) nor significant change of the expression levels of EGFR and apoptotic proteins (B).

Discussion

In the past decades, OPN has been found to play an important role in oncogenic processes contributing to HCC and liver cirrhosis (Sun, Dong et al. 2008, Fouad, Mohamed et al. 2015). Huang *et al.* showed that plasma OPN levels were positively correlated with hepatitis C virus infection and the grades of hepatic inflammation and fibrosis in human patients (Huang, Zhu et al. 2010). A previous study found that nonalcoholic steatohepatitis–related cirrhosis was increased by Hedgehog pathway–mediated OPN overexpression (Syn, Choi et al. 2011). In the present study, we focused on the effect of OPN on the development of chemically induced HCC and the underlying mechanism involving apoptosis. We showed that hepatic carcinogenesis was considerably inhibited by OPN deficiency at 36 weeks, accompanied by the increase of apoptotic cell death in OPN KO mice. Meanwhile, OPN KO mice at 26 weeks showed the development of hepatocellular adenoma in 2/15 mice, whereas WT mice had no tumors; there were no statistical significance. In comparison with the incidence of tumor at 26 weeks, no increase of tumor incidence at 36 weeks was observed in OPN KO mice, 8/13 WT mice had hepatocellular adenoma and carcinoma. Based on these results, tumor development and progression worsened by OPN. OPN expression was prominent in the tumor tissue of WT mice, whereas adjacent liver tissue rarely showed OPN expression. Similarly, strong

OPN expression was noted in most of human HCC samples. These results correspond to previous clinical studies that found OPN overexpression to be positively correlated with tumor progression.

Apoptosis is an essential process for maintaining homeostasis in normal tissue, and is connected with carcinogenesis because tumor cells may be able to evade apoptotic stimuli (Chiche, Rouleau et al. 2010). In a previous study, we suggested that OPN protected gastric epithelial cells and cancer cells from inducible nitric oxide synthase-mediated apoptosis through STAT1 downregulation, thereby promoting the development and progression of gastric cancer (Lee, Park et al. 2015). Likewise, some studies have reported that OPN played an important role in inhibiting apoptosis (Zhang, Liu et al. 2010, Zhang, Guo et al. 2014). In a mouse model, Hsieh *et al.* found that OPN deficiency promoted apoptosis and delayed the development of squamous papilloma (Hsieh, Juliana et al. 2006). In addition, it has been demonstrated through IHC that the anti-apoptotic effect of OPN may be related to the regulation of nuclear factor-kappa B (NF-κB) expression in human renal cell carcinoma (Matusan-Ilijas, Damante et al. 2011). In accordance with these results, we demonstrated that the tumor tissue samples and non-tumor tissue samples of OPN KO mice displayed a higher apoptotic index than was observed in WT mice, and that OPN suppression in human HCC cells also promoted apoptotic cell death. Previous studies have shown that OPN has two isoforms: a secreted form (sOPN) and an intracellular form (iOPN),

generated by alternative translation (Tilli, Mello et al. 2012). Based on the observation that the supplemental provision of rhOPN to OPN KD human HCC cells inhibited apoptosis, and that OPN overexpression in cells rarely affect cell viability and apoptotic cell death in the present study, it may be hypothesized that the anti-apoptotic effect of OPN is due to sOPN rather than iOPN (Fig. 9). Some reports support the possibility that the role of OPN in apoptotic cell death is mediated by interactions between OPN and its surface receptors with related downstream signaling. Zhao *et al.* previously found that OPN downregulation led to the inhibition of integrin expression, which could block the activity of NF-κB (Zhao, Dong et al. 2008). In addition, binding to the CD44 variants was able to exert significant suppressive effects on apoptosis of tumor cells through the phosphoinositide 3-kinase/Akt pathway (Lin and Yang-Yen 2001). Our data suggest that the increased apoptosis of hepatocytes and tumor cells may cause the suppression of hepatic carcinogenesis in OPN KO mice.

Next, we evaluated EGFR expression according to OPN regulation in order to explore the underlying mechanism through which OPN suppresses apoptosis. It has been confirmed that EGFR and downstream signaling significantly contribute to the carcinogenesis of various epithelial cancers (Rao, Janakiram et al. 2015, Xu, Lin et al. 2016). Similarly, EGFR blockade dramatically enhanced the apoptosis of cancer cells induced by ultraviolet radiation and chemotherapeutic agents (Jin,

Chen et al. 2012). In human cancer, sustained EGFR activation is commonly observed due to EGFR overexpression or the mutation of EGFR, leading to various tumor-promoting activities, including the inhibition of apoptosis (Peraldo-Neia, Migliardi et al. 2011, Guo, Gong et al. 2015). This anti-apoptotic effect of EGFR is mediated by the MAPK/ERK kinase (MEK)/MAPK signaling pathway in many types of normal cells as well as cancer cells (Zenz, Scheuch et al. 2003, Sordella, Bell et al. 2004). In agreement with previous studies, we found that WT mice showing a high EGFR expression level presented a lower apoptotic index in comparison to OPN KO mice, and that OPN suppression led to decreased EGFR expression and phosphorylation of ERK, as well as increased apoptotic cell death in human HCC cells. The activity of EGFR can be regulated ligand-dependently or transcriptionally, and the latter is mediated by promoter-binding factor (Guo, Gong et al. 2015, Wang 2016). Zenz *et al.* previously demonstrated that c-Jun, a member of the activator protein 1 family, played a crucial role in the transcriptional regulation of EGFR expression in a c-Jun conditional KO mice model (Zenz, Scheuch et al. 2003). They also showed that the lack of c-Jun ultimately led to apoptosis in keratinocytes. Based on this previous finding, we investigated the expression level of c-Jun depending upon OPN regulation, and found that c-Jun expression was suppressed by shRNA-mediated OPN KD. Additionally, it may have been the case that c-Jun-mediated EGFR expression was regulated by secreted OPN,

since supplemental rhOPN in OPN KD human HCC cells (not OPN overexpression) led to upregulated EGFR expression (Figure S3B). In combination with previous studies, our findings suggest that OPN is an important factor for inducing c-Jun-mediated EGFR transcription, resulting in the inhibition of apoptotic cell death.

In conclusion, we showed that OPN deficiency inhibited DEN-induced hepatic carcinogenesis in a mouse model, which could be linked with increased apoptotic cell death. In addition, *in vitro* study suggested the possibility that the anti-apoptotic effect of OPN may be related to the transcriptional upregulation of EGFR and the activation of the downstream molecule, p-ERK, which is mediated by c-Jun. Likewise, a positive correlation between OPN and EGFR expression was also identified in human HCC tissue as shown in a previous study (Tsai, Tsai et al. 2012). Though we concentrated on the effect of OPN on apoptosis in this study, OPN and related signaling also involve in cell proliferation, invasion and metastasis. Yoo *et al.* and Zhao *et al.* have previously described these roles of OPN in HCC using an *in vitro* and xenograft model (Zhao, Dong et al. 2008, Yoo, Gredler et al. 2011). On the other hand, Fan *et al.* proposed that OPN deficiency aggravates DEN-induced hepatic carcinogenesis based on the size and multiplicity of liver tumor. It was a new perspective in the roles of OPN in carcinogenesis (Fan, He et al. 2015). While they mainly focused on the roles of OPN in tumor progression because liver tumors developed in all mice at 36 weeks after

the injection of DEN, our mouse study could more logically explain the effect of OPN deficiency on tumor development considering many previous studies on the tumor-promoting effects of OPN. In the present study, we focused on the role of OPN in hepatocyte and cancer cells based on the histopathologic findings and IHC results from mouse and human HCC samples. However, further studies using liver-specific OPN KO mice rather than whole tissue-OPN KO mice or a comparison of these two types of OPN KO mice could be useful for determining the role of OPN in hepatic carcinogenesis in greater detail because human HCC can be closely related to immune response against to cellular damage and infectious agents. Despite some limitations of this study, our findings suggest that OPN directly contributes to the development of HCC, which is positively correlated with the EGFR-mediated anti-apoptotic effect. Therefore, the induction of apoptosis in cancer cells through targeting OPN and EGFR may be a helpful approach for the prevention and treatment of human HCC.

국문초록

마우스 위암과 간암 모델에서 Osteopontin 단백질의 역할

이 수 형

지도 교수: 김 대 용

서울대학교 대학원 수의학과 수의병리학 전공

Secreted phosphoprotein 1 *(Spp1)* 유전자에 의해 발현되는 Osteopontin (OPN)은 염증이나 종양성 질환 등 생체 내에서 일어나는 다양한 생리학적, 병리학적 과정에서 여러 가지 역할을 하는 것으로 알려져 있다. 선행연구에서는 면역 매개성 질환인 크론병이나 류마티스 관절염 또는 다양한 종양 환자의 혈액 내, 조직 내에서 OPN의 발현이 증가해 있다는 것이 임상적으로 확인되었다. 우리는 이번 연구에서 OPN을 결핍시킨 C57BL/6-Spp1$^{tm1Blh(-/-)}$마우스를 이용해 OPN이 *Helicobacter pylori*에 의해 유발된 위염이나 위암, 그리고 화학물질에 의해 유발된 간암 모델에서 어떠한 역할을 하는지 확인했다.

Helicobacter pylori 감염을 통해 유발된 위염 모델에서, OPN을 결핍시킨 마우스는 대조군 마우스에 비해 더 미약한 수준의 염증반응을 보였으며 대식세포의 침윤 정도나 IL-1β, TNF-α, and IFN-γ 등의 사이토카인 발현 역시 감소해 있었다. 또한 사람 및 마우스의 위암 세포주를 *Helicobacter*

*pylori*에 노출시킨 실험에서도 OPN의 발현을 감소시킨 세포주가 대조군 세포주에 비해 더 적은 양의 사이토카인 발현을 나타냈다. 이 후 사람 및 마우스의 위암 세포주를 키운 배지를 수거해, 이 배지에 대식세포를 배양했을 때, OPN발현을 감소시킨 대식세포가 더 낮은 화학주성을 띠었다. 한편, 이러한 염증성 병변의 차이 외에도 OPN이 결핍된 마우스의 위 점막 상피세포가 대조군 마우스에 비해 더 낮은 세포증식 정도를 보였으며, *Helicobacter pylori*와 공동 배양한 위암 세포주의 표현형 분석에서도 OPN 발현을 감소시켰을 때 G1/S 시기의 억압 및 세포 증식저해가 유발되는 것을 확인했다. 또한 위암 세포주에 IL-1β, TNF-α를 처리했을 때에도 유사한 결과가 나타났다. 이러한 결과는 OPN발현이 줄어들수록 IL-1β, TNF-α의 발현이 감소하며, 이와 연관된 MAP인산화 효소(mitogen-activated protein kinase) 신호전달체계가 억압되는 것과 관련이 있다는 것을 위암 세포주를 이용한 실험에서 확인했다.

이 후 화학물질 및 *Helicobacter pylori*투여로 유발한 위암 모델에서 OPN결핍 마우스는 대조군 마우스에 비해 현저히 낮은 종양발생률을 나타냈으며 종양의 크기 및 개수도 유의적으로 감소된 결과를 보였다. 또한 OPN이 결핍된 마우스에서는 *Helicobacter pylori*에 의해 유발된 만성 위염의 정도가 감소되어 있음이 다시 한번 확인되었고, 전암병변 역시 현저하게 줄어있었다. 뿐만 아니라 OPN결핍마우스에서는 대조군 마우스에 비해 종양 및 주변 점막에서 더 많은 세포자멸사가 관찰되었으며 signal transducer and activator of transcription 1 (STAT1)의 발현 및 유도형 산화질소 합성효소 (inducible nitric oxide synthase; iNOS) 발현 역시 높게 관찰되었다. 사람 위암세포주 및 단핵구 세포주를 이용한 실험에서도, OPN의 억압은 STAT1과 iNOS의 발

현을 증가시켰으며 이것은 세포자멸사의 증가라는 결과를 낳는 것이 관찰됐다. 이러한 OPN과 iNOS의 상관관계를 사람 위암 조직에서 확인하기 위해 OPN과 iNOS에 대한 면역조직화학염색을 실시했으며, 마우스 및 사람 세포주를 이용한 실험에서와 마찬가지로 OPN과 iNOS의 발현이 음의 상관관계를 보이고 있음이 확인되었다.

위와 같이 OPN의 억제가 위염 및 만성 위염과 밀접하게 연관되어 있는 위암의 감소와 밀접한 관계를 가지고 있다는 것을 확인한 후 간암에서도 유사한 역할을 하는지 확인하기 위해 대조군 마우스와 OPN결핍 마우스에 화학물질을 이용해 간암을 유발시켰다. 부검 결과, 화학물질 투여 후 36주에서 OPN결핍마우스가 대조군 마우스에 비해 유의적으로 낮은 간암 발생률을 나타냈으며, 세포자멸사 역시 화학물질 투여 후 26주, 36주 모두에서 현저히 증가해 있었다. 또한 OPN결핍 마우스의 간 조직에서 표피성장인자 수용체 (epidermal growth factor receptor; EGFR)의 감소가 동반되어 있었다. 사람 간암 세포주를 이용한 실험에서도 OPN의 억압은 EGFR의 전사 억제 및 단백질 발현 저해를 유발했으며 이는 전사인자 중 하나인 c-Jun의 발현 감소와 연관되어 있었고, 세포자멸사의 증가라는 결과를 초래했다. 또한 사람 간암조직에 OPN과 EGFR에 대한 면역조직화학염색 결과, OPN과 EGFR이 양의 상관관계를 보이고 있음이 확인되었다.

위의 결과들을 종합해볼 때, OPN의 결핍은 *Helicobacter pylori* 감염에 의해 유발되는 위염 및 이와 연관된 위암의 발생을 감소시키며, 다양한 신호전달체계 조절을 통해 세포자멸사를 촉진해 위암 및 간암 발생을 억제한다는 것을 알 수 있다.

핵심어: Osteopontin, 헬리코박터 파일로리, 대식세포, 유도형 산화질소 합성효소, 표피성장인자 수용체, 위암, 간암

학 번: 2011-21693

REFERENCES

Ahmed, M., R. Behera, et al. (2011). "Osteopontin: a potentially important therapeutic target in cancer." Expert Opin Ther Targets 15(9): 1113-1126.

Ambs, S. and S. A. Glynn (2011). "Candidate pathways linking inducible nitric oxide synthase to a basal-like transcription pattern and tumor progression in human breast cancer." Cell Cycle 10(4): 619-624.

Anborgh, P. H., J. C. Mutrie, et al. (2010). "Role of the metastasis-promoting protein osteopontin in the tumour microenvironment." J Cell Mol Med 14(8): 2037-2044.

Ashka, S., G. F. Weber, et al. (2000). "Eta-1 (osteopontin): an early component of type-1 (cell-mediated) immunity." Science 287(5454): 860-864.

Atkins, K., J. E. Berry, et al. (1998). "Coordinate expression of OPN and associated receptors during monocyte/macrophage differentiation of HL-60 cells." J Cell Physiol 175(2): 229-237.

Baffy, G., E. M. Brunt, et al. (2012). "Hepatocellular carcinoma in non-alcoholic fatty liver disease: A emerging menace." J Hepatol 56(6): 1384-1391.

Beales, I. L. (2002). "Effect of interlukin-1beta on proliferation of gastric epithelial cells in culture." BMC Gastroenterol 2: 7.

Behera, R., V. Kumar, et al. (2010). "Activation of JAK2/STAT3 signaling by osteopontin promotes tumor growth in human breast cancer cells." Carcinogenesis 31(2): 192-200.

Blaser, M. J. and D. E. Berg (2001). "*Helicobacter pylori* genetic diversity and risk of human disease." J Clin Invest 107(7): 767-773.

Brenes, F., B. Ruiz, et al. (1993). "*Helicobacter pylori* causes hyperproliferation of the gastric epithelium: pre- and post-eradication indices of proliferating cell nuclear antigen." Am J Gastroenterol 88(11): 1870-1875.

Brigati, C., D. M. Noonan, et al. (2002). "Tumors and inflammatory infiltrates: friends or foes? ." Clin Exp Metastasis 19(3): 247-258.

Brown, L. F., A. Papadopoulos-Sergiou, et al. (1994). "Osteopontin expression and distribution in human carcinomas." Am J Pathol 145(3): 610-623.

Bruix, J. and M. Sherman (2011). "Management of hepatocellular carcinoma: An update." Hepatology 53(3): 1020-1022.

Cantor, H. and M. L. Shinohara (2009). "Regulation of T-helper-cell lineage development by osteopontin: the inside story." Nat Rev Immunol 9(2): 137-141.

Chan, A. O., K. M. Chu, et al. (2007). "Association between *Helicobacter pylori* infection and interleukin 1beta polymorphism predispose to CpG island methylation in gastric cancer." Gut 56(4): 595-597.

Chang, W. L., H. B. Yang, et al. (2011). "Increased gastric osteopontin expression by *Helicobacter pylori* can correlate with more severe gastric inflammation and intestinal metaplasia." Helicobacter 16(3): 217-224.

Chen, C. N., F. J. Hsieh, et al. (2006). "Expression of inducible nitric oxide synthase and cyclooxygenase-2 in angiogenesis and clinical outcome of human gastric cancer." J Surg Oncol 94(3): 226-233.

Cheng, J., W. Wang, et al. (2014). "Meta-analysis of the prognostic and diagnostic significance of serum/plasma osteopontin in hepatocellular carcinoma." J Clin Gastroenterol 48(9): 806-814.

Chiche, J., M. Rouleau, et al. (2010). "Hypoxic enlarged mitochondria protect cancer cells from apoptotic stimuli." J Cell Physiol 222(3):

648-657.

Cho, H. J. and H. S. Kim (2009). "Osteopontin: a multifunctioal protein at the crossroads of inflammation, atherosclerosis, and vascular calcification." Curr Atheroscler Rep 11(3): 206-213.

Cho, S. O., J. W. Lim, et al. (2010). "Involvement of Ras and AP-1 in *Helicobacter pylori*-induced expression of COX-2 and iNOS in gastric epithelial AGS cells." Dig Dis Sci 55(4): 988-996.

Coligan, J. E. Current protocols in immunology. New York, John Wiley and Sons: v. (loose leaf).

Cook, A. C., A. F. Chambers, et al. (2006). "Osteopontin induction of hyaluronan synthase 2 expression promotes breast cancer malignancy." J Biol Chem 281(34): 24381-243899.

Correa, P. (1992). "Human gastric carcinogenesis: a multistep and multifactorial process--First American Cancer Society Award Lecture on Cancer Epidemiology and Prevention." Cancer Res 52(24): 6735-6740.

Correa, P. (1992). "Human gastric carcinogenesis: a multistep and multifactorial process—first american cancer society award lecture on cancer epidemiology and prevention. ." Cancer Res 52(24): 6735-6740.

Coussens, L. M. and Z. Werb (2002). "Inflammation and cancer." Nature 420(6917): 860-867.

Dai, N., Q. Bao, et al. (2007). "Protein expression of osteopontin in tumor tissues is an independent prognostic indicator in gastric cancer." Oncology 72(1-2): 89-96.

Davila, J. A., R. O. Morgan, et al. (2004). "Hepatitis C infection and the increasing incidence of hepatocellular carcinoma: a population-based study." Gastroenterology 127(5): 1372-1380.

de Freitas, D., M. Urbano, et al. (2004). "The effect of *Helicobacter*

pylori infection on apoptosis and cell proliferation in gastric epithelium." Hepatogastroenterology 51(57): 876-882.

de Vera, M. E., R. A. Shapiro, et al. (1996). "Transcriptional regulation of human inducible nitric oxide synthase (NOS2) gene by cytokines: initial analysis of the human NOS2 promoter." Proc Natl Acad Sci U S A 93(3): 1054-1059.

Edwards, P., J. C. Cendan, et al. (1996). "Tumor cell nitric oxide inhibits cell growth *in vitro*, but stimulates tumorigenesis and experimental lung metastasis *in vivo*." J Surg Res 63(1): 49-52.

Eslick, G. D., L. L. Lim, et al. (1999). "Association of *Helicobacter pylori* infection with gastric carcinoma: a meta-analysis." Am J Gastroenterol 94(9): 2373-2379.

Fabregat, I. (2009). "Dysregulation of apoptosis in hepatocellular carcinoma cells." World J Gastroenterol 15(5): 513-520.

Fan, X., C. He, et al. (2015). "Intracellular Osteopontin inhibits toll-like receptor signaling and impedes liver carcinogenesis." Cancer Res 75(1): 86-97.

Fan, X. G., D. Kelleher, et al. (1996). "Helicobacter pylori increases proliferation of gastric epithelial cells." Gut 38(1): 19-22.

Ferlay, J., H. R. Shin, et al. (2013). "GLOBOCAN 2012 v1.0, Cancer Incidence and Mortality Worldwide: IARC CancerBase No. 11 [Internet]."

Fouad, S. A., N. A. Mohamed, et al. (2015). "Plasma osteopontin level in chronic liver disease and hepatocellular carcinoma." Hepat Mon 15(9): e30753.

Fox, J. G. and T. C. Wang (2007). "Inflammation, atrophy, and gastric cancer." J Clin Invest 117(1): 60-69.

Gao, C., H. Guo, et al. (2007). "Osteopontin induces ubiquitin-dependent degradation of STAT1 in RAW264.7 murine macrophages." J

Immunol 178(3): 1870-1881.

Gao, C., Z. Mi, et al. (2007). "Osteopontin regulates ubiquitin-dependent degradation of stat1 in murine mammary epithelial tumor cells." Neoplasia 9(9): 699-706.

Giachelli, C. M., D. Lombardi, et al. (1998). " Evidence for a role of osteopontin in macrophage infiltration in response to pathological stimuli in vivo." Am J Pathol 152(2): 353-358.

Gong, M., Z. Lu, et al. (2008). "A small interfering RNA targeting osteopontin as gastric cancer therapeutics." Cancer Lett 272(1): 148-159.

Guo, G., K. Gong, et al. (2015). "Ligand-independent EGFR signaling." Cancer Res 75(17): 3436-3441.

Guo, H., Z. Mi, et al. (2010). "Osteopontin and protein kinase C regulate PDLIM2 activation and STAT1 ubiquitination in LPS-treated murine macrophages." J Biol Chem 285(48): 37787-37796.

Guo, H., P. Y. Wai, et al. (2008). "Osteopontin mediates Stat1 degradation to inhibit iNOS transcription in a cecal ligation and puncture model of sepsis." Surgery 144(2): 182-188.

Han, S. U., Y. B. Kim, et al. (2002). "*Helicobacter pylori* infection promotes gastric carcinogenesis in a mice model." J Gastroenterol Hepatol 17(3): 253-261.

Harada, K., G. Shiota, et al. (1999). "Transforming growth factor-alpha and epidermal growth factor receptor in chronic liver disease and hepatocellular carcinoma." Liver 19(4): 318-325.

Higashiyama, M., T. Ito, et al. (2007). "Prognostic significance of osteopontin expression in human gastric carcinoma." Ann Surg Oncol 14(12): 3419-3427.

Higuchi, Y., Y. Tamura, et al. (2004). "The roles of soluble osteopontin using osteopontin-transgenic mice in vivo: proliferation of CD4+

T lymphocytes and the enhancement of cell-mediated immune responses." Pathobiology 71(1): 1-11

Houghton, J., L. S. Macera-Bloch, et al. (2000). "Tumor necrosis factor alpha and interleukin 1beta up-regulate gastric mucosal Fas antigen expression in Helicobacter pylori infection." Infect Immun 68(3): 1189-1195.

Hsieh, Y. H., M. M. Juliana, et al. (2006). "Papilloma development is delayed in osteopontin-null mice: implicating an antiapoptosis role for osteopontin." Cancer Res 66(14): 7119-7127.

Hua, Z., J. Chen, et al. (2011). "Specific expression of osteopontin and S100A6 in hepatocellular carcinoma." Surgery 149(6): 783-791.

Huang, W., G. Zhu, et al. (2010). "Plasma osteopontin concentration correlates with the severity of hepatic fibrosis and inflammation in HCV-infected subjects." Clin Chim Acta 411(9-10): 675-678.

Hubbard, N. E., Q. J. Chen, et al. (2013). "Transgenic mammary epithelial osteopontin (spp1) expression induces proliferation and alveologenesis." Genes Cancer 4(5-6): 201-212.

Hur, E. M., S. Youssef, et al. (2007). "Osteopontin-induced relapse and progression of autoimmune brain disease through enhanced survival of activated T cells." Nat Immunol 8(1): 74-83.

Husain-Krautter, S., J. M. Kramer, et al. (2015). "The osteopontin transgenic mouse is a new model for Sjogren's syndrome." Clin Immunol 157(1): 30-42.

Imano, M., T. Satou, et al. (2009). "Immunohistochemical expression of osteopontin in gastric cancer." J Gastrointest Surg 13(9): 1577-1582.

Isoda, K. (2003). "Osteopontin Transgenic Mice Fed a High-Cholesterol Diet Develop Early Fatty-Streak Lesions." Circulation 107(5): 679-681.

Jin, W., B. B. Chen, et al. (2012). "TIEG1 inhibits breast cancer invasion and metastasis by inhibition of epidermal growth factor receptor

(EGFR) transcription and the EGFR signaling pathway." Mol Cell Biol 32(1): 50-63.

Jones, N. L., P. T. Shannon, et al. (1997). "Increase in proliferation and apoptosis of gastric epithelial cells early in the natural history of *Helicobacter pylori* infection." Am J Pathol 151(6): 1695-1703.

Jung, K. W., Y. J. Won, et al. (2014). "Cancer statistics in Korea: Incidence, mortality, survival, and prevalence in 2011." Cancer Res Treat 46(2): 109-123.

Kale, S., R. Raja, et al. (2014). "Osteopontin signaling upregulates cyclooxygenase-2 expression in tumor-associated macrophages leading to enhanced angiogenesis and melanoma growth via $\alpha 9\beta 1$ integrin." Oncogene 33(18): 2295-2306.

Kiefer, F. W., S. Neschen, et al. (2011). "Osteopontin deficiency protects against obesity-induced hepatic steatosis and attenuates glucose production in mice." Diabetologia 54(8): 2132-2142.

Kiefer, M. C., D. M. Bauer, et al. (1989). "The cDNA and derived amino acid sequence for human osteopontin." Nucleic Acids Res 17(1): 3306.

Kim, J. Y., B. N. Bae, et al. (2009). "Osteopontin, CD44, and NFkappaB expression in gastric adenocarcinoma." Cancer Res Treat 41(1): 29-35.

Konturek, P. C., W. Bielanski, et al. (1999). "*Helicobacter pylori* associated gastric pathology." J Physiol Pharmacol 50(5): 695-710.

Kumar, V., R. Behera, et al. (2010). "p38 kinase is crucial for osteopontin-induced furin expression that supports cervical cancer progression." Cancer Res 70(24): 10381-10391.

Kuroda, T., Y. Kitadai, et al. (2005). "Monocyte chemoattractant protein-1 transfection induces angiogenesis and tumorigenesis of gastric carcinoma in nude mice via macrophage recruitment." Clin

Cancer Res 11(21): 7629-7636.

Kusmartsev, S. and D. I. Gabrilovich (2013). "Stat1 signaling regulates tumor-associated macrophage-mediated T cell deletion." J Immunol 174(8): 4880-4891.

Kwon, H. J., Y. S. Won, et al. (2012). "Vitamin D(3) upregulated protein 1 deficiency promotes N-methyl-N-nitrosourea and *Helicobacter pylori*-induced gastric carcinogenesis in mice." Gut 61(1): 53-63.

Laffon, A., R. Garcia-Vicuna, et al. (1991). "Upregulated expression and function of VLA-4 fibronectin receptors on human activated T cells in rheumatoid arthritis." J Clin Invest 88(2): 546-552.

Lee, I. O., J. H. Kim, et al. (2010). "*Helicobacter pylori* CagA phosphorylation status determines the gp130-activated SHP2/ERK and JAK/STAT signal transduction pathways in gastric epithelial cells." J Biol Chem 285(21): 16042-16050.

Lee, J. L., M. J. Wang, et al. (2007). "Osteopontin promotes integrin activation through outside-in and inside-out mechanisms: OPN-CD44V interaction enhances survival in gastrointestinal cancer cells." Cancer Res 67(5): 2089-2097.

Lee, S. H., J. W. Park, et al. (2015). "Ablation of osteopontin suppresses N-methyl-N-nitrosourea and *Helicobacter pylori*-induced gastric cancer development in mice." Carcinogenesis 36(12): 1550-1560.

Li, J. J., H. Y. Li, et al. (2014). "Diagnostic significance of serum osteopontin level for pancreatic cancer: a meta-analysis." Genet Test Mol Biomarker 18(8): 580-586.

Li, X., A. B. O'Regan, et al. (2003). "IFN-gamma induction of osteopontin expression in human monocytoid cells." J Interferon Cytokine Res 23(5): 259-265.

Liaw, L., E. D. Birk, et al. (1998). "Altered wound healing in mice lacking a functional osteopontin gene (spp1)." J Clin Invest 101(7):

1468-1478.

Lin, F., Y. Li, et al. (2011). "Overexpression of osteopontin in hepatocellular carcinoma and its relationships with metastasis, invasion of tumor cells." Mol Biol Rep 38(8): 5205-5210.

Lin, Y. F., M. S. Wu, et al. (2006). "Comparative immunoproteomics of identification and characterization of virulence factors from *Helicobacter pylori* related to gastric cancer." Mol Cell Proteomics 5(8): 1484-1496.

Lin, Y. H., C. J. Huang, et al. (2000). "Coupling of OPN and its cell surface receptor CD44 to the cell survival response elicited by interleukin-3 or granulocyte-macrophage colony-stimulating factor." Mol Cell Biol 20(8): 2734-2742.

Lin, Y. H. and H. F. Yang-Yen (2001). "The osteopontin-CD44 survival signal involves activation of the phosphatidylinositol 3-kinase/Akt signaling pathway." J Biol Chem 276(49): 46024-46030.

Liu, X., S. Tian, et al. (2016). "Wogonin inhibits the proliferation and invasion, and induces the apoptosis of HepG2 and Bel7402 HCC cells through NFkappaB/Bcl-2, EGFR and EGFR downstream ERK/AKT signaling." Int J Mol Med: doi: 10.3892/ijmm.2016.2700.

Lund, S. A., C. M. Giachelli, et al. (2009). "The role of osteopontin in inflammatory processes." J Cell Commun Signal 3(3-4): 311-322.

Luo, J. C., V. Y. Shin, et al. (2005). "Tumor necrosis factor-alpha stimulates gastric epithelial cell proliferation." Am J Physiol Gastrointest Liver Physiol 288(1): G32-38.

Luo, X., M. K. Ruhland, et al. (2011). "Osteopontin stimulates preneoplastic cellular proliferation through activation of the MAPK pathway." Mol Cancer Res 9(8): 1018-1029.

Mannick, E. E., L. E. Bravo, et al. (1996). "Inducible nitric oxide synthase, nitrotyrosine, and apoptosis in *Helicobacter pylori* gastritis: effect of antibiotics and antioxidants " Cancer Res 56(14): 3238-3243.

Matusan-Ilijas, K., G. Damante, et al. (2011). "Osteopontin expression correlates with nuclear factor-kappaB activation and apoptosis downregulation in clear cell renal cell carcinoma." Pathol Res Pract 207(2): 104-110.

Meloche, S. and J. Pouyssegur (2007). "The ERK1/2 mitogen-activated protein kinase pathway as a master regulator of the G1- to S-phase transition." Oncogene 26(22): 3227-3239.

Mikula, M., A. Dzwonek, et al. (2003). "Quantitative detection for low levels of *Helicobacter pylori* infection in experimentally infected mice by real-time PCR." J Microbiol Methods 55(2): 351-359.

Milne, A. N., F. Carneiro, et al. (2009). "Nature meets nurture: molecular genetics of gastric cancer." Hum Genet 126(5): 615-628.

Mishima, R., F. Takeshima, et al. (2007). "High plasma osteopontin levels in patients with inflammatory bowel disease." J Clin Gastroenterol 41(2): 123-125.

Miyazaki, Y., T. Tashiro, et al. (1995). "Expression of osteopontin in a macrophage cell line and in transgenic mice with pulmonary fibrosis resulting from the lung expression of a tumor necrosis factor-alpha transgene." Ann N Y Acad Sci 760: 334-341.

Muntane, J. and M. D. la Mata (2010). "Nitric oxide and cancer." World J Hepatol 2(9): 337-344.

Murakami, K., T. Fujioka, et al. (1997). "*Helicobacter pylori* infection accelerates human gastric mucosal cell proliferation." J Gastroenterol 32(2): 184-188.

Nagoshi, S. (2014). "Osteopontin: Versatile modulator of liver disease." Hepatol Res 44(1): 22-30.

Nam, K. T., S. Y. Oh, et al. (2004). "Decreased *Helicobacter pylori* associated gastric carcinogenesis in mice lacking inducible nitric oxide synthase." Gut 53(9): 1250-1255.

Nuciforo, P., N. Radosevic-Robin, et al. (2015). "Quantification of HER familiy receptors in breast cancer." Breast Cancer Res 17: doi: 10.1186/s13058-13015-10561-13058.

Oldberg, A., A. Franzen, et al. (1986). "Cloning and sequence analysis of rat bone sialoprotein (osteopontin) cDNA reveals an Arg-Gly-Asp cell-binding sequence." Proc Natl Acad Sci U S A 83(23): 8819-8823.

Osman, M. A., G. S. Bloom, et al. (2013). "*Helicobacter pylori*-induced alteration of epithelial cell signaling and polarity: a possible mechanism of gastric carcinoma etiology and disparity." Cytoskeleton (Hoboken) 70(7): 349-359.

Oz, H. S., J. Zhong, et al. (2012). "Osteopontin ablation attenuates progression of colitis in TNBS model." Dig Dis Sci 57(6): 1554-1561.

Pan, H. W., Y. H. Ou, et al. (2003). "Overexpression of osteopontin is associated with intrahepatic metastasis, early recurrence, and poorer prognosis of surgically resected hepatocellular carcinoma." Cancer 98(1): 119-127.

Park, J. W., S. H. Jang, et al. (2014). "Cooperativity of E-cadherin and Smad4 loss to promote diffuse-type gastric adenocarcinoma and metastasis." Mol Cancer Res 12(8): 1088-1099.

Park, J. W., S. H. Lee, et al. (2015). "Osteopontin depletion decreases inflammation and gastric epithelial proliferation during *Helicobacter pylori* infection in mice." Lab Invest 95(6): 660-671.

Park, J. W., D. M. Park, et al. (2014). "Establishment and characterization of metastatic gastric cancer cell lines from murine gastric adenocarcinoma lacking Smad4, p53, and E-cadherin." Mol Carcinog 54(11): 1521-1527.

Parsonnet, J., G. D. Friedman, et al. (1991). "*Helicobacter pylori* infection and the risk of gastric carcinoma." N Engl J Med 325(16): 1127-

1131.

Patouraux, S., D. Rousseau, et al. (2014). "Osteopontin deficiency aggravates hepatic injury induced by ischemia-reperfusion in mice." Cell Death Dis 5: e1208.

Peek, R. M., Jr., C. Fiske, et al. (2010). "Role of innate immunity in *Helicobacter pylori*-induced gastric malignancy." Physiol Rev 90(3): 831-858.

Peek, R. M., Jr., S. F. Moss, et al. (1997). "*Helicobacter pylori* cagA+ strains and dissociation of gastric epithelial cell proliferation from apoptosis." J Natl Cancer Inst 89(12): 863-868.

Peraldo-Neia, C., G. Migliardi, et al. (2011). "Epidermal Growth Factor Receptor (EGFR) mutation analysis, gene expression profiling and EGFR protein expression in primary prostate cancer." BMC cancer 11: 31.

Popivanova, B. K., F. I. Kostadinova, et al. (2009). "Blockade of a chemokine, CCL2, reduces chronic colitis-associated carcinogenesis in mice." Cancer Res 69(19): 7884-7892.

Rahn, W., R. W. Redline, et al. (2004). "Molecular analysis of *Helicobacter pylori*-associated gastric inflammation in naive versus previously immunized mice." Vaccine 23(6): 807-818.

Rao, C. V., N. B. Janakiram, et al. (2015). "Simultaneous targeting of 5-LOX-COX and EGFR blocks progression of pancreatic ductal adenocarcinoma." Oncotarget 6(32): 33290-33305.

Rieder, G., J. A. Hofmann, et al. (2003). "Up-regulation of inducible nitric oxide synthase in *Helicobacter pylori*-associated gastritis may represent and increased risk factor to develop gastric carcinoma of intestinal type." Int J Med Microbiol 293(6): 403-412.

Ringelhan, M. and U. Protzer (2015). "Oncogenic potential of hepatitis B virus encoded proteins." Curr Opin Virol 14: 109-115.

Rittling, S. R. (2011). "Osteopontin in macrophage function." Expert Rev Mol Med 13: e15.

Rittling, S. R., H. N. Matsumoto, et al. (1998). "Mice lacking osteopontin show normal development and bone structure but display altered osteoclast formation in vitro." J Bone Miner Res 13(7): 1101-1111.

Robertson, B. W. and M. A. Chellaiah (2010). "Osteopontin induces beta-catenin signaling through activation of Akt in prostate cancer cells." Exp Cell Res 316(1): 1-11.

Rogers, A. B., N. S. Taylor, et al. (2005). "*Helicobacter pylori* but not high salt induces gastric intraepithelial neoplasia in B6129 mice." Cancer Res 65(23): 10709-10715.

Rokkas, T., S. Ladas, et al. (1999). "Relationship of Helicobacter pylori CagA status to gastric cell proliferation and apoptosis." Dig Dis Sci 44(3): 487-493.

Rollo, E. E., L. D. Laskin, et al. (1996). "Osteopontin inhibits nitric oxide production and cytotoxicity by activated RAW264.7 macrophages." J Leukoc Biol 60(3): 397-404.

Roussel, Y., A. Harris, et al. (2007). "Novel methods of quantitative real-time PCR data analysis in a murine Helicobacter pylori vaccine model." Vaccine 25(15): 2919-2929.

Russo, A., T. Franchina, et al. (2015). "A decade of EGFR inhibition in EGFR-mutated non small cell lung cancer (NSCLC): Old successes and future perspectives." Oncotarget 6(29): 26814-26825.

Santos, J. C., M. S. Ladeira, et al. (2012). "Relationship of IL-1 and TNF-alpha polymorphisms with *Helicobacter pylori* in gastric diseases in a Brazilian population." Braz J Med Biol Res 45(9): 811-817.

Sato, T., T. Nakai, et al. (2005). "Osteopontin/Eta-1 upregulated in Crohn's disease regulates the Th1 immune response." Gut 54(9): 1254-1262.

Schumacher, M. A., J. M. Donnelly, et al. (2012). "Gastric Sonic Hedgehog acts as a macrophage chemoattractant during the immune response to *Helicobacter pylori*." Gastroenterology 142(5): 1150-1159.

Shevde, L. A. and R. S. Samant (2014). "Role of osteopontin in the pathophysiology of cancer." Matrix Biol 37: 131-141.

Shigematsu, Y., T. Niwa, et al. (2013). "Interleukin-1beta induced by *Helicobacter pylori* infection enhances mouse gastric carcinogenesis." Cancer Lett 340(1): 141-147.

Shinohara, M. L., M. Jansson, et al. (2005). " T-bet-dependent expression of osteopontin contributes to T cell polarization." Proc Natl Acad Sci U S A 102(47): 17101-17106.

Shinohara, M. L., H. J. Kim, et al. (2008). " Alternative translation of osteopontin generates intracellular and secreted isoforms that mediate distinct biological activities in dendritic cells." Proc Natl Acad Sci U S A 105(1): 7235-7239.

Shinohara, M. L., J. H. Kim, et al. (2008). "Engagement of the type I interferon receptor on dendritic cells inhibits T helper 17 cell development: role of intracellular osteopontin." Immunitiy 29(1): 68-78.

Shinohara, M. L., L. Lu, et al. (2006). "Osteopontin expression is essential for interferon-alpha production by plasmacytoid dendritic cells." Nat Immunol 7(5): 498-506.

Singhal, H., D. S. Bautista, et al. (1997). "Elevated plasma osteopontin in metastatic breast cancer associated with increased tumor burden and decreased survival." Clinical Can Res 3(4): 605-611.

Sodek, J., B. Ganss, et al. (2000). "Osteopontin." Crit Rev Oral Biol Med 11(3): 279-303.

Song, G., G. Ouyang, et al. (2009). "Osteopontin promotes gastric cancer metastasis by augmenting cell survival and invasion through Akt-mediated HIF-1alpha up-regulation and MMP9 activation." Journal of cellular and molecular medicine 13(8B): 1706-1718.

Sordella, R., D. W. Bell, et al. (2004). "Gefitinib-sensitizing EGFR mutations in lung cancer activate anti-apoptotic pathways." Science 305(5687): 1163-1167.

Sukowati, C. H., K. E. El-Khobar, et al. (2016). "Significance of hepatitis virus infection in the oncogenic initiation of hepatocellular carcinom." World J Gastroenterol 22(4): 1497-1512.

Sun, B. S., Q. Z. Dong, et al. (2008). "Lentiviral-mediated miRNA against osteopontin suppresses tumor growth and metastasis of human hepatocellular carcinoma." Hepatology 48(6): 1834-1842.

Syn, W. K., S. S. Choi, et al. (2011). "Osteopontin is induced by hedgehog pathway activation and promotes fibrosis progression in nonalcoholic steatohepatitis." Hepatology 53(1): 106-115.

Syu, L. J., M. El-Zaatari, et al. (2012). "Transgenic expression of interferon-gamma in mouse stomach leads to inflammation, metaplasia, and dysplasia." Am J Pathol 181(6): 2114-2125.

Tang, H., J. Wang, et al. (2007). "Inhibition of osteopontin would suppress angiogenesis in gastric cancer." Biochem Cell Biol 85(1): 103-110.

Tilli, T. M., K. D. Mello, et al. (2012). "Both osteopontin-c and osteopontin-b splicing isoforms exert pro-tumorigenic roles in prostate cancer cells." Prostate 72(15): 1688-1699.

Tsai, W. C., W. C. Tsai, et al. (2012). "Association between Osteopontin and EGFR Expression with Clinicopathological Parameters in Hepatocellular Carcinoma." Chin J Physiol 55(6): 412-420.

Tsung, K., J. P. Dolan, et al. (2002). "Macrophages as effector cells in interleukin 12-induced T cell-dependent tumor rejection." Cancer Res 62(17): 5069-5075.

Uaesoontrachoon, K., D. K. Wasgewatte Wijesinghe, et al. (2013). "Osteopontin deficiency delays inflammatory infiltration and the onset of muscle regeneration in a mouse model of muscle injury." Dis Model Mech 6(1): 197-205.

Ue, T., H. Yokozaki, et al. (1998). "Co-expression of osteopontin and CD44v9 in gastric cancer." Int J Cancer 79(2): 127-132.

Uede, T. (2011). "Osteopontin, intrinsic tissue regulator of intractable inflammatory diseases." Pathol Int 61(5): 265-280.

Wai, P. Y., L. Guo, et al. (2006). "Osteopontin inhibits macrophage nitric oxide synthesis to enhance tumor proliferation." Surgery 140(2): 132-140.

Wang, Z. (2016). "Transactivation of epidermal growth factor receptor by G protein-coupled receptor: Recent progress, challange and future research." Int J Mol Sci 17(1) doi:10.3390/ijms17010095.

Weber, G. F., G. S. Lett, et al. (2011). "Categorical meta-analysis of osteopontin as a clinical cancer marker." Oncol Rep 25(2): 433-441.

Weigert, A. and B. Brune (2008). "Nitric oxide, apoptosis and macrophage polarization during tumor progression." Nitric Oxide 19(2): 95-102.

Whitney, A. E., T. S. Emory, et al. (2000). "Increased macrophage infiltration of gastric mucosa in *Helicobacter pylori*-infected children." Dig Dis Sci 45(7): 1337-1342.

Wroblewski, L. E., R. M. Peek, Jr., et al. (2010). "*Helicobacter pylori* and gastric cancer: factors that modulate disease risk." Clin Microbiol Rev 23(4): 713-739.

Wu, C. Y., M. S. Wu, et al. (2007). "Elevated plasma osteopontin associated with gastric cancer development, invasion and survival." Gut 56(6): 782-789.

Xia, H. H., S. K. Lam, et al. (2005). "Macrophage migration inhibitory factor stimulated by *Helicobacter pylori* increases proliferation of gastric epithelial cells." World J Gastroenterol 11(13): 1946-1950.

Xu, S. T., C. Guo, et al. (2015). "Role of osteopontin in the regulation of human bladder cancer proliferation and migration in T24 cells." Mol Med Rep 11(5): 3701-3707.

Xu, Y. P., G. Lin, et al. (2016). "C-Met as a molecular marker for esophageal squamous cell carcinoma and its association with clinical outcome." J Cancer 7(5): 587-594.

Yamamoto, T., M. Kita, et al. (2004). "Role of tumor necrosis factor-alpha and interferon-gamma in *Helicobacter pylori* infection." Microbiol Immunol 48(9): 647-654.

Yanai, A., Y. Hirata, et al. (2003). "*Helicobacter pylori* induces antiapoptosis through nuclear factor-kappaB activation." J Infect Dis 188(11): 1741-1751.

Yang, J. D., W. S. Harmsen, et al. (2011). "Factor that affect risk for hepatocellular carcinoma and effects of surveillance." Clin Gastroenterol Hepatol 9(7): 617-623.

Yiu, A. J. and C. Y. Yiu (2016). "Biomarker in colorectal cancer." Anticancer Res 36(3): 1093-1102.

Yoo, B. K., R. Gredler, et al. (2011). "c-Met activation through a novel pathway involving osteopontin mediates oncogenesis by the transcription factor LSF." J Hepatol 55(6): 1317-1324.

Zenz, R., H. Scheuch, et al. (2003). "c-Jun regulates eyelid closure and skin tumor development through EGFR signaling." Dev Cell 4(6): 879-889.

Zhang, A., Y. Liu, et al. (2010). "Osteopontin silencing by small interfering RNA induces apoptosis and suppresses invasion in human renal carcinoma Caki-1 cells." Med Oncol 27(4): 1179-1184.

Zhang, H., M. Guo, et al. (2014). "Osteopontin knockdown inhibits alphav,beta3 integrin-induced cell migration and invasion and promotes apoptosis of breast cancer cells by inducing autophagy and inactivating the PI3K/Akt/mTOR pathway." Cell Physiol Biochem 33(4): 991-1002.

Zhang, R., X. Pan, et al. (2011). "Osteopontin enhances the expression and activity of MMP-2 via the SDF-1/CXCR4 axis in hepatocellular carcinoma cell lines." PloS One 6(8): e23831.

Zhao, J., L. Dong, et al. (2008). "Down-regulation of osteopontin suppresses growth and metastasis of hepatocellular carcinoma via induction of apoptosis." Gastroenterology 135(3): 956-968.

Zhu, B., K. Suzuki, et al. (2004). "Osteopontin modulates CD44-dependent chemotaxis of peritoneal macrophages through G-protein-coupled receptors: evidence of a role for an intracellular form of osteopontin." J Cell Physiol 198(1): 155-167.

Zhu, W., L. Guo, et al. (2014). "Combination of osteopontin with peritumoral infiltrating macrophages is associated with poor prognosis of early-stage hepatocellular carcinom after curative resection." Ann Surg Oncol 21(4): 1304-1313.